INFORMATION TO USERS

This manuscript has been reproduced from the microfilm master. UMI films the text directly from the original or copy submitted. Thus, some thesis and dissertation copies are in typewriter face, while others may be from any type of computer printer.

The quality of this reproduction is dependent upon the quality of the copy submitted. Broken or indistinct print, colored or poor quality illustrations and photographs, print bleedthrough, substandard margins, and improper alignment can adversely affect reproduction.

In the unlikely event that the author did not send UMI a complete manuscript and there are missing pages, these will be noted. Also, if unauthorized copyright material had to be removed, a note will indicate the deletion.

Oversize materials (e.g., maps, drawings, charts) are reproduced by sectioning the original, beginning at the upper left-hand corner and continuing from left to right in equal sections with small overlaps.

Photographs included in the original manuscript have been reproduced xerographically in this copy. Higher quality 6" x 9" black and white photographic prints are available for any photographs or illustrations appearing in this copy for an additional charge. Contact UMI directly to order.

Bell & Howell Information and Learning
300 North Zeeb Road, Ann Arbor, MI 48106-1346 USA

UMI®
800-521-0600

A Study of Heat and Mass Transfer in Dual Water Heaters

by

Abdussalam Mohamed Shawesh

A Thesis Submitted to the Faculty of Graduate Studies and Research
in Partial Fulfillment for the Degree of Master of Engineering of
McGill University in Montreal
Submitted February 12, 1998

Abstract

An improved hot water generator that combines direct water heating in a packed column and indirect water heating in a submerged combustion chamber is the subject of this investigation. Advantages of the heater over the conventional hot water generators include higher efficiency, lower cost of equipment, lower pressure drop and a simpler control system.

The experimental work has been conducted on a prototype dual water heater located at the Natural Gas Technology Center at Boucherville, Quebec. The heater consists of an immersed firetube and two packed columns. It provides hot water at two temperatures. The effects of the controlling parameters, such as the flow rates of the water, air, and fuel gas, on the performance of the heater were analyzed. Equations governing the heat and mass transfer were formulated. Simplified forms of these equations were used to determine heat and mass transfer coefficients.

Résumé

Le sujet de cette expérimentation porte sur une génératrice d'eau chaude améliorée permettant le chauffage direct de l' eau chaude dans une colonne remplie d'anneaux de type Pall et le chauffage indirect de l'eau dans une chambre a combustion submergée. Comparé aux génératrices d'eau chaude conventionnelles, les avantages de ce chauffe-eau comportent une meilleure efficacité, un équipement a prix réduit, un échappement de pression plus bas et un système de contrôle plus simple.

La recherche expérimentale a été effectuée sur un prototype de chauffe-eau double. Le chauffe-eau consiste en un tube immerge (chambre a combustion) et deux colonnes. Il procure de l'eau chaude selon deux températures. Les effets des paramètres de contrôle tels que les flux d'eau, l'air et des gaz de combustion sur la performance du chauffe-eau ont été analyses. L'équation s'appliquant a la chaleur et au transfert de la masse a été formulée et des formes simplifiées ont été utilisées pour déterminer les coefficients de chaleur et de transfert de masse.

Acknowledgments

The author wishes to express his gratitude to the following people who made the completion of this work possible:

To his director, Dr. N. E. Cooke for his valuable assistance and guidance to this work.

To Mr. Stephane Brunet for his valuable help and support.

To the academic and technical staff of the Department of Chemical Engineering for their support and understanding.

To the Natural Gas Technology Centre of Quebec for making available their facilities and in particular the equipment used in this research.

And finally, to my family and friends.

Table of Contents

List of Figures

List of Tables

1. 0 INTRODUCTION

Low temperature water for process heating or direct usage is a major use of energy in the industrial and residential sectors. To recover energy as a hot water, two major pieces of equipment are required; combustion equipment, and heat transfer equipment. In applications using boilers, sophisticated controls and combustion chambers designs have reached a level in which it is impractical to achieve a much more improvement in the thermal efficiency. Direct contact heat transfer between hot combustion gases and water as a method to increase the efficiency of heat transfer and lower the cost, has recently received attention. Besides the substantial increase in the overall efficiency, direct contact water heating eliminates the use of steam as a secondary heating medium.

In direct contact heat transfer, the transfer of heat is achieved through intimate contact of two material streams without the presence of an intervening solid wall. The method is used in various branches of industry, such as drying, gas quenching, water desalination and water cooling or heating. Advantages of direct contact heat exchangers over surface heat exchangers include greater heat transfer area, lower equipment cost, lower pressure drop and the ability to transfer heat at a much lower temperature difference. In addition, the absence of the intervening solid wall reduces corrosion problems and avoids deterioration of heat transfer efficiency due to fouling. One disadvantage of direct contact heat exchangers is contamination. The design methods are less comprehensive than with conventional exchangers. Kierth & Boeheum [1988] considered that the lack of reliable design methods for direct contact heat exchangers discouraged process engineers from using this method and caused them to favour surface heat exchangers.

Gas-liquid direct contact heat transfer applications are usually available as spray columns, baffle columns, and packed columns. In this type of equipment, there is a trade--off between heat transfer performance and gas-side pressure drop. Spray columns have the lowest pressure drop, but low heat transfer performance per unit volume due to deterioration of the uniformity of spray pattern as distance from the spray nozzles

increases, and the large degree of back-mixing of the gas. The baffle columns have a higher pressure drop than the spray columns with higher heat transfer performance. Spray chambers are suitable when there is a large temperature gradient while baffle columns are recommended when solid deposits are expected to form during the exchange of heat.

Packed columns have the highest heat transfer performance because of the large interfacial area on the packing surface but they also have a higher pressure drop. Packed columns are very effective when moderate pressure drop or low liquid hold up is important and a high transfer area or high volumetric efficiency is needed. They are also useful for corrosive gas or liquid service. The most important feature of packed columns, is the packing materials, which are generally classified as being random or structured. There are many factors affecting the proper selection of type, material, and size of packing including cost, capacity, pressure drop and service conditions. The design of packed columns depends greatly upon the heat transfer, mass transfer, flooding, and pressure drop characteristics of packing. An important aspect in the mechanical design of spray or packed columns, is to ensure the uniformity of gas and liquid distribution. In heat transfer applications, pressure fed distributors such as pipe orifice and spray nozzles are used for liquid distribution. The choice depends upon gas or liquid feeding rates, turndown requirements, plugging or fouling tendencies, cost, and other mechanical factors.

In gas-liquid direct contact heat transfer applications, heat and/or mass transfer take place in the form of droplets, bubbles, or falling films. Mass transfer accompanied the heat transfer can be either a benefit or a hindrance. In some situations, mass transfer is desirable. For example, a cooling tower functions better when large amounts of water are evaporated. There are situations where direct-contact heat exchanger designs may benefit from the minimization of mass transfer and significant amount of mass transfer could be considered undesirable. For example, direct contact between combustion products and water usually results in dissolution of these gases into water.

Available hot water generators that utilize direct contact heat transfer between hot combustion gases and water can be split into two classes:

I. Equilibrium Hot Water Generators.

In this type of generators, the exit flue gas and hot water are at the same temperature. The hot combustion gas from an immersed combustion chamber is bubbling through a water bath. Keeping the combustion chamber surrounded by water minimizes the heat losses, and the need for the use of high temperature material. The main drawback, however is the low water temperature produced which is normally in the range of 40 to 50°C. Higher water temperature can be produced at the expense of the efficiency.

II. Counter-current / Co-current Hot Water Generators.

Heat transfer from a flame to a stream of water is achieved by direct gas firing into water. Design details of such units are still under development and details are generally unavailable. Rao and Mohtadi [1982] have developed a small unit that utilized a hydrocyclone to provide a combustion zone, followed by a co-current gas-water mixing zone. At higher outlet water temperatures, the thermal efficiency is low. This may be attributed to the nature of simultaneous heat and mass transfer involved. Heap [1992] has conducted extensive field trials with different types of counter-current hot water generators and found that both direct and indirect water heating were required for production of hot water at a temperature up 90°C.

One attractive application is a Dual Water Heater (DWH) which is a compromise between direct gas firing and submerged combustion chamber. Both sensible and latent heat are removed from the combustion products in this device. Indirect and direct water heating are both involved. The Natural Gas Technology Centre (NGTC) in Boucherville, Quebec, has been carrying out developmental research on water heating using direct gas firing. Their aim was to develop a Dual Water Heater (DWH) that can give a continuous supply of water at two temperatures; 60°C (sanitary hot water) and 85°C (heating or sterilization) with an overall efficiency of 95%.

Cold water is introduced at the top of a packed column. It contacts the upward flowing combustion products in the packed section. When it leaves the packing it flows over the combustion chamber for further heating. The heated water moves through a closed circuit heat exchanger where its heat is transferred to another fluid. The water is then re-circulated to the packed section. The hot saturated gas passes to a second packed tower, wherein it moves counter-currently to a descending fresh stream of water. The cooled gas passes to the atmosphere. The output hot water is slightly contaminated by combustion products (CO_2, NO and O_2). Standard Water Quality Tests have shown that the water can be used in the industrial applications such as loundries , tanneries, and dairy industry. However, it is not suitable for direct human consumption or for use in food products [Heap, 1992]. Comparison between available generators is show in Table (1.1).

The primary features that distinguish the DWH from other devices such as boilers, submerged combustion generators are:

1. The temperature of approach at the exit of the heater is less than 20 ° C
2. The latent heat in the flue gas is recovered.
3. The system is relatively compact.
4. Hot water is continuously produced at a temperature in the range of 60 to 90° C
5. The efficiency is about 98%
6. Only simple control of air-gas ratio is required.
7. Low emissions of CO, NO_x, and SO_2 and lower fuel consumption may eliminate the need for additional pollution control equipment. However, The hot water produced requires chemical and biochemical processing before it could be used for domestic purposes.

The main component of the Dual Water Heater is the direct contact packed tower, where simultaneous heat and mass transfer take place. To develop an efficient unit, one needs to determine the optimum heat transfer rates per unit volume. This determines the size and therefore the cost of the unit. Because there are few design techniques for predicting the performance of direct contact heat transfer, a systematic study is necessary to fully understand the transport phenomena involved and then a general reliable design method could be developed.

The objective of this study is to assist in the development of a technically viable system(DWH) that combines an immersed combustion chamber and a direct-contact heat transfer equipment. This includes the followings;

1. A general description of the processes involved.

2. A comprehensive review of the related literature, a discussion of the elementary principles of simultaneous heat and mass transfer, a formulation of the general governing equations and presentation of the simplified forms that have been used for the analysis of the system.

3. A general description of the heater including the measuring instruments used in collecting the experimental data.

4. An analysis of the effect of the following controlling parameters on the system performance, heat and mass transfer coefficients:

a. Gas and liquid flow rates

b. Amount of excess air.

c. Packing size and height.

Table (1.1) Comparison between available hot water generators.

Item	Duel Water Heaters	Conventional boilers	Direct Contact Hot Water Generators
Cost	Low	High	Low
Control system	Simple	Sophisticated	Simple
Water temperature	60- 90 °C	Steam as a secondary heating medium	Up to 60 °C
Design details	Under development	Totally available	Under development
Overall efficiency	above 95%	Up 80%	Below 95%

2.0 PROCESS DESCRIPTION

The dual water heater consists of two units. The first unit consists of an immersed firetube at the bottom with a packed tower at the top. The second unit is a second packed tower. A sketch of the main components of heater is shown in Fig(2.1). A detailed description is presented in Chapter (4). A description of the processes involved in each unit follows:

2.1 First Unit

Air and natural gas are fed to a burner. The hot gas from the burner port passes through a horizontal immersed firetube, and then is released under the packed section. Water sprayed at the top of the unit flows down through the packing , over the firetube and is collected as a hot water at the bottom. Hot water produced is circulated in a closed loop through a surface heat exchange where its heat is transferred to a clean water, to be used for domestic purposes, and then re-circulated to the top of the unit. The firetube is kept submerged in water to prevent the formation of vapor pockets which might cause the tube to overheat. For the purpose of the process description, the unit is divided into two sections; combustion section, and direct contact section.

2.1.1 Combustion Section

In the combustion section, the premixed air-gas mixture is burned inside the horizontal immersed tube. Gas analysis at standard condition [15°C, 101.325 kPa] is shown in Table(2.1). The average higher heating value is 37.6 MMJ/m^3 and the average specific gravity is 0.59. The combustion reactions of the gas with theoretical amount of air are as follows:

Basis: 1.00 mole of natural gas

$$0.956\ CH_4 + 1.912\ O_2 + 7.189\ N_2 \rightarrow 0.956\ CO_2 + 1.912\ H_2O + 7.189\ N_2 \quad (2.1)$$

$$0.021\ C_2H_6 + 0.0735\ O_2 + 0.2764\ N_2 \rightarrow 0.042\ CO_2 + 0.063\ H_2O + 0.2764\ N_2 \quad (2.2)$$

$$0.001\ C_3H_8 + 0.005\ O_2 + 0.0188\ N_2 \rightarrow 0.003\ CO_2 + 0.004\ H_2O + 0.0188\ N_2 \quad (2.3)$$

$$0.0005\ C_4H_{10} + 0.00325\ O_2 + 0.0122\ N_2 \rightarrow 0.002\ CO_2 + 0.0025\ H_2O + 0.0122\ N_2 \quad (2.4)$$

$$0.018\ N_2 \rightarrow 0.018\ N_2 \quad (2.5)$$

$$0.0035\ CO_2 \rightarrow 0.0035\ CO_2 \quad (2.6)$$

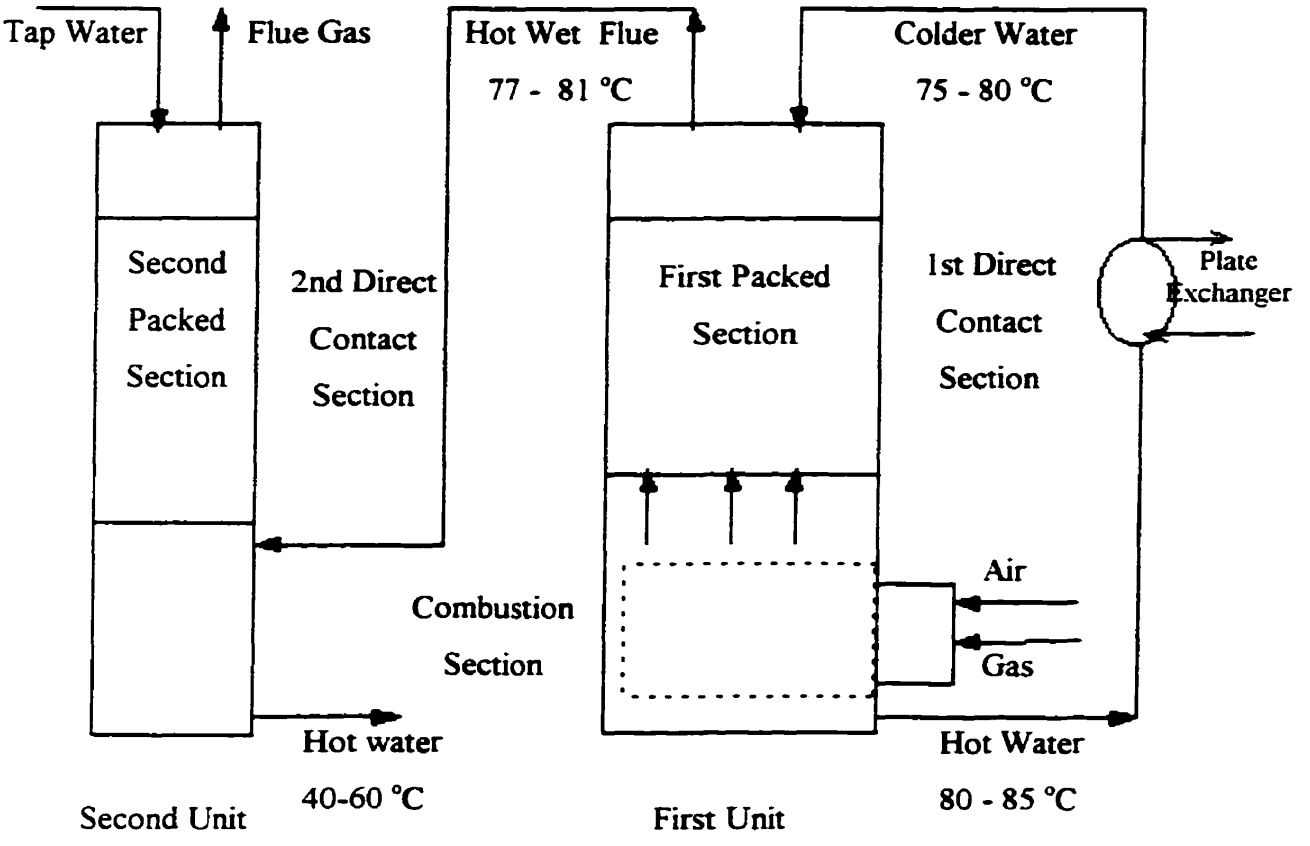

Fig(2.1): A sketch of the Dual Water Heater

Table (2.1): Typical input gas analysis at standard conditions

Component	Mol. %
CH_4	95.6
C_2H_6	2.10
C_3H_8	0.10
C_4H_{10}	0.05
N_2	1.80
CO_2	0.35
Total	100

Traces of CO, NO_x and hydrocarbons are sometimes found in the combustion products. The combustion products are partially cooled as they flow through the combustion tube, transferring their heat through the walls of the tube to the surrounding water. On the water side, heat is transferred by both conduction and convection. On the gas side, heat is transferred by radiation and convection. The amount of the combustion species changes as the level of excess air changes. The temperature of the flame and the mode of heat transfer on the gas side are also affected by the percentage excess air.

The design of the firetube is governed by heat transfer and pressure drop. The cooling of the combustion products is a function of tube size and length, as well as the properties and velocity of the gases. Rapid cooling of the combustion products to temperatures well below the adiabatic flame temperature must be prevented because this results in flame instability and formation of soot. Burners that accomplish complete combustion in short length are required for a stable and compact system

2.1.2 Direct Contact Section

The hot gases (800-1100°C) leaving the combustion section enter the bottom of the first packed section and exit from this packed section in the range of 1-3 °C above the inlet water temperature. Water normally enters the top of the section in the range of (75-80 °C) and leaves at (77-82°C). However, the inlet water temperature is fixed by the cold water temperature into the plate exchanger and its performance. The temperature of water leaving the first unit is normally in the range of (80-85°C). A small amount of fresh water is added periodically to replace the amount lost either by vaporization or entrainment.

As long as the water temperature is higher than the dew point of the combustion gases, the water will continue to evaporate and mix with the gases. Sensible heat is transferred through the interface to the bulk water. The total heat transferred equals the heat used to raise the temperature of the water and to vaporize the portion of it. As the hot gases travel through the section, they are humidified and cooled, while water is being heated. The wet-bulb temperature of the gas mixture and therefore the maximum allowable temperature of water produced in the direct contact section are increased as a consequence of the increased moisture content. The amount of heat transferred from the

combustion gases to the bulk water is proportional to the difference in enthalpy of the gases between the entering and the leaving conditions.

Quenching of the hot gases with water is very rapid. However, depending on contacting conditions and the geometry of the contacting system, there are three distinct posibilities:

I. The gases leave the unit unsaturated. They are being humidified and cooled. The total heat transferred, Q_t, includes the sensible heat transfer, Q_s, and the latent heat transfer, Q_v,

$$Q_t = Q_s + Q_v \tag{2.7}$$

The amount of heat transferred to the liquid, Q_L, is

$$Q_L = Q_s \tag{2.8}$$

Hence, the liquid temperature rise is less than that for the case of direct contact without mass transfer for the same conditions.

II. The gases reach saturation at some point in the direct contact section. After this point the water vapor in the gas condenses and mixes with the bulk water.

III. The temperature of water is lower than the dew point of the humidified gases. Water vapor can be removed from the unsaturated gases by direct contact with cold water. Water vapor condenses and mixes with the bulk water. The gases are cooled and dehumidified. Both sensible and latent heat are transferred to the water.

The inlet water temperature, the gas-air ratio, and the gas and liquid flow rates determine the exhaust gas temperature and consequently the thermal efficiency of the first unit of the heater. The outlet water temperature of the direct section is determined by the type and volume of the contacting tower.

2.2 Second Unit

The cooled and humidified gases in the temperature range of 75 to 81°C coming from the first unit, pass through the second unit where they rise counter-current to a descending stream of fresh water. The gases exit to the atmosphere in the temperature range of 10 to 20 °C above the water inlet temperature. The fresh water enters the top of the unit in the range of (20-25)°C in the summer time and in the range of (2-15)°C in the winter time. The hot water leaves the bottom at (45- 60)°C. This water is not re-circulated.

The temperature and humidity of the hot gases entering the second unit are greater than the temperature and humidity of the liquid-gas interface. Water vapor is removed from the gases by direct contact with cold water. As the gases travel along the unit, the water condenses, and mixes with the bulk water, while the gases are cooled and dehumidified. Both sensible and latent heat are transferred to the water.

$$Q_L = Q_t = Q_S + Q_v \qquad (2.9)$$

Hence, the liquid temperature rise is caused by both sensible and latent heat.

In addition to the transfer of heat, CO_2, CO, N_2, NO_x ,O_2 and hydrocarbons dissolve in the water along the direct contact sections of the heater. The rate of dissolution of these components depends on a number of factors such as mass transfer coefficients, temperatures, concentrations in each phase, the interfacial area and solubilities of the gases. The rate of dissolution of these gases in the unit is too small to affect the heat transfer process and can be neglected.

3.0 ELEMENTARY PRINCIPLES & LITERATURE REVIEW

3.1 Gas -liquid indirect heat transfer

Water heating by cooling a hot combustion gas in an immersed firetube involves the three modes of heat transfer ; conduction , convection , and radiation. The overall convective/conduction heat transfer coefficient can be approximated by,

$$\frac{1}{U_{con}} = \frac{1}{h_G} + \frac{x}{\gamma_{wall}} + \frac{1}{h_L} \tag{3.1}$$

The water-side heat transfer coefficient, h_L, is large compared to the gas-side coefficient. For a firetube with a thin wall, equation(3.1) simplifies to,

$$U_{con} \cong h_G \tag{3.2}$$

and hence the convective heat transfer is approximately,

$$Q_{con} = h_G \, \pi \, D \, l \, (t_G - t_L) \tag{3.3}$$

The convective heat transfer coefficient, h_G, for flow of gases inside tubes can be predicted by available correlations. In gas quenching by contact with cold wall, Gambill[1967] recommended the following equations for local Nusselt number for turbulent flow regime:

$$Nu = \frac{0.021(Re)^{0.8}(Pr)^{0.4}}{\left(t_{wall}/t_G\right)^{0.29-0.0019\left(\frac{L}{D}\right)}} \tag{3.4}$$

For turbulent flow of combustion gases ($(Pr)^{0.4} \cong 1.0$) inside a tube with L/D<60, Pritchard et.al[1977] recommended the following correlation:

$$Nu = 0.023(Re)^{0.8}[1 + (D/l)^{0.7}] \tag{3.5}$$

Pritchard et.al[1977] recommended that the heat transfer by radiation, Q_{rad}, be approximated by,

$$Q_{rad} = \sigma \, \pi \, D \, l \, (\varepsilon_G t_G^{\,4} - \zeta_{Gwall} t_w^{\,4}) \tfrac{1}{2} (\varepsilon_{wall} + 1) \tag{3.6}$$

In the case of non-luminous gases the effective emissivity, ε_G, is mainly made up of the emissivity of CO_2, and H_2O molecules. ζ_{Gwall} is the absorpance of gases at the wall temperature

The total heat transfer, Q_t, is

$$Q_t = Q_{conv} + Q_{rad} \tag{3.7}$$

A steady state heat balance on the gas in the tube element, l, is as follows:

$$G(H_{Go} - H_{Gl}) - h_G(\pi D l)(\overline{t_G} - \overline{t_{wall}}) - \frac{1}{2}(\sigma)(\pi D l)(\varepsilon_{wall} + 1)(\varepsilon_G \overline{t_G}^4 - \zeta_{Gwall} \overline{t_{wall}}^4) = 0 \qquad (3.8)$$

Where $\overline{t_G}$ and $\overline{t_{wall}}$ are the average gas and wall temperatures.

Since $\overline{t_{wall}} << \overline{t_G}$, the term $\zeta_{Gwall} \overline{t_{wall}}^4$ can be neglected,

$$G(H_{Go} - H_{Gl}) - h_G(\pi D l)(\overline{t_G} - \overline{t_{wall}}) - \frac{1}{2}(\sigma)(\pi D l)(\varepsilon_{wall} + 1)(\varepsilon_G \overline{t_G}^4) = 0 \qquad (3.9)$$

Equation(3.9) is an approximate relation to predict the gas temperature profile along the fire tube and is derived based on the following assumptions:

1. The wall temperature is considered uniform and very close to the outlet water temperature. The heat transfer from the tube wall to the water is enhanced by forced convection caused by water circulation around the tube and hence the liquid-side resistance to heat transfer is negligible.
2. The wall resistance to heat transfer is small. Scale formation, if any, is not considered.
3. Steady state, plug flow.
4. Radiant interchange along the tube is very small and neglected.
5. The convective heat transfer coefficient is constant over the tube length.

A reasonable agreement between experimental measurement and the results obtained using the use of equation(3.9) was reported by Pritchard et.al[1977]. He also applied the momentum equation to determine the pressure drop through the tube and consequently the flue height. In the dual water heater, the design pressure includes in addition the pressure drop through the direct contact section.

By assuming complete combustion at the tube entrance which implies the inlet gas temperature is equal the adiabatic flame temperature, equation(3.9)can be applied to estimate the gas temperature at the end of the tube. Since the change of water temperature is very small compared to the change of flue gas temperature, the logarithmic temperature difference at the tube ends can be used as the overall driving force temperature.

The overall heat transfer coefficient between water and the flue gases, U, is,

$$U = \frac{\bar{L}(H_{Lm} - H_{Lout})}{(\pi D l)(\Delta t)_{LM}} \tag{3.10}$$

The thermal efficiency of the firetube , η, is defined as,

$$\eta = \frac{\bar{L}(H_{Lm} - H_{Lout})}{GH_{Gin}}(100) \tag{3.11}$$

Investigators correlated the efficiency of immersed firetubes in terms of amount of excess air, tube length, rate of heat input, and tube diameter. For example, Patrick and Thornton[1958] recommended the following correlation:

$$\eta = 80.9 - 28.3 \exp(-0.02\, l / D) \tag{3.12}$$

3.2 Gas-liquid direct-contact heat and mass transfer

Direct contact heat transfer between water and the flue gases can be divided into two categories according to the direction of mass transfer; heat transfer with humidification(evaporation), and heat transfer with dehumidification(condensation).They have the following differences:

a. In humidification, the heat and mass move in opposite directions while in dehumidification they have the same direction (Fig(3.1a,b)).

b. The vapour enters the interface at the liquid temperature in case of evaporation while it enters the interface at the gas temperature in case of condensation.

c. The gas film is thicker in case of vaporization but thinner in case of condensation.

d. Condensation commences when the partial pressure of component A(water vapor) in the gas phase(P_{AG}) is higher than the partial pressure at the interface(P_{Ai})while evaporation commences when the partial pressure of component A(water vapor) at the interface is higher than the corresponding partial pressure in the gas phase.

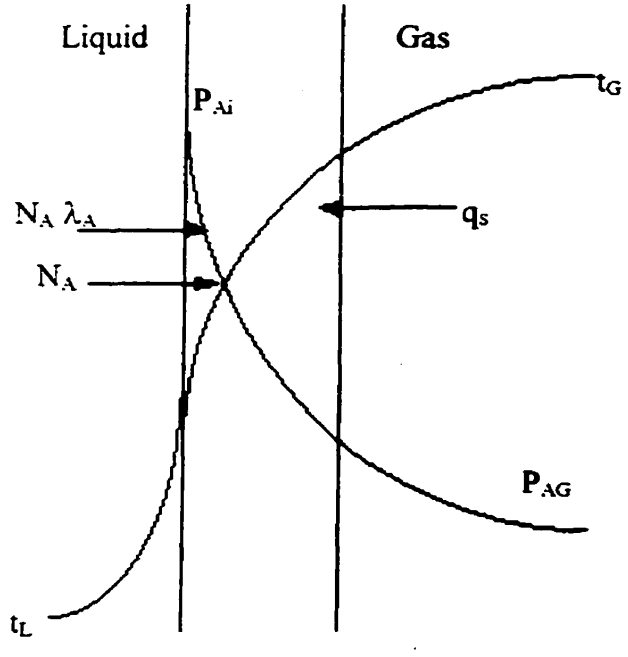

Fig(3.1a):Heat transfer with humidification

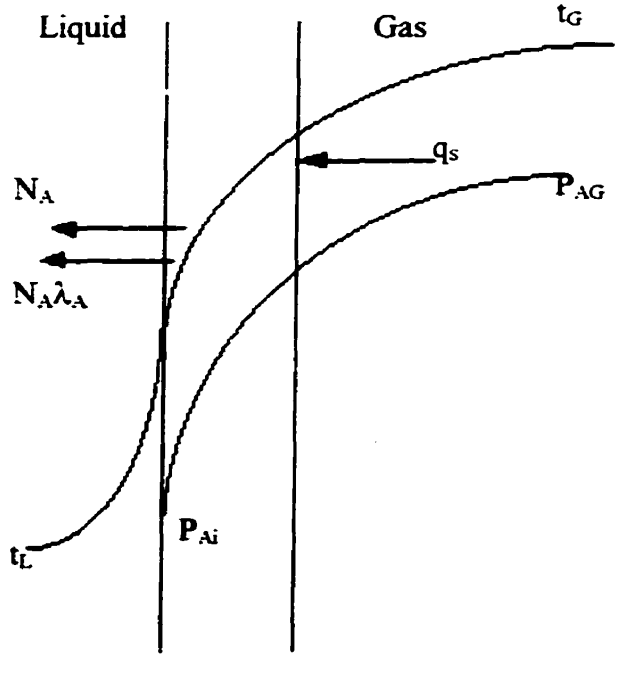

Fig(3.1b):Heat transfer with dehumidification

3.2.1 BASIC OF INTERPRETATION

Each direct contact section in the Dual Water Heater may be represented as shown in Fig. (3.2). Flue gas enters the bottom of the direct contact section at a temperature t_{G1}, a humidity Y_1' and an enthalpy H_{G1} . The flue gas leaves at the top of the column at a temperature t_{G2}, a humidity Y_2', and an enthalpy H_{G2}. Water enters at the top at a bulk temperature t_{L2} and an enthalpy H_{L2} and leaves at the bottom of the section at a temperature t_{L1} and an enthalpy H_{L1}. The mass velocity of the gas is G_S of vapor-free gas per hour per square unit of the column cross section. The mass velocities of the water at the outlet and inlet are, respectively, L_1 and L_2 per hour per square unit of the tower cross section.

The method of setting up the mass and energy balances will be undertaken with the following simplifying assumptions:

- The gas is insoluble in the liquid phase.
- Water as vapor or liquid is the only one component that is transferring between the phases.
- The process is adiabatic.
- Heat transfer by radiation is neglected.
- Heat and mass fluxes may transfer in any direction between the phases. The rate equations are written as if the transfer were from gas to the liquid.
- No mist is formed in the gas phase.
- The gas is ideal.

An overall mass balance over the column,

$$L_2 - L_1 = G_S(Y'_2 - Y'_1) \qquad (3.13a)$$

or in differential form, $$dL = G_S\, dY' \qquad (3.13b)$$

Similarly, an enthalpy balance is

$$L_2H_{L2} + G_SH_{G1} = L_1H_{L1} + G_SH_{G2} \qquad (3.14a)$$

or in differential form, $$G_S dH_G = d(LH_L) \qquad (3.14b)$$

The above equations can be applied at any point along the column.

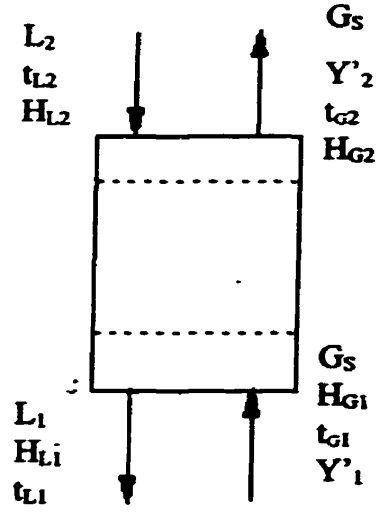

Fig(3.2): Direct contact section

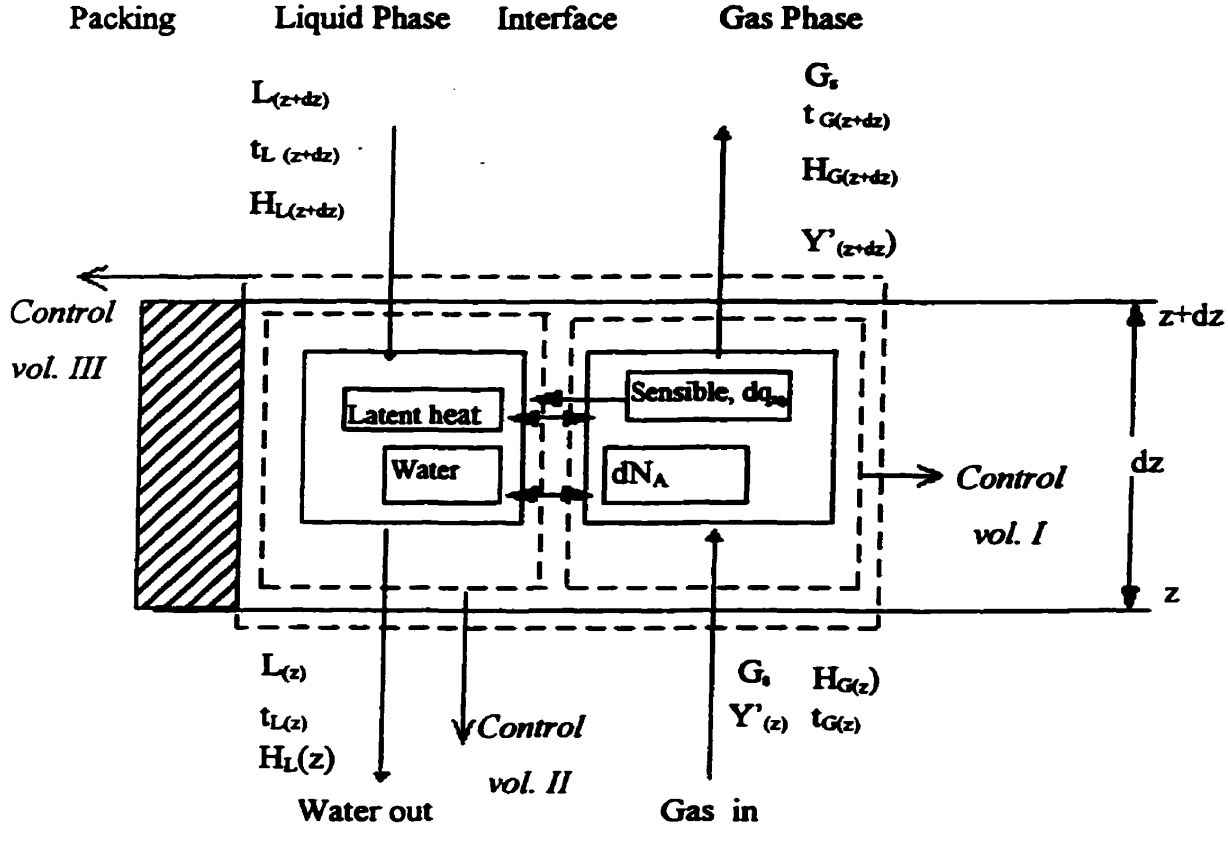

Fig (3.3) : Differential section of a packed column

Consider a differential height, dZ, across the contacting column as shown in Figure(3.3), which that shows the differential section of the contacting column is split in three control volumes I, II, and III to set up the heat and mass balance equations.

The mass and heat transfer rates are:

Mass transfer rate of component A(i.e.water vapor) per square unit of tower cross section is , [Treybal, 1968],

$$dN_A = F_G \ln\left(\frac{1-\frac{P_{Ai}}{P_t}}{1-\frac{P_{AG}}{P_t}}\right) a_M dZ = -G_S dY' \qquad (3.15)$$

or approximately,

$$dN_A \cong k_G(P_{AG} - P_{Ai})a_M dZ \cong k_Y(Y'_{AG} - Y'_{Ai})a_M dZ \qquad (3.15b)$$

The sensible heat of gas per square unit of tower cross section, is

$$dq_{SG} = h_G a_H (t_G - t_i)dZ \qquad (3.16)$$

While heat transfer in liquid phase per square unit of tower section is,

$$dq_{SL} = h_L a_H (t_i - t_L)dZ \qquad (3.17)$$

The total differential change of the enthalpy of liquid phase can be defined as:

$$d(LH_L) = LC_L dt_L + C_L(t_L - t_o)dL \qquad (3.18)$$

The specific gas enthalpy is,

$$H_G = C_S(t_G - t_o) + \lambda_o Y' \qquad (3.19)$$

The total differential change of the enthalpy of gas phase can be defined as:

$$G_S dH_G = G_S C_S dtG + G_S C_{AV} t_G dY' - G_S C_{AV} t_o dY' + G_S \lambda_o dY' \qquad (3.20a)$$

or approximately,

$$G_S dH_G = G_S C_S dtG + G_S \lambda_o dY' \qquad (3.20b)$$

By conducting mass and enthalpy balances based on the control volumes sketched in Figure (3.3), the following governing equations can be easily obtained.

Control volume I

$$-G_S C_S dt_G = h_G a_H (t_G - t_i)dZ \qquad (3.21)$$

Control volume II

$$LC_L dt_L = [G_S C_{AL} dY' - h_L a_H dZ](t_i - t_L) \quad (3.22a)$$

Or approximately,

$$LC_L dt_L = h_L a_H (t_i - t_L) dZ \quad (3.22b)$$

Control volume 3

$$LC_L dt_L = G_S \{C_S dt_G + [C_{AV}(t_G - t_o) - C_{AL}(t_L - t_o) + \lambda_o] dY'\} \quad (3.23a)$$

or approximately,

$$LC_L dt_L = G_S C_S dt_G + \lambda_o dY' \quad (3.23b)$$

If the heat and mass transfer coefficients are available, equations (3.15), (3.22), and (3.23) can be numerically integrated. Extensive trial and error is required. The design of a direct gas -liquid contactor based in the general relations presented above can be performed efficiently when a computer is available. Laso and Bomio[1993] developed a computer model to simulate heat and mass transfer in packed columns. They used the heat - mass analogy, with corrections for high heat and mass fluxes, for prediction of mass and heat transfer coefficients. When they compared their model with experimental data obtained for columns operating close to the boiling point of water they found a good agreement. The application of the model for design purposes still requires the knowledge of the characteristics of the column internals such as; heat and mass transfer coefficients and the wetting area.

3.2.2 Combination of heat transfer coefficients

The method of combining gas and liquid heat transfer coefficients into the overall heat transfer coefficient Ua depends on whether there is significant condensation or vaporization accompanying the sensible cooling of the gas. According to the design summary provided by Fair[1961], the overall heat transfer coefficient can be described by the following equations:

For sensible gas cooling with coolant vaporization,

$$1/Ua = [1/\alpha\, h_G a] + [1/h_L a]\,[Q_L/Q_t] \quad (3.24)$$

and for sensible gas cooling with coolant partial condensation,

$$1/Ua = [1/h_L a] + [1/\alpha h_G a]\,[Q_V/Q_t] \quad (3.25)$$

Where α is called Ackermann correction factor[Ackermann 1937]. It accounts for the effect of mass transfer on the heat transfer. Fair in his summary, provided a graph from which the value of α can be directly read for a given value of mass transfer rate per unit volume.

The total volume required to accomplish the desired heat transfer, Q_t, can be obtained by integrating the following equation, [Chilton and Colburn 1934]

$$V_T = \int_0^{Q_t} \frac{dQ}{Ua(t_G - t_L)} \tag{3.26}$$

The difficulty of integrating the above equation arises due to :

a. The driving force (temperature difference, t_G-t_L , is not constant over the whole contacting device.

b. The heat transfer coefficients are not constant thoughout the contacting system.

In the direct contact section of the first unit, flue gas is quenched quickly from temperature t_{G1} to a temperature t_{G2} while the liquid water is heated from temperature t_{L1} to a temperature t_{L2} . The overall heat transfer can be determined from an experimental data by the following approximation,

$$Ua \cong \frac{Q_t}{V_T(\Delta t)_{lm}} \tag{3.27a}$$

If the change of water temperature is small, The heat transfer coefficient in the gas phase can be obtained by integration of equation(3.21),

$$h_G a = \frac{G_s C_s}{Z} \ln\left[\frac{t_{G2} - t_L}{t_{G1} - t_L}\right] \tag{3.27b}$$

3.2.3 Determination of Heat and Mass Transfer Coefficients

Phase mass - heat transfer coefficients are needed for sizing the gas -liquid direct contactors. The methods of obtaining the transfer coefficients include, constant water temperature or wet-bulb temperature runs; the graphical methods; the mass-heat transfer analogy approach; the overall enthalpy driving potentials method and the experimental correlations. They will be discussed in details in the following sections.

3.2.3.1 Wet-bulb temperature method.

This method requires two experimental runs; the first run has to be conducted at constant liquid temperature throughout the apparatus. It leads to equality of the liquid temperature and the interface temperature. The heat transfer resistance in the liquid phase is eliminated. Such an operation affords an opportunity to obtain the interfacial temperatures and humidities, and then equations (3.15), and (3.21) can be integrated directly and the values of mass and heat transfer coefficients in the gas phase can be obtained.

In the other run , the liquid temperature varies. Runs have to be made with the same gas and water flow rates in the same apparatus. Using the values of gas phase mass and heat transfer coefficients obtained at constant liquid temperature run(assumed to be applicable), the liquid heat transfer coefficients can be calculated by solution of equations (3.21) and (3.22).

The method requires the experimental measurement of small driving forces. McAdams et.al[1949] and Yoshida & Tanaka[1952]used this method to determine the heat transfer performance of packed columns for air-water system with low water concentration operating under humidification, dehumidification and water cooling.

3.2.3.2 Mass -heat transfer analogy

Because there is no relation between the conditions at the interface and in the bulk gas, direct integration of the governing equation is not possible in absence of the transfer coefficients. One approach is to lump the driving forces for heat and mass transfer in a single driving force. An addition relationship between the heat and mass transfer coefficients is required. The analogy of heat and mass transfer determines the relation between the two coefficients. For air-water mixture, the ratio of heat transfer coefficient to mass transfer was found to approximately equal the humid heat of the mixture,

$$\frac{h_G}{k_G} = C_s \qquad (3.28)$$

Equation(3.28) is called the Lewis relation and is applicable for low concentration of water vapor in air provided the area of heat and mass transfer are the same. Substitution of Lewis relation in the governing equations simplifies the calculation by expressing the

driving forces in terms of enthalpy instead of temperature and humidities. The method has been known in the literature as a total heat method and has been applied successfully to the design of cooling towers.

For systems other than air-water or when there are high mass and heat fluxes, the Lewis relation may be written as,

$$\frac{h_G}{k_G P_{BM}}\left[\frac{a_H}{a_M}\right] = C_p(Le)^{2/3} \qquad (3.29)$$

Another approach to utilize the heat and mass transfer analogy is to use the available correlations for mass transfer coefficients to obtain the corresponding heat transfer coefficients or vise versa. Huang and Fair[1989] used the correlation presented by Bravo and Fair[1982] for calculation of the effective area for mass transfer, together with the models of Onda et.al [1968] to determine the individual phase mass transfer coefficients for air-water system in a packed column. When they compared the measured heat and mass transfer coefficients and the predicted values obtained from the analogy they found the analogy holds reasonably well. Additional confirmation has been provided by Fair [1990], who utilized this approach to design a hot gas recovery system.

Recently, Bohn and Swanson [1991] measured the heat transfer coefficient for nitrate salt-air system at elevated temperatures in 150 mm packed column filled with 610 mm bed of Pall rings. They found that the system behaved as a simple heat exchanger with exchange effectiveness of unity. Using the mass transfer model of Onda et.al[1968] and mass-heat transfer analogy, they determined the connective heat transfer coefficient at the liquid/gas interface. At the gas/dry packing interface they used the correlation of Witaker[1972]. When they compared the film coefficients predicted by these two correlations, they found that the dry gas film coefficients were about three times larger than the gas-liquid heat transfer coefficients and the overall heat transfer was affected by 1-2%. However, this effect will depend on the unwetted area fraction. As the unwetted area fraction increases the rate of heat transfer increases and probably the rate of mass transfer decreases and hence the mass heat transfer analogy approach is not applicable. This may explain why the experimental values of mass transfer coefficients were found to be less than the predicted values by the use of heat - mass transfer analogy.

3.2.3.3 Graphical Methods

Simplified graphical or numerical design methods are attractive and they give a clear explanation of the principal variables that affect both the heat and mass processes and the system design, provided the simplifications involved have a minor effect. A graphical procedure based on the enthalpy-temperature diagram was developed by Mickley[1949] to evaluate the heat transfer performance in direct contact heat transfer equipment. It incorporates the determination of the liquid -side heat transfer coefficient form a single experimental test. The experimental determinations of heat and mass transfer coefficients require extreme precision of the measurement of the final gas temperature and humidity. Trial and error is involved. The method is applicable for air-water system with low mass fluxes .

For systems other than air-water for which equation(2.28) does not hold, Lewis and White [1953] proposed a graphical design method by the use of a modified enthalpy concept instead of the true enthalpy. They used a modified form of the Lewis relation,

$$\frac{h_G}{K_Y} = f b C_s \qquad (3.30)$$

Where b is a constant and equal the Lewis number for the system under consideration and f is the ratio of the heat transfer area to the mass transfer area. They used a modified Latent heat of vaporization, λ', defined as,

$$\lambda' = \frac{\lambda}{f\,b} \qquad (3.31)$$

They defined the modified enthalpy of a gas as,

$$H_G' = C_S(t_G - t_o) + Y'\lambda' \qquad (3.32)$$

If heat and mass transfer coefficients are known , the design procedure is similar to Mickely's method. The steps are based on the modified enthalpy instead of the gas enthalpy. The authors claimed that the method could be used for the determination of heat and mass transfer coefficients from an experimental run however, extensive trial and error are required because a construction of the modified enthalpy-temperature diagram in addition to the true enthalpy- temperature diagram is included in the trial and error calculations. The method is applicable only for dilute gas - vapor mixtures for which the

humidity can be used as the mass transfer driving force and the Lewis number may be considered constant.

Gribb and Nelson[1956] modified Mickley's method to apply to moist coal gas-water system. Instead of using the enthalpy, they used the enthalpy transfer potential, θ_G, defined as,

$$\theta_G = C_S(t_G - t_o) + \lambda \omega_G Y' \tag{3.33}$$

Where:

$$\omega_G = \ln\left(1 + \frac{P_{AG}}{P_t - P_{AG}}\right) / \frac{P_{AG}}{P_t - P_{AG}} \tag{3.34}$$

ω_G accounts for using the humidity as a driving force for high mass fluxes.

The method requires a construction of two charts , i.e. the temperature - enthalpy and the temperature - humidity charts. The method can be used only if the individual coefficients are known.

3.2.3.4 Overall - driving potential method

This method is based on the assumption that all the resistance to heat transfer lies within the gas phase and that the temperature at the interface is equal to the temperature of the bulk of the liquid. In direct water heaters, this is a reasonable assumption since the heat transfer coefficient for water is much higher than the corresponding value for gas. With the use of mass heat transfer analogy, the driving forces can be expressed in terms of overall enthalpy driving force. The overall enthalpy driving force is the difference between the specific gas enthalpy at the bulk gas temperature, H_G, and the specific enthalpy of the saturated gas at the corresponding liquid temperature, $H_{w,}$. The transfer coefficient corresponding to this driving force is called the overall enthalpy transfer coefficient and has the practical advantage of being easily measured. For small heat and mass fluxes, the following equation can be easily derived. See [Nemunitias &Eckert, 1975],

$$K_Y a = \frac{G_S}{Z}\int_1^2 \frac{dH_G}{(H_w - H_G) + \overline{C}_S(t_L - t_o)(Le - 1)} = \frac{\overline{L}C_L}{Z}\int_1^2 \frac{dt_L}{(H_w - H_G) + \overline{C}_S(t_L - t_o)(Le - 1)} \tag{3.35}$$

If Lewis relation holds, this equation reduces to a simpler form,

$$K_Y a = \frac{G_S}{Z}\int_1^2 \frac{dH_G}{(H_w - H_G)} = \frac{\bar{L}C_L}{Z}\int_1^2 \frac{dT_L}{(H_w - H_G)} \qquad (3.36)$$

In the case of high mass fluxes, Carey and Williamson[1950] have shown that the overall enthalpy potential method can be used if a correction is introduced for the variation of the partial pressure of the inert gas in the gas -vapor mixture. The method is extended to apply for determination of the transfer coefficients in the dehumidification section of the direct water heater. The formulation of the rate equations is briefly presented in the following paragraphs. More details can be found in the original paper of Carey and Williamson[1950].

The method is based the following assumptions:

1. Since the heat transfer coefficient for water is much higher than the corresponding value for gas, only the gas transfer coefficient needs to be considered. This leads to equating the temperature and humidity at the interface conditions to that at the bulk liquid conditions.

2. The heat transfer area and mass transfer area are the same. This is function of liquid flow rate and liquid distribution used especially in packed towers.

3. Since the sensible heat transferred is a small fraction of the amount of latent heat transferred, the Lewis relation can be approximated by,

$$\frac{h_G a}{k_G a P_{BM}} = \frac{C_P'}{\rho_{ns}} \qquad (3.37)$$

4. The heat and mass transfer coefficient are constant throughout the contacting unit.

The heat and mass transfer rate equations are:

The rate of mass transfer of water vapor(A),

$$V_n \rho_{ns} dS_{rG} = K_G a \times (P_G - P_w) A dZ \qquad (3.38)$$

Where,

Cp': volumetric specific heat of gas-vapor mixture.

V_n : Volumetric flow rate of the dry flue gas at normal conditions (0°C, 101.325 kPa)

ρ_{ns} : Normal density of the steam

S_{rG}: volume of steam/volume of dry gas at t_G.

P_w : Partial pressure of water vapor at liquid temperature, t_L,

P_G : Partial pressure of water vapor at gas temperature, t_G,

K_G : Overall mass transfer coefficient based on partial pressure difference as a driving force.

The partial pressures of water vapor are related to the steam ratio, S_r, by

$$P_G = P_t \times \frac{S_{rG}}{1+S_{rG}} \tag{3.39a}$$

and

$$P_w = P_t \times \frac{S_{rw}}{1+S_{rw}} \tag{3.39b}$$

where S_{rw} is the steam ratio at water temperature.

Expressing the water vapor transfer equation in terms of steam ratio yields,

$$V_n \rho_{ns} ds_{rG} = K_G a \times P_t \times \left(\frac{S_{rG}}{1+S_{rG}} - \frac{S_{rw}}{1+S_{rw}} \right) \times AdZ \tag{3.40}$$

The sensible heat transfer rate is,

$$V_n C_P'(1+S_{rG})dt_G = h_G a(t_G - t_L)AdZ \tag{3.41}$$

Substitution of equation(3.37) into equation(3.41),

$$V_n C_p'(1+S_{rG})dt_G = \frac{K_G a A P_{BM}}{\rho_{ns}}(C_p' t_G - C_p' t_L)dZ \tag{3.42}$$

The sum of equation(3.42) and equation(3.40) multiplied by the latent heat of water gives the total heat transfer rate equation,

$$V_n[\lambda \rho_{ns} dS_{rG} + C_p'(1+S_{rG})]dt_G = \frac{K_G a P_t}{\rho_{ns}} \times \left[\frac{H_G'}{1+S_{rG}} - \frac{H_w'}{1+S_{rw}} \right] AdZ \tag{3.43}$$

With the assumption of no liquid resistance to the heat transfer, the heat transferred from the gas must equal the heat gained by water,

$$\frac{K_G a P_t}{\rho_{ns}} \times \left[\frac{H_G'}{1+S_{rG}} - \frac{H_w'}{1+S_{rw}} \right] dZ = \bar{L} dt_L \tag{3.44}$$

where H_G' and H_w' are the exact enthalpy of gas-vapor mixture per unit normal volume of dry gas at gas and water temperatures.

Equation(3.44) can be integrated over the whole unit to give the overall transfer equation,

$$\bar{L} \times (t_{L2} - t_{L1}) = \frac{K_G a P_t}{\rho_{ns}} \times Z \left(\frac{H_G'}{1 + S_{rG}} - \frac{H_w'}{1 + S_{rW}} \right)_{mean} \qquad (3.45)$$

Carey and Williamson[1950] have devised charts to permit the rapid calculation of the mean driving force if values of the driving force are obtained at the terminal conditions and the central point of the operating range. The driving force profile over the tower was approximated to a parabola. By the use of equation (3.45), the value of $K_G a$, can be experimentally estimated.

For convenience, the results can presented in terms of the Height of Transfer Unit, HTU, defined as ,

$$HTU = \frac{V_n \times \rho_{nG}}{K_G a P_{BM}} \qquad (3.46a)$$

Where,

ρ_G : Normal density of dry flue gas.

The height of heat transfer unit is defined as,

$$\text{Height of heat transfer unit} = \frac{V_n \times \rho_{nG} C_p}{h_G a} = \frac{G_s C_s}{h_G a} \qquad (3.46b)$$

The number of transfer unit, NTU, is related to the height of transfer unit as,

$$NTU = \frac{Z}{HTU} \qquad (3.47)$$

The transfer unit concept offers the characteristic of a contacting device to be expressed as a dimenisonless number or as a unit of length.

3.2.3.5 Experimental correlations

Experimental data for heat transfer and mass transfer coefficients are usually correlated by the general form,

$$\text{Coefficient} = \text{Constant } (G)^m (L)^n$$

Where m, n are empirical constants. The Constant values in all the following experimental correlations in this section are based on the lb.ft.hr units.

McAdams et.al [1949] and Yoshida and Tanaka [1951] found the resistance of the liquid film to enthalpy transfer for air-water system in a packed tower to be 27-46% of the total resistance of both phases. McAdams et.al [1949] used a 102 mm diameter tower packed with 25.4 mm carbon Raschig rings. The heat transfer coefficient in the gas phase was determined by operating the tower at constant water temperature(wet bulb method) and was correlated by,

$$(h_G a)_{t_f} = 1..78(G_s)^{0.7}(L)^{0.07}e^{0.0023t_f} \qquad (3.48)$$

For values of air flow rate, G, ranging from 1690 to 5000 (kg.dry air)/(hr)(m^2) and the liquid flow rates, L, from 2450 to 12,700 (kg.)/(hr)(m^2). The gas film temperature t_f ranged from 46 to 96 °C.

The liquid heat transfer coefficient in the same apparatus at the same gas and liquid loading when operated as a cooling tower was correlated by the following equation,

$$h_L a = 0.82(G_s)^{0.7}(L)^{0.5} \qquad (3.49)$$

Yoshida and Tanaka [1951] used a 254 mm diameter column , randomly packed with 15, 25, or 35 mm ceramic Rasching rings, to a depth of 318 mm. They studied the heat and mass transfer between air and water under three modes of operations; constant water temperature humidification, water cooling, and dehumidification. The air flow rate ranged from 700 to 2900 (kg.dry air)/(hr)(m^2) and the liquid water rates ranged from 970 to 20,300 (kg.)/(hr)(m^2). The results were correlated by following equations:

$$h_G a = 0.117(G_s)(L)^{0.2} \qquad (3.50)$$

$$h_L a = 8.0(L)^{0.8} \qquad (3.51)$$

$$k_Y a = 0.45(G_s)(L)^{0.2} \qquad (3.52)$$

Where k_Y is the gas -film mass transfer coefficient based on humidity as driving force.

Inspection of the above correlations shows that the gas heat transfer coefficient may be under-estimated while the liquid heat transfer coefficient may be over-estimated. This might be because of the following reasons:

a. The wall effects might have a considerable effect because of low tower to packing diameter.

b. The effective transfer area may not be the same for different modes of operation.

c. The heat transfer area does not equal the mass transfer area.

Similar work was reported by Hensel and Treybal [1952] over a wide range of air and water flow rates. They used a square tower (546 mm " on the side) packed with 38.1 mm. Berl saddles. By utilizing the wet bulb method they confirmed that the gas heat and mass transfer coefficients were exponentially proportional to the liquid and gas flow rates.

Huang and Fair[1989] studied the heat and mass transfer between air and water in a 0.305-m square cooling tower, packed with different types of packing to a depth of 0.305 m. The air flow rate ranged from 1940 to 5900 (kg.dry air)/(hr)(m^2) and the water rates ranged from 2840 to 19,550 (kg)/(hr)(m^2). They used Mickley's method to determine the heat and mass transfer coefficients. For 25.4 mm Pall rings, the results were correlated by the following equations:

$$h_G a = 0.019(G_s)^{1.12}(L)^{0.33} \tag{3.53}$$

$$h_L a = 0.296(G_s)^{0.45}(L)^{0.87} \tag{3.54}$$

$$k_G a = 0.073(G_s)^{1.12}(L)^{0.33} \tag{3.55}$$

Different constants and exponents were obtained for other types of packing.

In gas cooling operations, Parekh [1942] studied the cooling of hot air at atmospheric pressure by water in a column packed with Raschig rings. The results were correlated as follows,

$$Z = m\frac{H_{G2} - H_{G1}}{(H_G - H_{w)_{LM}}}\sqrt{\frac{G}{L}} \tag{3.56}$$

Where:

m = 1.4 for 25.4-mm

= 1.7 for 38.1-mm

= 2.1 for 50.8-mm

H_G = Specific enthalpy of gas, Btu/lb

Zhavoronkov and Furmer[1944] studied the heat and mass transfer between hot, dry air and water in a 300mm diameter tower, packed with Raschig rings of several sizes. The height of the packing was 1.0 m. The air flow rate ranged from 600 to 2340 (kg.dry

air)/(hr)(m^2) and the water rates ranged from 3500 to 25,000 (kg)/(hr)(m^2). They correlated the heat transfer coefficient by the following equation:

$$h_G a = 0.0201(G_s)^{0.7}(L)^{0.7} \quad (3.57)$$

Nemunaitias and Eckert [1975] measured the overall heat transfer coefficients for air-water system in a 762 mm diameter packed tower operating under humidification and dehumidification conditions. The packing employed were 50.8 mm polypropylene Pall rings and 50.8 mm porcelain Intalox saddles with a bed height of 0.91 m. Liquid and gas rates were varied from 2400 to 24,400 (kg.)/(hr)(m^2), and 2450 to 14,650 (kg.)/(hr)(m^2) respectively. The overall heat transfer coefficient was correlated by the following equations:

For 50.8-mm Pall rings, Humidification:

$$Ua = 0.0279(G)^{0.57}(L)^{806} \quad (3.58)$$

For 50.8-mm Pall Rings, Dehumidification:

$$Ua = 4.0 \times 10^{-5}(H_s)^{0.608}(G)(L)^{0.684}(0.075/\rho_G)^{0.5} \quad (3.59)$$

Where: H_s= Inlet gas enthalpy, Btu/mole of dry gas

Comparison between these equations for the same systems(air-water), shows large discrepancies in determining heat and mass transfer coefficients. Possible explanations for the discrepancies include experimental errors which can be very large because of close approach temperatures at the top of the column. Another possible explanation is that the area for heat transfer is not the same as that for mass transfer. Hence the correlations for heat and mass transfer may good for the system tested and can not be used for other systems and conditions. Most of previous experimental work has dealt only with cases for which the heat and mass fluxes are low. It is apparent that there is a need for more experimental data covering cases that involve high mass and heat fluxes.

3.3 Hydraulic parameters

In designing direct contact heaters the hydraulic parameters are usually considered first. The diameter of the contactor is determined based on the approach to the flooding and the allowable pressure drop. A simplified design procedure is available in Coker[1991].

3.3.1 Flooding

For columns containing random packing such as Raschig rings, Pall rings, and saddles, the method of Eckert [1970] is often used.

3.3.2 Pressure drop

The pressure drop through the packing is a function of a function of the gas and liquid flow rates. For random packings, empirical methods given by Eckert[1970] and Mersmann & Deixler[1986] are convenient.

4.0 EXPERIMENTAL APPARATUS AND PROCEDURE

4.1 General

Experimental work was conducted on the prototype Dual Water Heater at the Laboratory of the Natural Gas Technology Center (NGTC). A schematic diagram of the experimental set-up is shown in Fig(4.1). The heater consists of two rectangular units each 2-m high. The first unit has a cross section of 610 mm × 1829 mm and is divided into two parts. The lower part houses an immersion firetube and the upper part contains a water distributor and a packed section. The second unit (457 mm × 762 mm) includes water spray nozzles and a packed section. The material of the walls of both units is 304 stainless steel. The heater is provided with a rectangular base that houses an air blower, two water pumps, control trains for gas and air, and a control cabinet.

4.2 Description of The Prototype DWH

4.2.1 First unit

4.2.1.1 Lower Part.

The lower part houses the combustion chamber which is a submerged horizontal tube. A gas burner with its discharge sleeve fitted to the tube was mounted tangentially to the wall of the unit. The mouth of the tube was equipped with a vertical gas distributor by which the flow of the combustion products was divided into two streams. A shield with a steep angle was provided to prevent water entering through the tube. The burner was equipped with pressure and flow control valves to control the gas rate and a butterfly valve to regulate the air-gas ratio. Design details of the combustion chamber are the confidential property of the NGTC.

A 15-hp. centrifugal water pump was used to recirculate the water through the unit. A plate heat exchanger was used to simulate the heating demand. The water flow rate was controlled so that the combustion chamber was always kept immersed in the water.

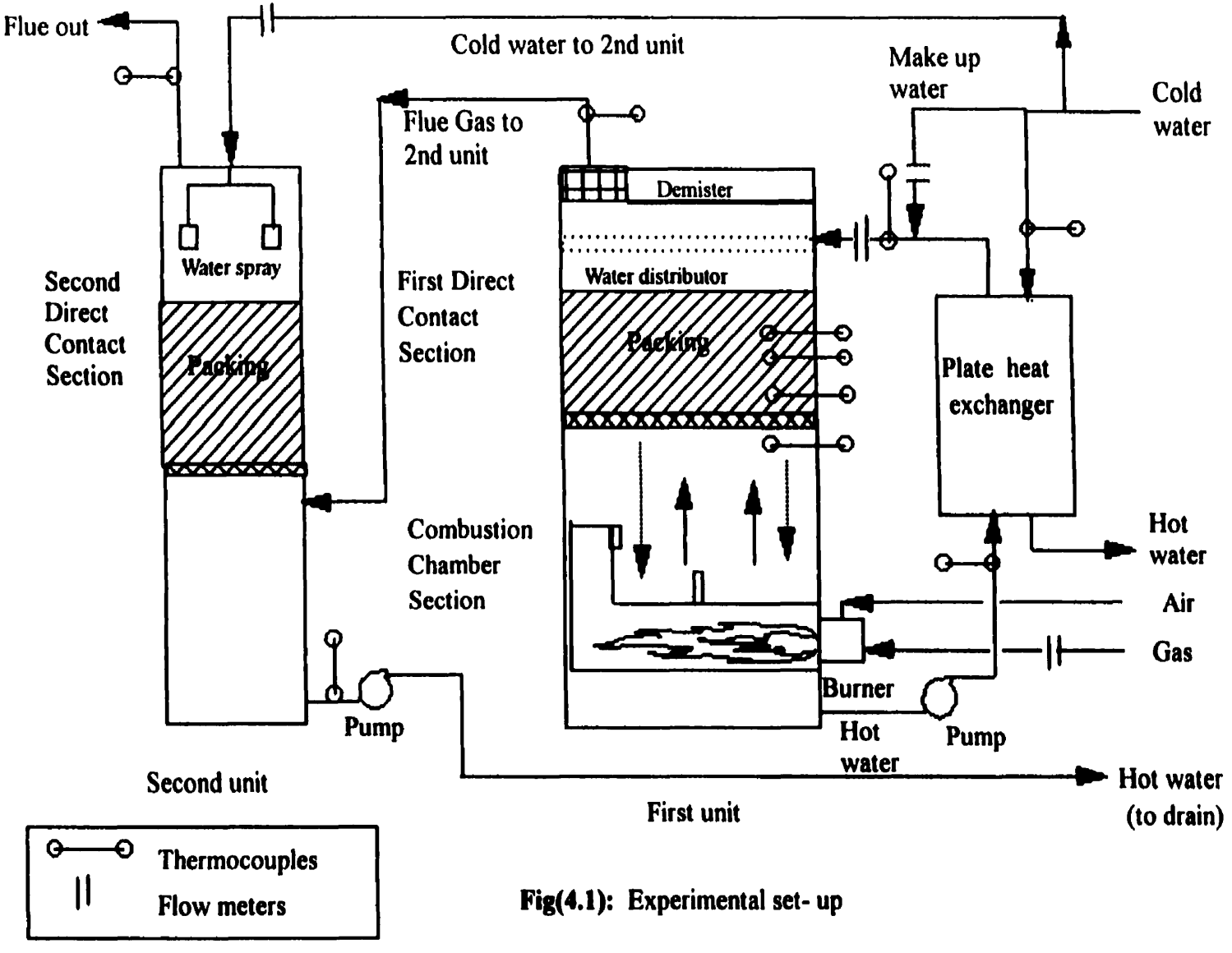

Fig(4.1): Experimental set- up

The water level around the combustion chamber was maintained constant at about 737 mm(± 50) by periodic additions of water. A level sensor was provided to actuate the make up control valve. The main features of this section are as follows:

a. Gas burner specifications:

Burner type	Maxon-Ovenpak, EB version
Gas flow rate	up to 85 m^3/hr (under normal conditions)
Maximum Capacity	879 kW (based on the higher heating value)
Turndown ratio	1:10

b. Air blower specifications:

Blower type	External, fan, The New York Blower Company
Power	5 hp
Air flow rate	up to 1500 m^3/hr (under normal conditions)
Pressure	104.663 kPa

c. Firetube specifications:

Diameter	≈0.5 m
Length	≈1.8 m
Thickness	≈4.0 mm

The gas/air ratio is controlled via an actuating valve installed on the gas line. At any given air flow rate, the valve actuates the gas control valve to adjust the gas flow rate so that the pressure drop in both gas and air leading lines are equal. The air flow rate is set based on the flue gas analysis.

4.2.1.2 Upper Part

This part forms the first direct contact section in the heater. It consisted of 457 mm of packing , 254 mm of spray above the packing , and 330 mm space for droplets below a perforated support plate. Water was introduced at the top through a distribution manifold. The water distributor was a 102 mm. diameter pipe with 80 holes each approximately 10 mm, in the bottom. Flue gas leaving the fire tube below the support plate traveled upward through the packing where were directly contacted with the water flowing downward.

A zig-zag and V-notch demistors were installed at the top to catch water droplets carried by the flue gases leaving the unit.

4.2.2 Second unit.

This unit forms the second direct contact section in the heater. Tap water was delivered to spray nozzles at the top of this unit. The water flow rate was controlled by a valve and a flow meter. The water travelled through a packed bed and then to a storage zone at the bottom of the unit. A 3-hp centrifugal water pump was installed at the bottom. The pump was used to simulate the hot water demand. The water level at the bottom of the unit was kept constant to approximately 508 mm(±75mm). The flue gases from the first unit were passed through a 254 mm interconnecting pipe to the second unit where they were fed below a support plate through a 152 mm nozzle. The gases were directly contacted the water in the packed bed and then discharged out of the unit. The total height available for the packing was 762 mm. The characteristic of the water distributor used is as follows:

Type	(2) Square spray nozzles (Full cone) supplied by Fulljet.
Size	10 mm
Angle of spray	80°
Spray distance	254-305 mm
Coverage	432-508 mm each.

4.3 Instrumentation

4.3.1 Flow Rate measurements:

The fuel gas flow rate was measured using an in-line mass flow meter supplied by Sierra. An orifice plate was installed in the air line to measure and control the air flow rate. The pressure drop through the orifice was measured by a U-tube manometer. The gas flow rate was controlled through the control panel to keep the outlet water temperature of the first unit to a pre-set value. The water flow rate to the second unit was adjusted automatically by the control panel in order to keep the outlet water temperature at a set value. The inlet water flow rate to each unit was measured by a magnetic inductive flow

meter supplied by Krohne. A rotameter was installed on the make up water line . Gas and water flow meters were calibrated by the manufacture with an accuracy of ± 1.0% .

4.3.2 Temperature measurements:

Inlet water temperature was measured by T-type thermocouples inserted just before the distributor manifolds. Outlet water temperature was measured using T-type thermocouples inserted in water outlet lines. A K-type thermocouple was inserted in the outlet nozzle of the firetube to measure the inlet temperature of the combustion products to the direct contact section of the first unit. The gas temperature was measured using T-type thermocouples inserted in the inlet and outlet gas lines. The wall temperature was measured by a potable surface thermocouple.Thermocouples were embedded along the packing to measure the water temperature profile. All thermocouples were calibrated using a water thermostat. Gas and water temperatures and flow rates measurements were recorded using a data acquisition system.

4.3.3 Humidity measurements:

To obtain a representative sample, a sampling system was constructed which consisted of a sampling tube equipped with the following:

- Water trap to capture the liquid water entrained in the gas,
- Wet test meter,
- Thermocouple and pressure indicator,
- Humidity measuring device,
- A valve to regulate the sampling flow rate,
- Heating tapes to keep the temperature of the gas sample above its dew point,
- Insulation.

The water trap was a vertical column filled with a glasswool .The sampling tube was provided with two outlet openings. A thermocouple was inserted in one of the opening, and a continuous gas sample was withdrawn through the other opening by virtue of the gage pressure in the heater. The glass wool was replaced by a steel mesh because it was found that the glasswool rapidly flooded with water.

The water content of the gas sample was measured by the following techniques:

1. Gravimetric method

A measured gas sample was passed through a drying column filled with Dririete. The water content of the gas was determined from the weight difference of the column before and after sampling and the temperature and pressure conditions of the sample.

2. Cooling method

A measured gas sample was passed through a cooled vessel. The water content of the gas was determined by measuring the condensate collected and the temperature and pressure conditions of the sample.

3. Electrical conductivity method

An instrument sensor marketed as (HMP235) was used to measure the humidity and the temperature of the gas. The humidity measurement is based on measuring the electrical conductivity of the sensor which is related to the amount of water absorbed by the material of the sensor.

4. Wet and dry bulb temperature method

A psychometric sensor was used to measure the humidity of the gas streams. The sensor was equipped with a portable computer-controlled unit (Hygrophill,model 4456). A gas sample was drawn in by a small fan and then passed over two temperature-sensitive semi conductor sensors. One of the sensors was constantly surrounded by water and measured the wet bulb temperature, while the other sensor measured the dry bulb temperature. It was also used to measure the temperature and humidity of the air.

Exact determination of the water content of the gas was difficult due the following reasons:

- condensation of water vapor in sampling and measuring network,
- escape of water droplets from the sampling tube,
- neither the humidity nor the gas temperature was steady constant during the measurement,
- the gas was very close to saturation.

The measured relative humidity of the gas leaving the second unit was found to be in the range of 90 - 100% by all the above methods. Since the lowest gas temperature was

at the outlet of the second unit, the gas leaving the second unit was assumed saturated and by the use of the energy and water balances, the water content of the gas at other locations was estimated. Inlet and outlet gas temperatures were measured using the thermocouples accommodated in the sampling probes.

4.3.4 Dry flue gas analysis

Horiba gas analyzers(510 series) were used. The characteristics of these analyzers are listed in Table (4.1).The analyzers were calibrated using standard gas bottles of known compositions. Air was used to periodically test the oxygen analyzer. The unit uses nitrogen as a carrier gas. At steady state, a continuous gas sample from the sampling probe, which was located at the outlet nozzle of the first unit, was passed through a drying tube, and then fed to the analyzers. The oxygen content of the flue gas was used to determine to the air flow rate and to set the gas-air ratio.

Table (4.1): Characteristics of the flue gas analyzers

Species	Measuring method	Repeatability	Units
O_2	Magnetic Pressure type	±0.5% full scale	vol %
CO_2	Non-Dispersive infrared	±0.5% full scale	vol %
CO	Non-Dispersive infrared	±0.5% full scale	ppm
CH_4	Non-Dispersive infrared	±0.5% full scale	ppm
NO	Chemiluminescent	±0.5% full scale	ppm

4.3.5 Safety

The heater was equipped with the following safety features:

a. High temperature alarm and shutdown switch, low and high water level alarm to protect the pumps and the combustion chamber.

b. Typical gas-air control trains which included high and low pressure switches, shut down valves, as well as a flame detector.

c. Air purging and water circulation were incorporated prior to the start-up of the heater.

d. Overflow lines to prevent water flooding were installed which were S shaped in order to prevent the leakage of the gases.

4.4 Experimental Procedure

Preliminary experimental runs were carried out in order to test the heater at its projected capacity for the following :

I. Complete and stable combustion

By adjusting the air control valve and analyzing the flue gases leaving the first unit, the air flow rate to the burner was set to operate at about 26% percent excess air. The fuel gas flow rate was set at 73 m^3/hr. The content of CH_4, CO, CO_2 and NO_x in the combustion products were continuously analyzed in order to monitor the combustion efficiency. The flame stability was monitored through a window.

II. Water temperature

The water flow rate circulating through the first unit was set at about 57 m^3/hr. The cooling water flow rate fed to the plate heat exchanger was set at about 4.5 m^3/hr in order to keep the temperature of water leaving the first unit above 80 °C. The water flow rate fed to the second unit was adjusted through the control panel to keep the temperature of water leaving the second unit at about 60 °C.

The experimental work was concentrated on measuring the heat and mass transfer coefficients in the direct contact sections. The packing used in both units was Stainless steel Ballast rings manufactured by Glitsch Inc. Their characteristics are listed in Table(4.2). The height of the packing in the first unit was 457 mm. The total height of the first contact section was 1219 mm. The height of the packing in the second unit was 305

and 610 mm. In addition to the packing, the second direct contact section includes 305 mm of spray above the packing and 305 mm of droplet below the packing. The size of packing used was 25.4 and 50.8 mm.

Tests were made by varying the water flow rate at different gas flow rates. Variation in gas and water flow rates was limited by following factors:

a. Loading and wetting characteristics of the packing

b. The capacity of the gas burner.

c. The capacity of the pump circulating water through the first unit.

d. Keeping all solid parts of the combustion section wet.

e. Availability of water.

The fuel gas flow rate was in the range of (40 - 85) m^3/hr at standard conditions. The water flow rate to first unit was in the range of (52 - 68) m^3/hr while the water flow to the second unit was in the range of (3.5 - 8.0) m^3/hr. The heater was operated at 26% and 40% excess air.

At each combination of gas, air and water flow rates, gas and water temperatures at the inlet and outlet of both units, air temperature and humidity, were recorded. The temperature of the water leaving the second unit was maintained in the range of 40-70°C From this experimental data heat, mass, and enthalpy transfer rates were estimated and analyzed.

Table(4.2): Characteristics of Ballast Rings used in the Experimentation

Size (mm)	Wall Thickness (mm)	Packing Density (kg/m^3)	Specific Surface Area (m^2/m^3)	Free Space (Void) (%)	Packing Factor
25.40	0.609	497	207	94	48
50.80	0.762	401	128	95	28

5.0 RESULTS AND DISCUSSION

5.1 Performance

Measurements of input and output data such as gas and water flow rates and temperatures for each run are recorded every 10 seconds and the average readings are evaluated and used for energy and materiai balance calculations. The heat balances are calculated from a datum of 0°C and 101.325 kPa. The maximum error in the closure of the heat balances is ± 4%.

In all runs, the exhaust gas was analyzed for unburned fuel and the concentrations of CO, and NOx. The concentration of CH_4 was in the range of (4 -10)ppm and the concentration of CO was (1-4)ppm. The maximum concentration of NO_x was 110 ppm. The results indicated that nearly complete combustion with perfect quenching has been achieved.

The prototype heater was operated at the following conditions:

Fuel gas flow rate = 73.1 m^3/hr.

Excess air = 26% (mol%)

Water flow rate to the first unit = 57.2 m^3/hr

Temperature of inlet water to the first unit = 75.5 °C

Water flow rate to the second unit = 4.5 m^3/hr

Temperature of inlet water to the second unit = 14 °C

The time required to reach steady state was 15 minutes. The heater was able to maintain the outlet water temperatures to ± 2.5°C as can be observed in Fig(5.1). The average outlet water temperatures were 82.3 °C for the first unit and 62.1 °C for the second unit. The small variation of outlet temperatures was due to the periodic additions of water to maintain a constant water level around the combustion chamber. The amount of water added varied with the outlet gas temperature and flow rate. The maximum rate was 0.5 m^3 /hr.

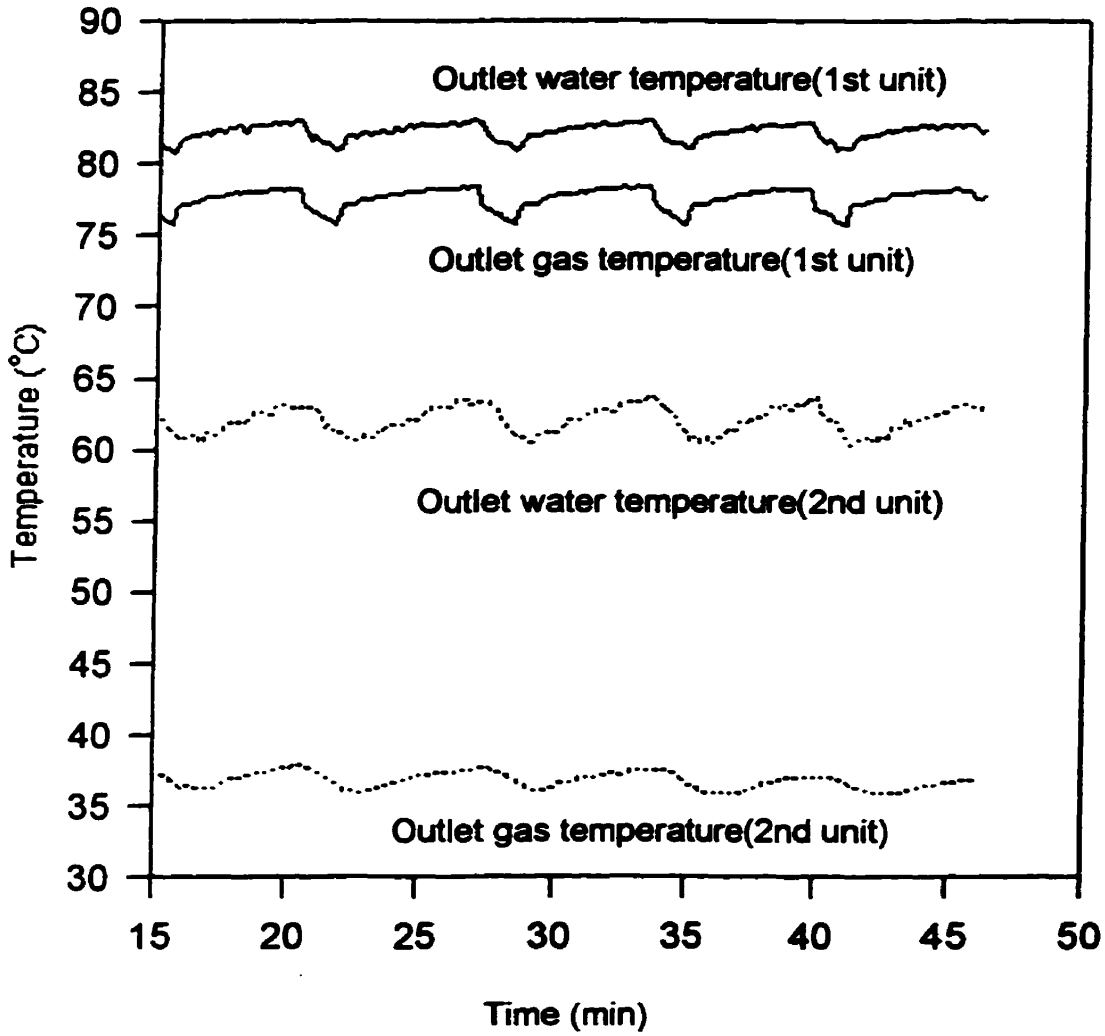

Fig(5.1) : Performance of DWH at steady state

The performance of the heater is analyzed in terms of the thermal efficiency. The thermal efficiency is defined as the percentage of the total heat input transferred to the liquid water. The overall thermal efficiency of the heater is more than 95%. It is a combination of the efficiency of the first and the second unit. In the first unit, the fraction of the heat transferred to liquid water is determined by the thermal performance of both the firetube and the direct contact section. The thermal efficiency of the firetube is in the range of 25 - 45%. In the direct contact sections there is a trade-off between the thermal efficiency and the level of temperature at which the hot water is obtained.

The thermal efficiency of the first unit has been calculated using equation (3.11) and was found to decrease as the inlet water temperature increases. This is because the enthalpy of the flue gases leaving the unit increases as the inlet water temperature increases. The inlet water temperature is fixed by the flow rate of the cold water into the plate heat exchanger. The temperature of water leaving the first unit is required to be above 80°C. To meet this objective, the first unit has to be operated below 60% efficiency as can be observed in Fig(5.2) in which the thermal efficiency of the first unit is plotted against the water temperature. The effect of the inlet water temperature to the first unit on the percentage of total heat liberated by combustion and transferred to liquid water in each unit is illustrated in Fig(5.3). Normally, the second unit has to handle up to 50% of the total heat input to the heater. The thermal efficiency of the second unit is determined by the inlet water temperature and flow rate. For water outlet temperatures between 50 to 60 °C, the thermal efficiency is 90-95%. The heat losses are very small. The maximum wall temperature measured during experimentation was less than 100 °C.

The performance of the first unit is also analyzed using the Dimensionless Temperature Parameter[Rao&Mohtadi 1982]. The Dimensionless Temperature Parameter, DTP, is calculated as the absolute temperature difference between exit and inlet water temperature(° K) divided by the absolute inlet water temperature(° K). The effect of inlet water temperature on Dimensionless Temperature Parameter, DTP, is shown in Fig(5.4). The variation of the DTP with the inlet water temperature in the firetube section is very small. In the direct contact section, the DTP is strongly influenced by the inlet water temperature. The relation between the DTP in the direct contact section of the first unit

and the inlet water temperature at three firing rates is shown in Fig(5.5). As the inlet water temperature is increased, the DTP decreases. If the inlet water temperature is increased above 355 °K (≈82°C), the DTP in the direct contact section approaches zero. At this point, the thermal efficiency of the direct contact section is zero. All the sensible heat of the flue gases is used to evaporate water. The point at which the DTP in the direct contact section approaches zero is a function of the firing rate. It is actually function of the inlet specific enthalpy of the flue gases rather than the flue gas flow rate. The effect of the firing rate on DTP at constant inlet water temperature is illustrated in Fig(5.6).

Another parameter used to analyze the thermal performance of the heater at different operating conditions is the temperature of approach. The temperature of approach at the exit of the first unit is calculated as the difference between the outlet gas temperature and the inlet water temperature. The temperature of approach decreases as the inlet water temperature increases. Such an effect is shown in Fig(5.7) in which the temperature approach at the exit of the unit is plotted against the water temperature. The variation of temperature approach with the firing rate at constant water temperature is shown in Fig(5.8). The temperature of approach in the second unit is in the range of (10 - 20)°K and the DTP is in the range of (0.12 - 0.20), varying with the inlet water temperature and flow rate. The variation of the temperature of approach and the DTP with inlet water temperature are mainly due the nature of heat and mass transfer taking place in the direct contact sections.

Increasing the air flow rates reduces the thermal efficiency of the first unit. This may be explained in terms of the heat transfer in the immersed firetube and direct contact section. At high air flow rates, the thermal efficiency of the firetube is lower while in the direct contact section the rate of mass transfer(evaporation) is higher causing lower sensible heat transfer to the liquid water. Although the thermal efficiency of first unit decreases as the percentage excess air increases, it appears that the performance of the second unit is enhanced. This may be attributed to the increase of the superficial gas velocity through the second unit. Variations of the temperature of approach and the DTP in the first unit with inlet water temperature at three firing rates with 40% excess air are shown in Fig(5.9a,b).

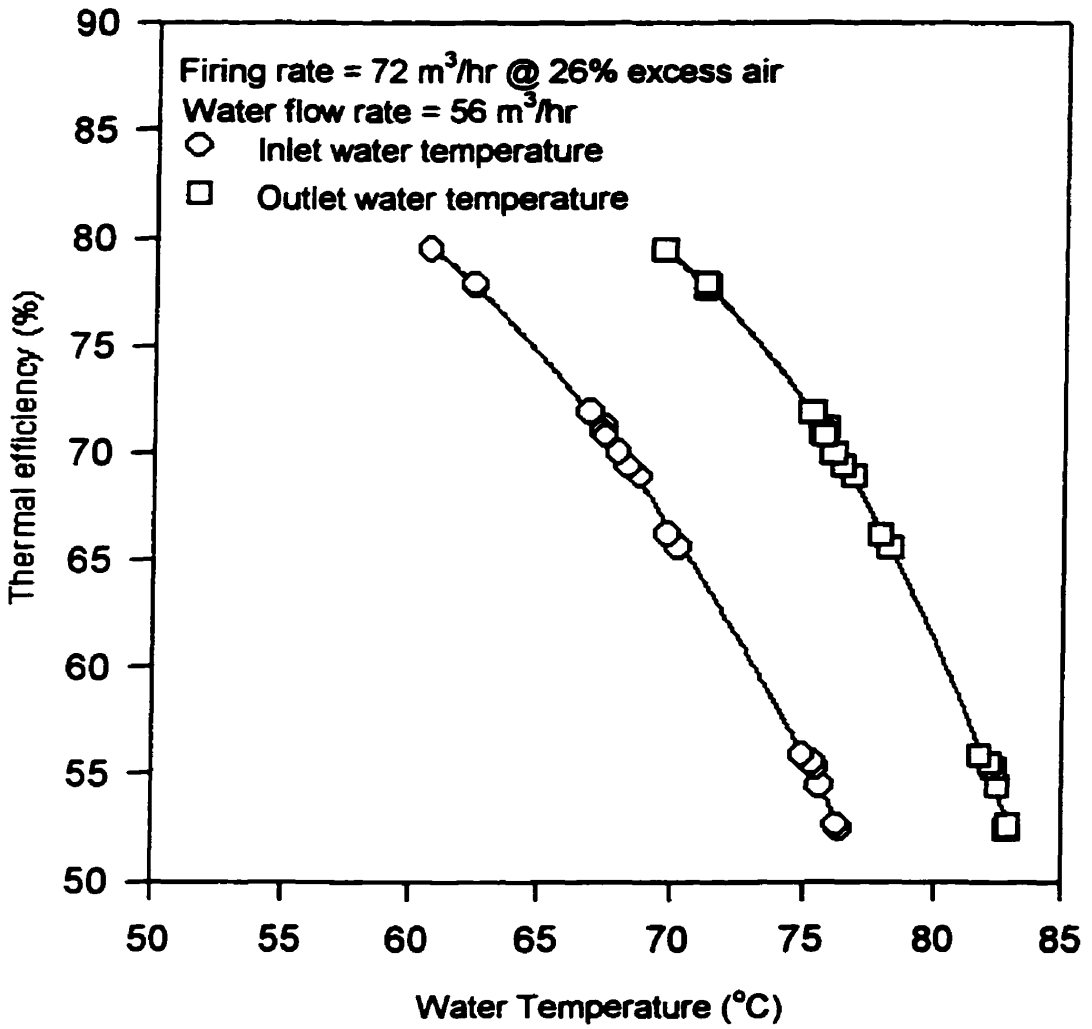

Fig(5.2): Thermal efficiency of first unit vs. inlet and outlet water temperature.

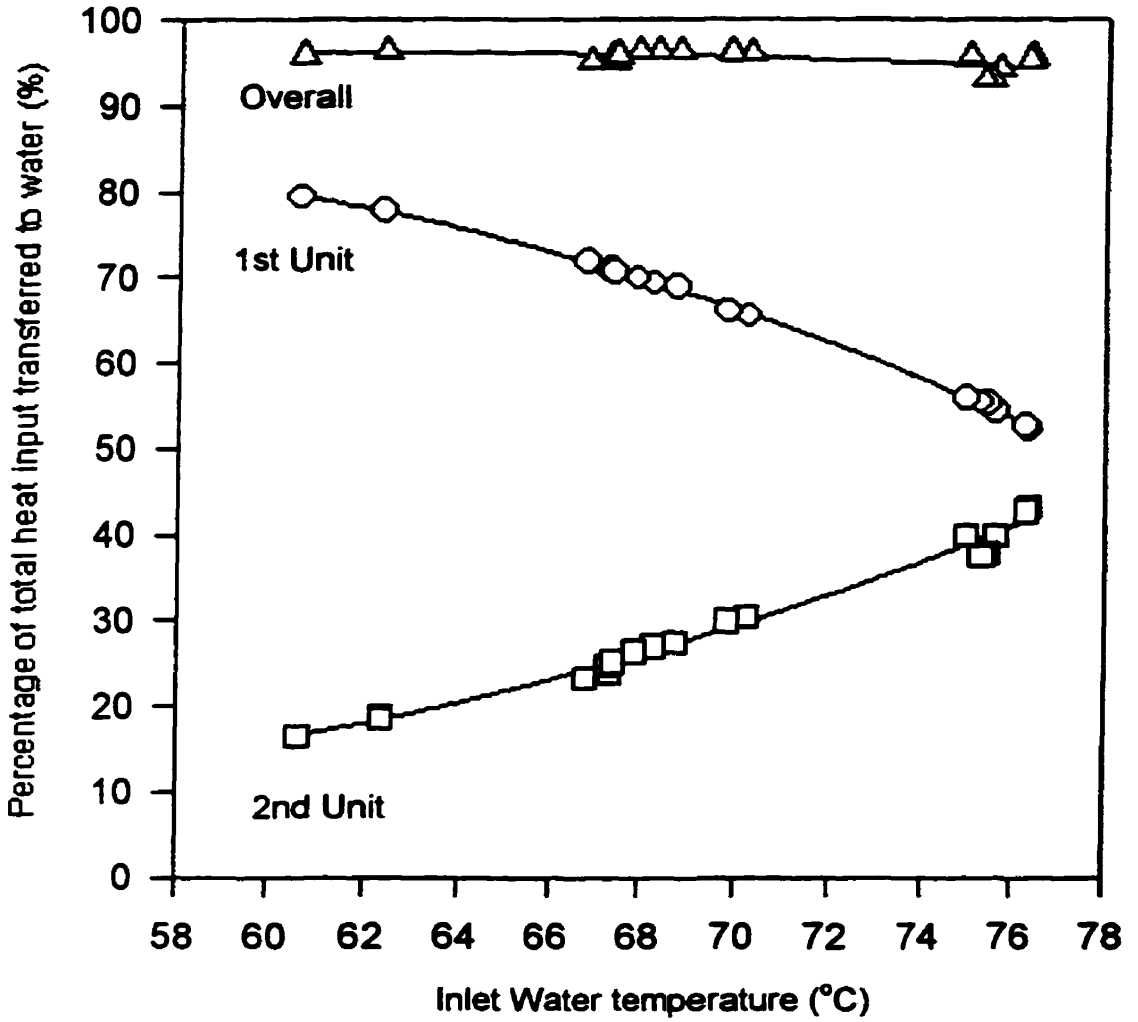

Fig(5.3): Thermal perfomance of each unit vs. inlet water temperature to 1st unit

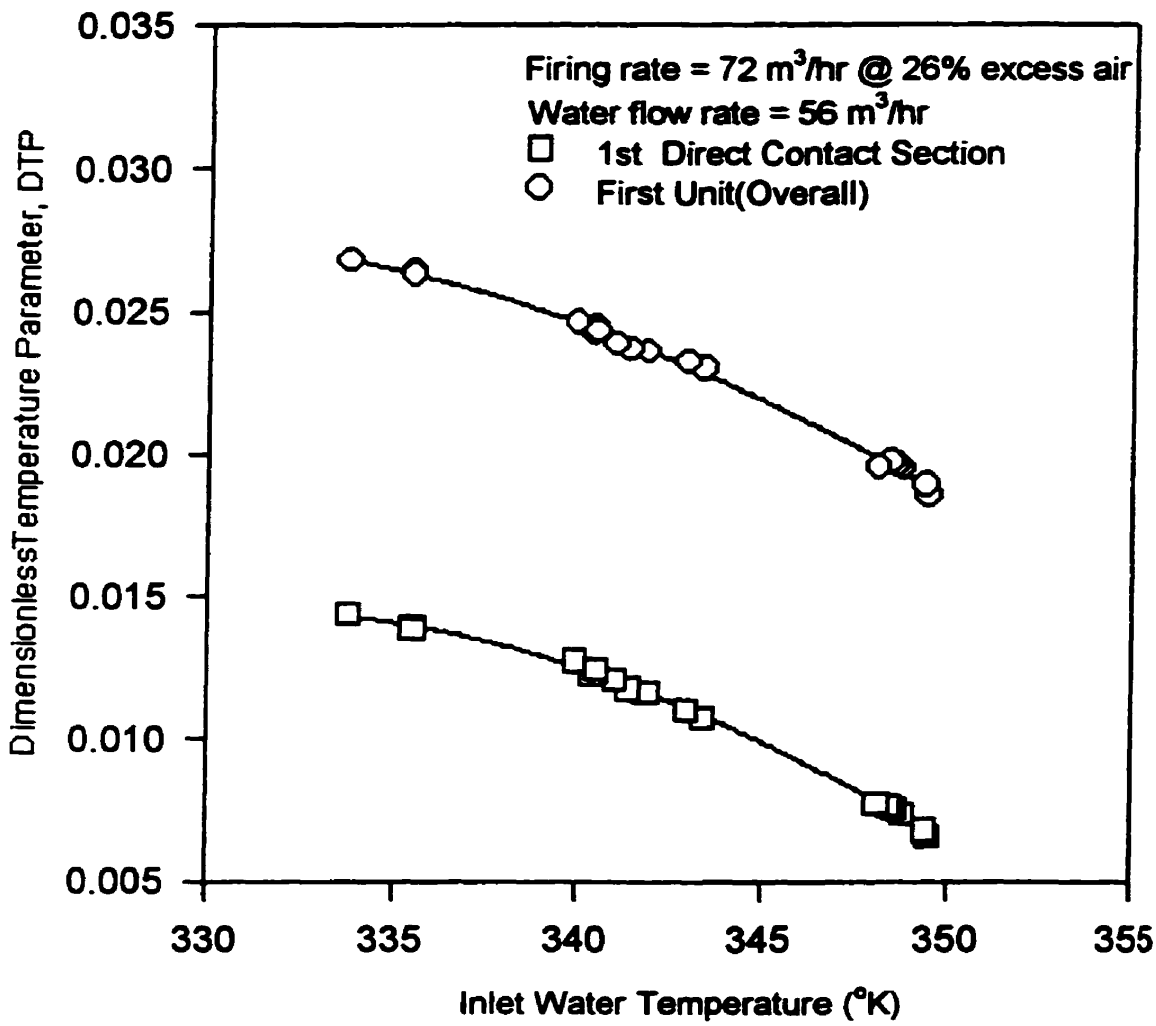

Fig(5.4): Variation of the DTP in the 1st unit with water temperature.

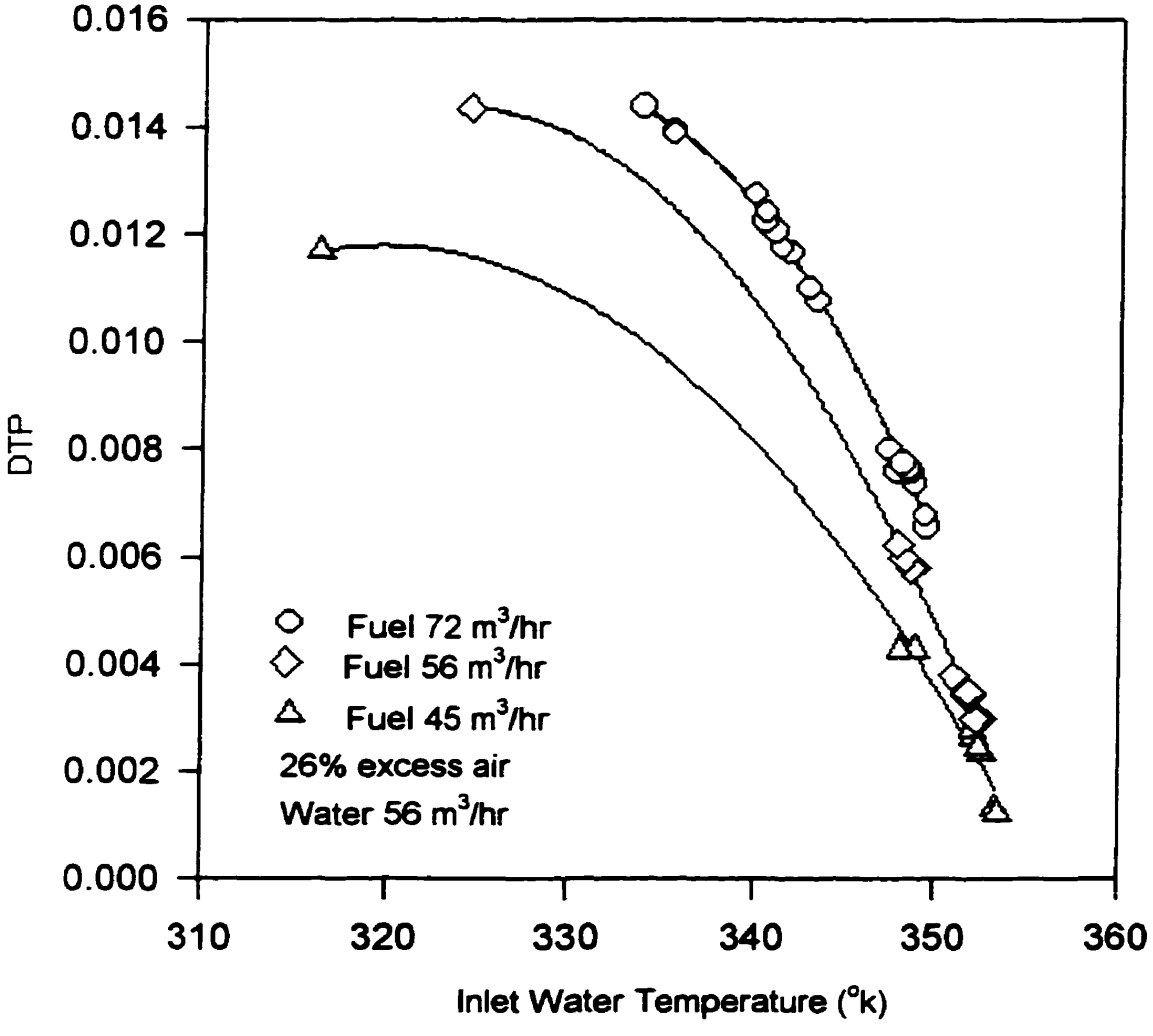

Fig(5.5): Variation of DTP in the direct contact section of the first unit with inlet water temperature and gas flow rate

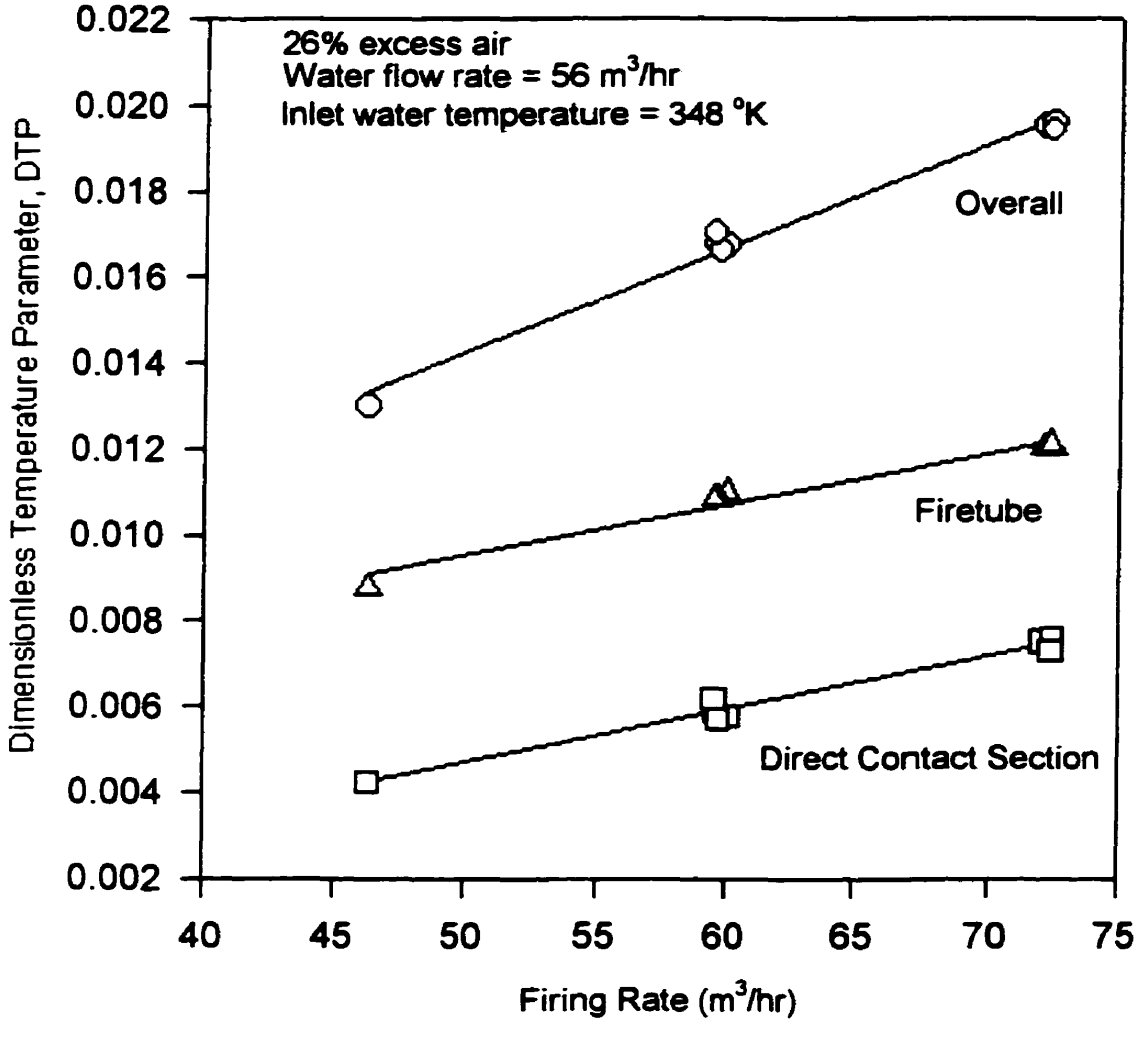

Fig(5.6): Variation of the DTP in the 1st unit with the firing rate.

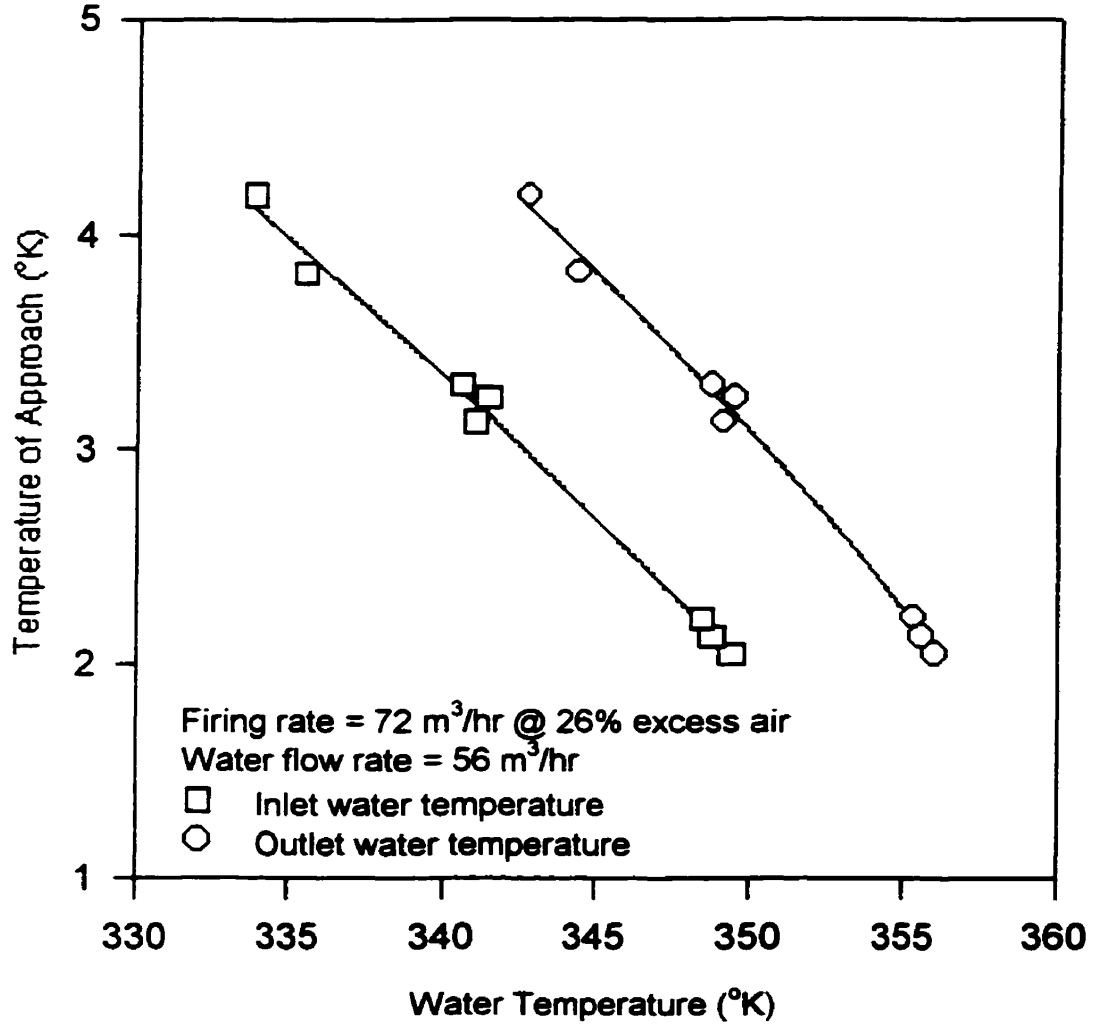

Fig(5.7): Temperature of approach in the first unit vs. water temperature

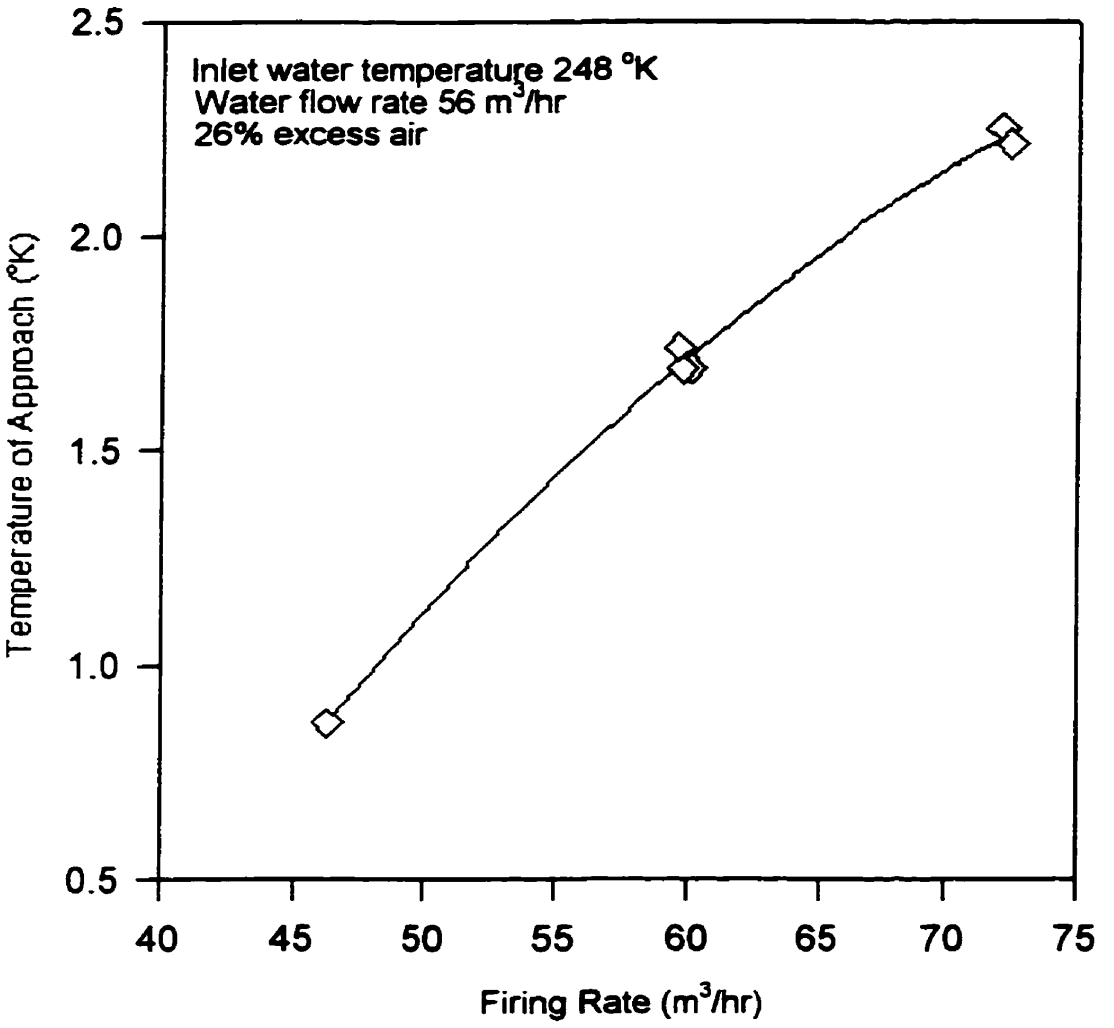

Fig(5.8): Effect of the firing rate on the temperature of approach(1st unit).

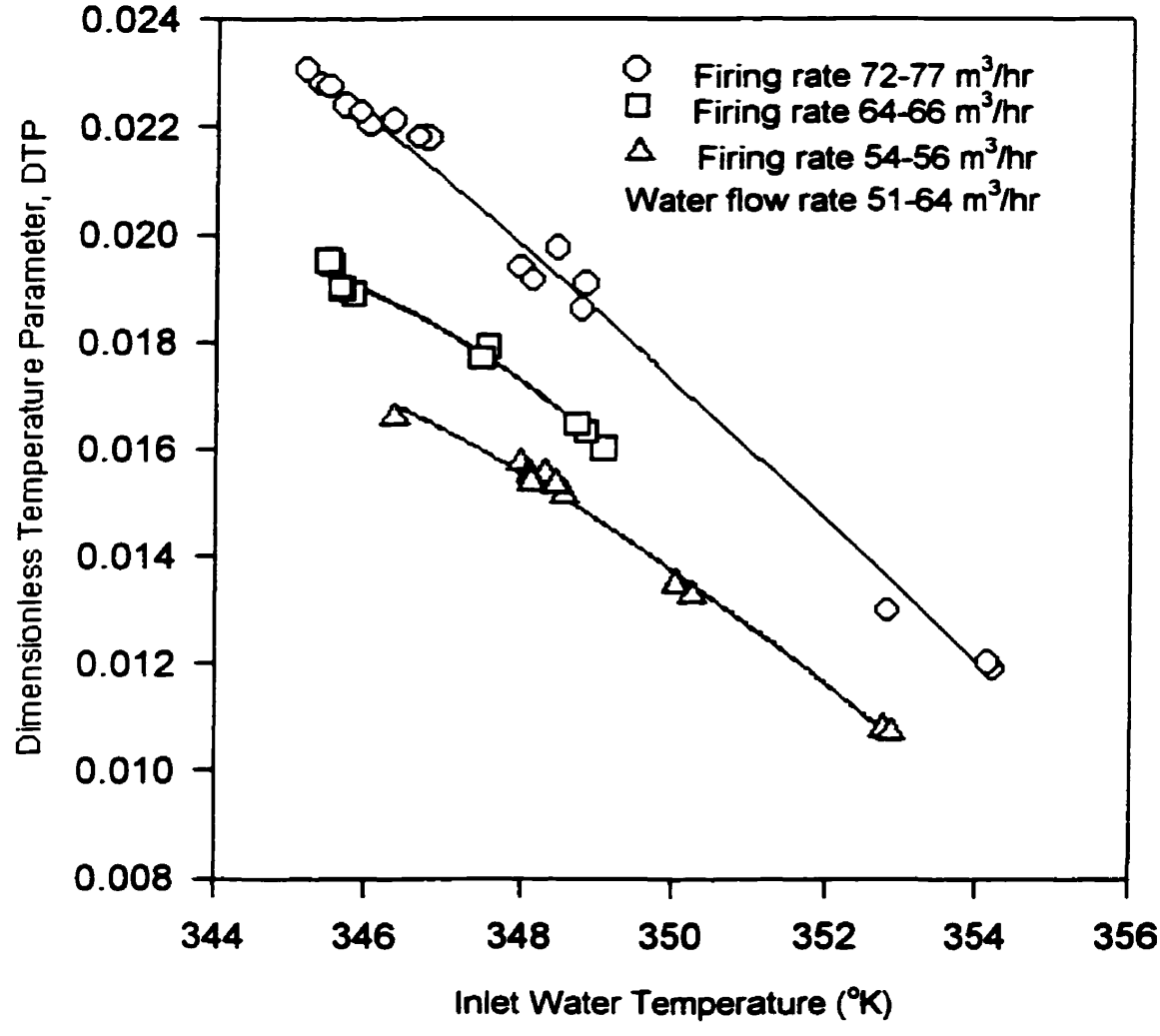

FiG(5.9a): Variation of the DTP in the first unit with inlet water temperature and firing rate at 40% excess air

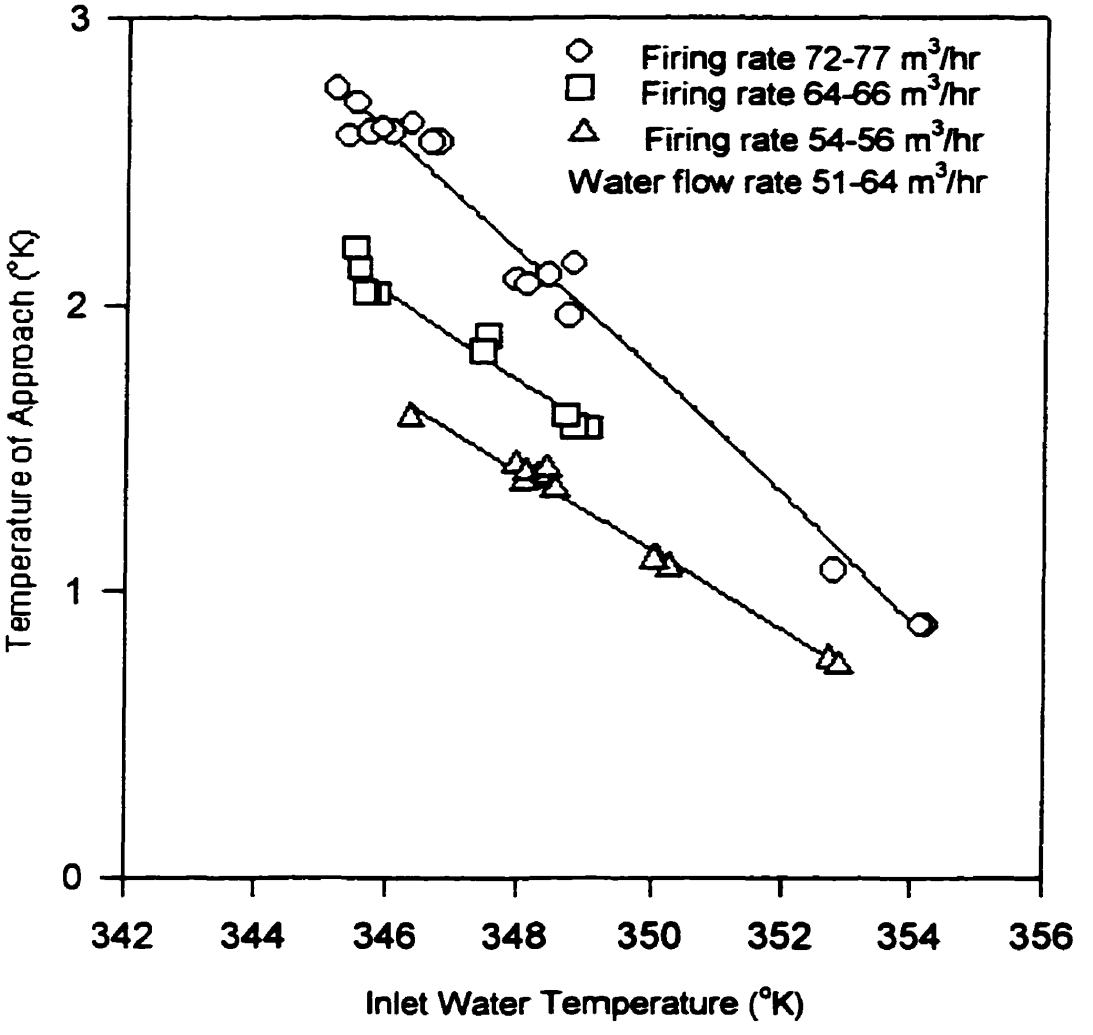

Fig(5.9b): Temperature of approach in the 1st unit at 40% excess air

5.2 Heat and Mass Transfer Considerations

5.2.1 Immersed Firetube

The heat transfer coefficient between the hot gas flowing through the firetube and the liquid water has been calculated using equation(3.10). The temperature difference at the inlet of the firetube was taken to be the difference between the theoretical adiabatic flame temperature and the temperature of the water leaving the unit. The temperature difference at the outlet of the firetube was taken to be the difference between the temperature of flue gases leaving the firetube(measured) and the water temperature. This water temperature was estimated by calculating an energy balance around the firetube. Measured overall heat transfer coefficients are in the range of (160 - 240) $kJ/m^2.hr.°C$. varying with gas and air flow rates.

The variation of the overall heat transfer coefficient with gas flow rate is shown in Figure (5.10). The overall heat transfer coefficient includes both the radiation and convection. According to equation(3.9) the heat transfer by radiation accounts for more than 80% of the total heat transferred in the firetube.

Values of the temperatures of the flue gas leaving the firetube estimated by using equation(3.9) were found slightly higher than the measured ones as illustrated in Figure(5.11). This may be attributed to the following:

1. The convective heat transfer coefficient was under-estimated.
2. The measured flue gas temperature was lower than the actual gas temperature.
3. The source of radiation heat transfer was not only due to CO_2 and H_2O but possibly due to some solid particles(soot).

According to Figure (5.11),the measured flue gas temperature and that predicted using equation (3.9) are related by following empirical expression:

Predicted gas temperature(°C) - Measured gas temperature (°C) $\approx$ 2(Firing rate, m^3/hr).

This differnce might be due to the tube-thermocouple relative heat transfer.

It is most likely that the rate of heat transfer by convection is under-estimated. The convective heat transfer coefficient in the fire tube is approximately twice that obtained by empirical correlations(equation 3.4 & 3.5).

The effect of increasing the excess air modifies the heat transfer in the firetube in the following ways:

1. It reduces the inlet gas temperature(flame temperature) which results in a lower average gas temperature and a higher gas emissivity.
2. It reduces the concentration of radiating species which results in a lower gas emissivity.
3. The total gas flow rate is increased, resulting in higher convective heat transfer coefficients.
4. Increasing the amount of air reduces the maximum firing rate of the burner, due to a higher pressure drop through the heater.

An approximate estimation of the rate of heat transfer at 26% and 40% excess air using equation(3.9) have showed that the overall heat transfer coefficient and the thermal efficiency are slightly decreased as the level of excess air is increased. At constant air - fuel gas raio, the amount of heat transferred increases as the firing rate increases because both the velocity and the average gas temperature increase accordingly. However the thermal efficiency of the firetube decreases as the firing rate increases. The variation of the thermal efficiency with the firing rate and excess air is shown in Fig(5.12) in which the thermal efficiency of the firetube is plotted against the logarithm of the firing rate at two levels of excess air.

The temperature of water splashing onto the surface of the firetube was never more than 90° C while the temperature of the gas inside the tube is more than ten times the water temperature. This large temperature gradient subjected the exposed parts of firetube to cracking of the walls of the tube resulting in tube failure. A tube failure in the exposed part was experienced during the experimentation.

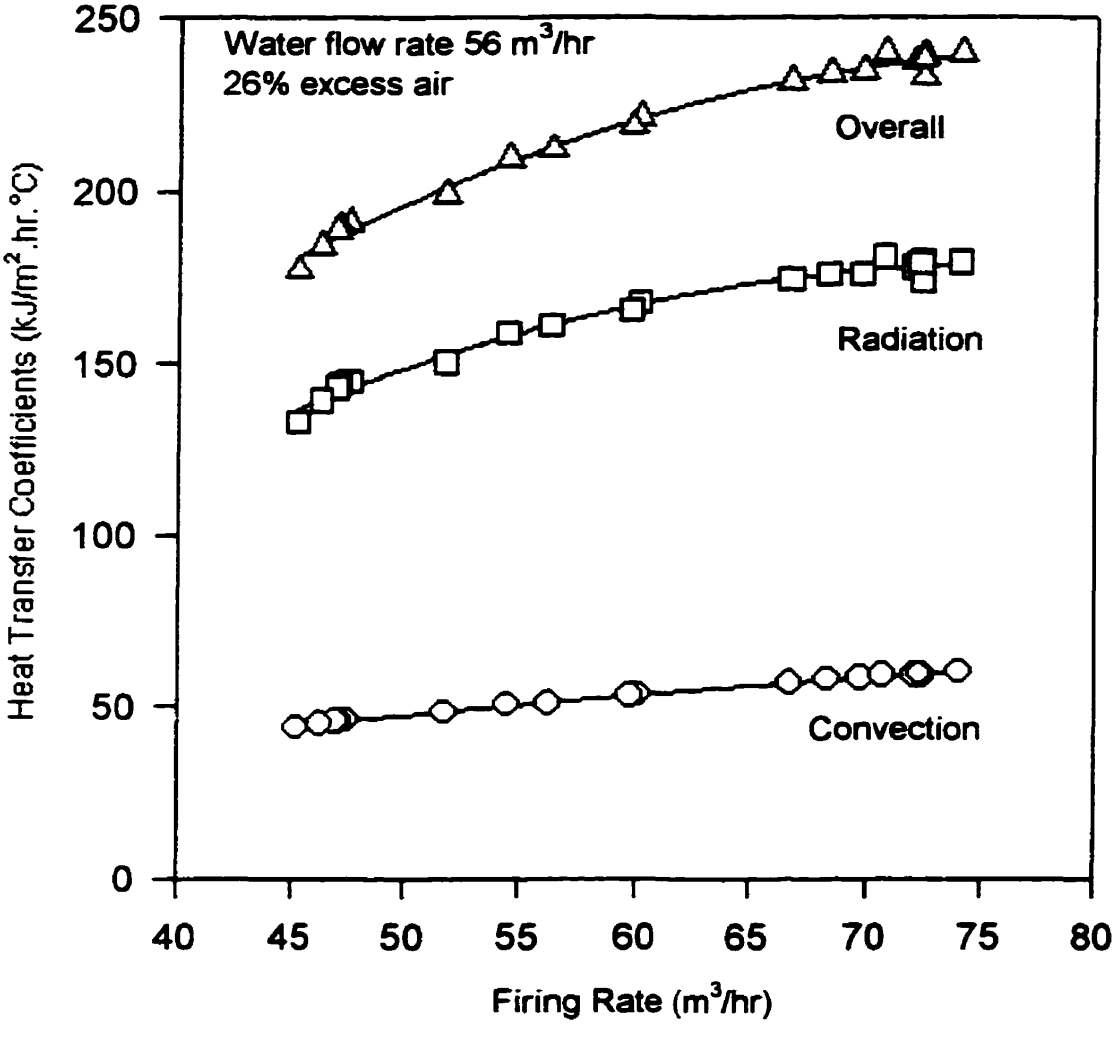

Fig(5.10): Variation of heat transfer coefficients (firetube) with firing rate.

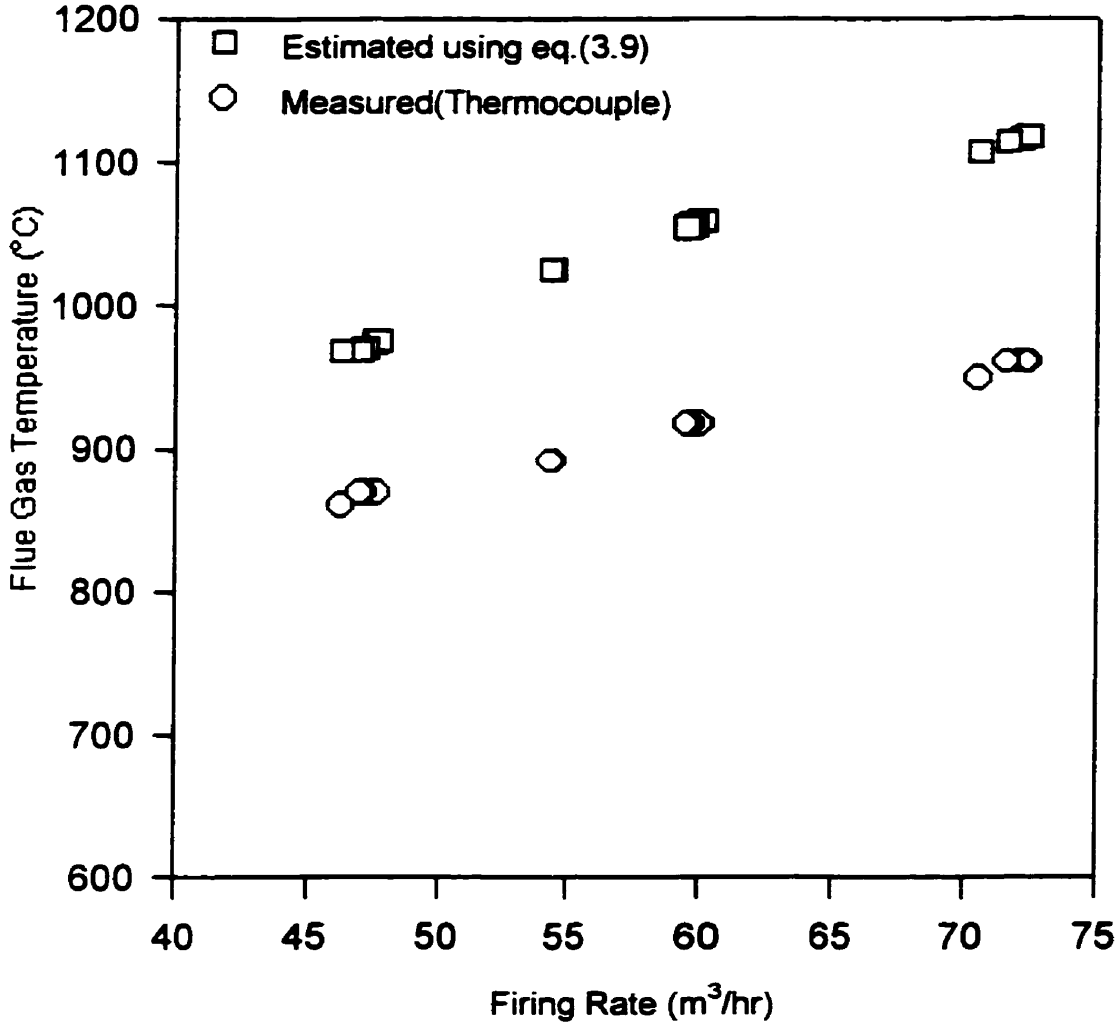

Fig(5.11): Measured and estimated gas temperature at the exit of the firetube.

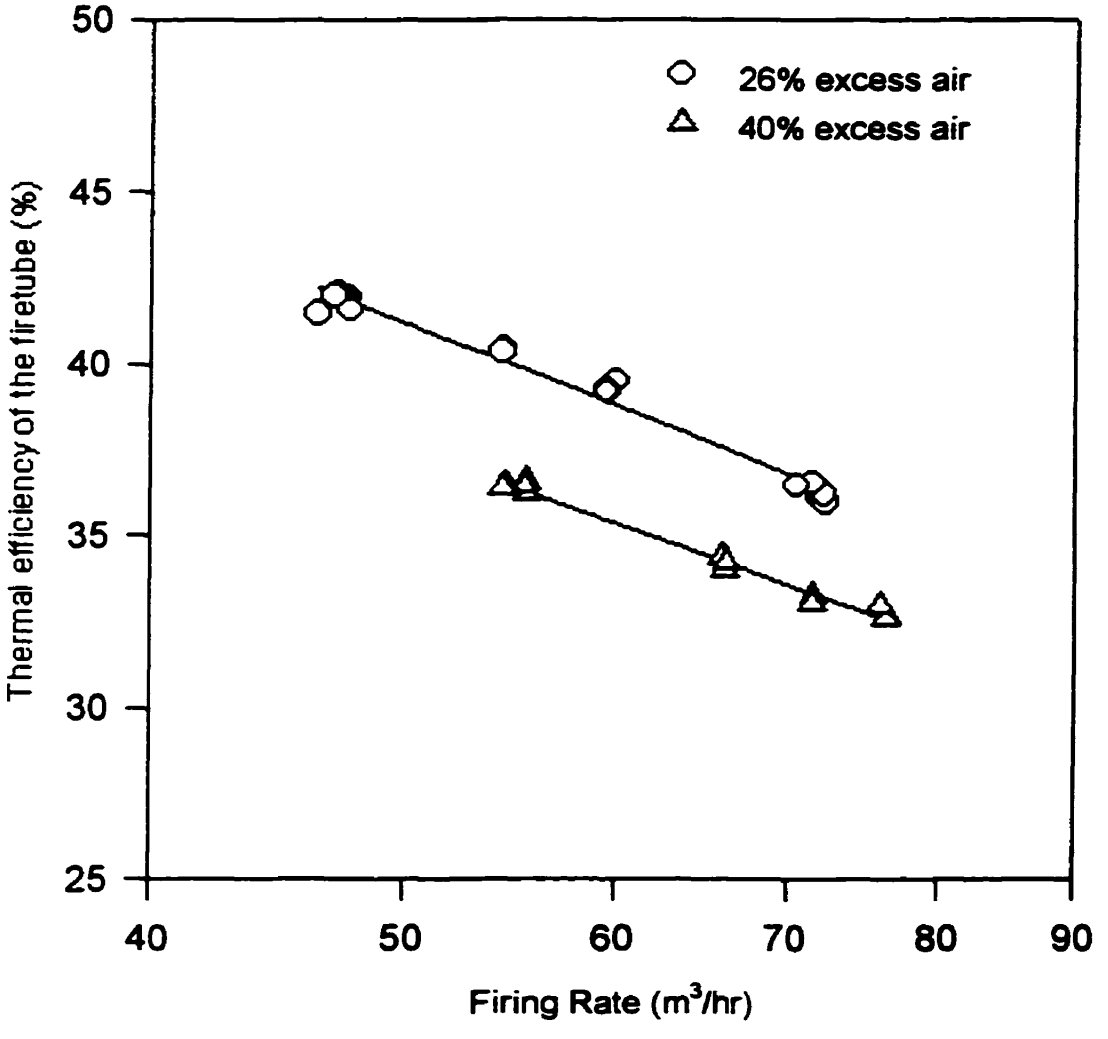

Fig(5.12): Effect of gas and air flow rate on the thermal efficiency of the firetube

5.2.2 First Direct Contact Section

The amount of heat that can be transferred to liquid water by quenching the hot flue gases leaving the firetube is a function of the temperature difference between the adiabatic saturation temperature of the gases and the inlet water temperature. The adiabatic saturation temperature is determined by inlet temperature and humidity of the flue gases. For particular level of excess air, the humidity of the flue gases is constant and the change of the temperature of flue gases with the firing rate is small resulting in a small change of the adiabatic saturation temperature. For example, at 26% excess air, the adiabatic saturation temperature of flue gases leaving the firetube is (81-84°C). Normally this is the maximum water temperature that can be obtained by direct contact between the hot gases and liquid water. However, with an inlet water temperature higher than the adiabatic saturation temperature, the temperature of water can be raised above the adiabatic saturation temperature. Zero temperature difference between the inlet water temperature and the adiabatic saturation temperature means that all the sensible heat of the gas is used to evaporate water and there will be no change in the temperature of liquid water. As the temperature difference increases, or more specifically as the inlet water temperature decreases the enthalpy change of water increases and net amount of water evaporated decreases while the level of the temperature of hot water obtained is lowered. On the other hand, the actual change in water temperature and the actual temperature of approach are determined by the gas and liquid flow rates, inlet water temperature, and the size of the contacting section.

Overall heat transfer coefficient between liquid water and the flue gases in the direct section of the first unit has been calculated based on the total enthalpy change of the water per unit volume of the contact section, per unit log-mean temperature difference(equation 3.27a). The temperature difference between the flue gases and liquid water at the bottom is much higher than that at the top. The reason for using the log-mean temperature difference as the mean driving force is that the cooling of the hot gases with water to a temperature below 100 °C takes place in a very short contact height.

It was found that the overall heat transfer coefficient is strongly affected by the inlet water temperature. This effect is shown in Fig(5.13). As discussed above, the

increase of the heat transfer coefficient with the decrease of the inlet water temperature can be attributed to the fact that at lower water temperatures a greater amount of heat is transferred and/ or returned to the bulk liquid. As the inlet water temperature at the top of the unit increases the actual temperature approach at the top decreases and approaches zero when the inlet water temperature equals the adiabatic saturation temperature. For water temperatures above 75°C , the amount of sensible heat transferred to liquid water is less than 30% of the total heat entering the direct section and hence the water temperature may be assumed constant. For constant water temperature, equation(3.27b) is used to estimate the sensible heat transfer coefficient between the flue gases and the liquid water. The variation of the sensible heat transfer coefficient with inlet water temperature at constant gas and liquid flow rates is also shown in Fig(5.13). It is interesting to note that, for water temperatures above 60°C(dew point), the ratio of the overall heat transfer coefficient to the sensible heat transfer coefficient is smaller than one, while for water temperatures below the dew point the ratio is greater than one. As the inlet water temperature increases, the sensible heat transfer coefficient increases while the overall heat transfer decreases. The height of heat transfer unit obtained using equation (3.46b) is in the range (0.15 - 0.25 m) while the number of transfer units is in the range (5 - 8). The second term of equation(3.27b) is the number of transfer units.

Overall and sensible heat transfer coefficients at constant inlet water temperature for three firing intensities are shown in Fig(5.14). Increasing the firing rate results in an increase in the flue gas flow rate per unit area of the contacting section and in the same time it results in an increase in the inlet flue gas temperature. The total inlet enthalpy per unit area of the section is used to combine the effects of both the flue gas flow rate and the specific enthalpy on the heat transfer coefficients. It is found that straight lines could be drawn through the experimental data. The slopes at an average inlet water temperature of 75 °C are calculated and found to be 0.6 and 0.65 as shown in Figure(5.15). This indicates that the heat transfer coefficients increase exponentially with total inlet flue gas enthalpy per unit area of the contact; gas mass velocity, and gas specific enthalpy.

The effect of increasing the level of excess air modifies the heat transfer in the direct quenching section in the following ways:

1. Increases the superficial gas velocity which results in an increase in the heat transfer coefficients.
2. Reduces the inlet specific enthalpy (temperature and pressure) of the flue gases resulting in reduction of the overall and sensible heat transfer coefficients.
3. The maximum firing rate is reduced as the level of excess air is increased due to the increase of the pressure drop through the heater

Sensible heat transfer coefficients obtained with 40% excess air is shown in Fig(5.16). Comparing the heat transfer coefficient obtained at 26% and 40% of excess air reveals that there is an increasing trend of sensible heat transfer coefficient and a decreasing trend of overall heat transfer coefficient with increasing the pecentage excess air. However, within the range of the this work, the effect is small.

The variation of the rate of evaporation of water with the inlet water temperature at different gas flow rates is shown in Fig(5.17). The rate of evaporation determines the amount of water which needs to be added to keep the firetube always immersed in water. There is a good agreement between the calculated amount of water evaporated and the amount of water added periodically as indicated by the flow meter installed on the make up water line.

Liquid water mass velocity was in the range of 45,000 - 60,000 $kg/m^2.hr$. Within this range, the overall heat transfer coefficients are slightly increased as the liquid flow rate is increased. Operating below this range may subject the exposed solid parts of the firetube to overheating. Water temperature measurements along the first unit are shown in Fig(5.18). The water temperature rise per unit volume of the direct contact section is not constant.

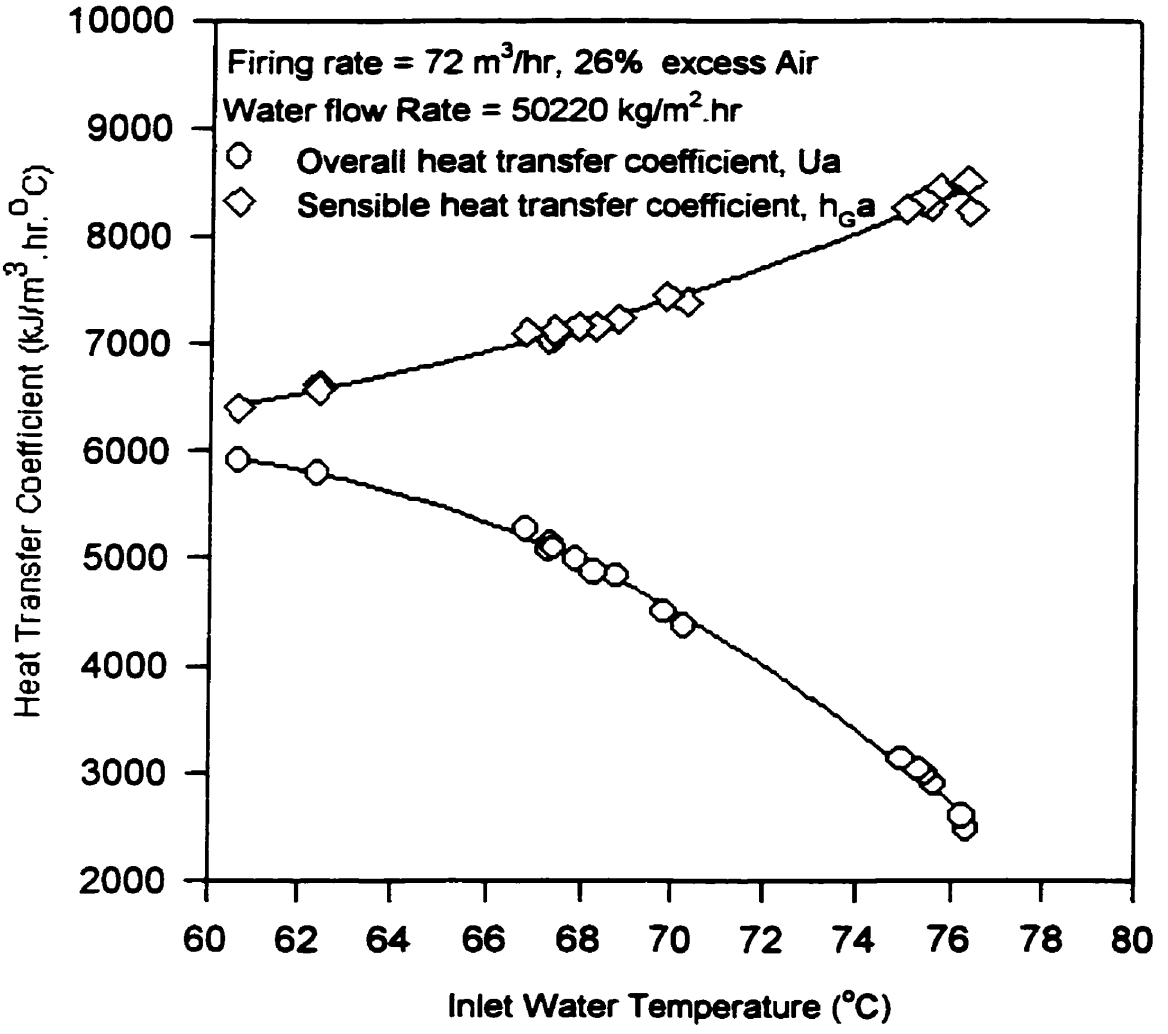

Fig(5.13): Heat transfer coefficients in the first direct contact section vs. inlet water temperature.

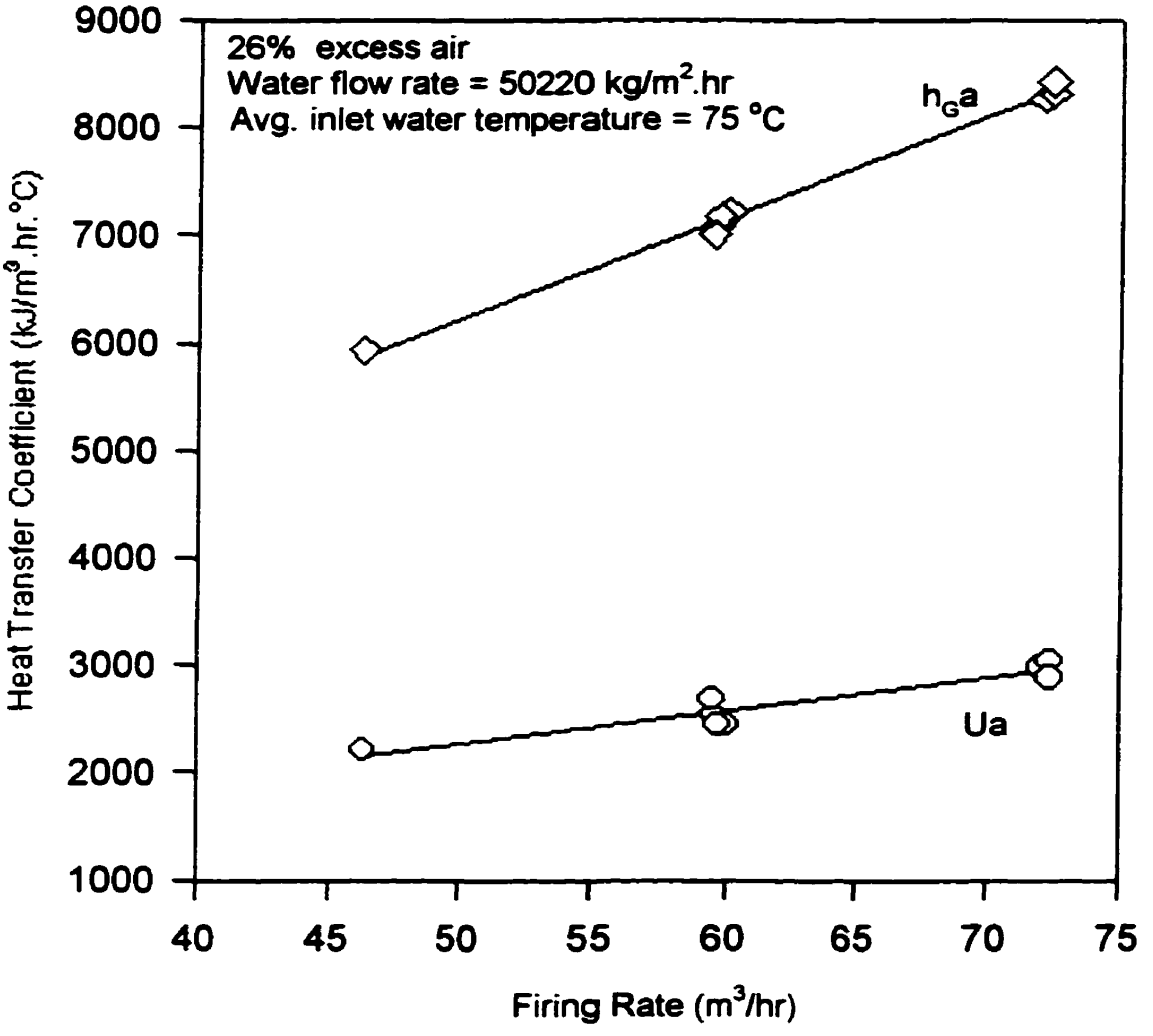

Fig(5.14): Heat transfer coefficients in the 1st direct contact section vs. firing rate at constant inlet water temperature.

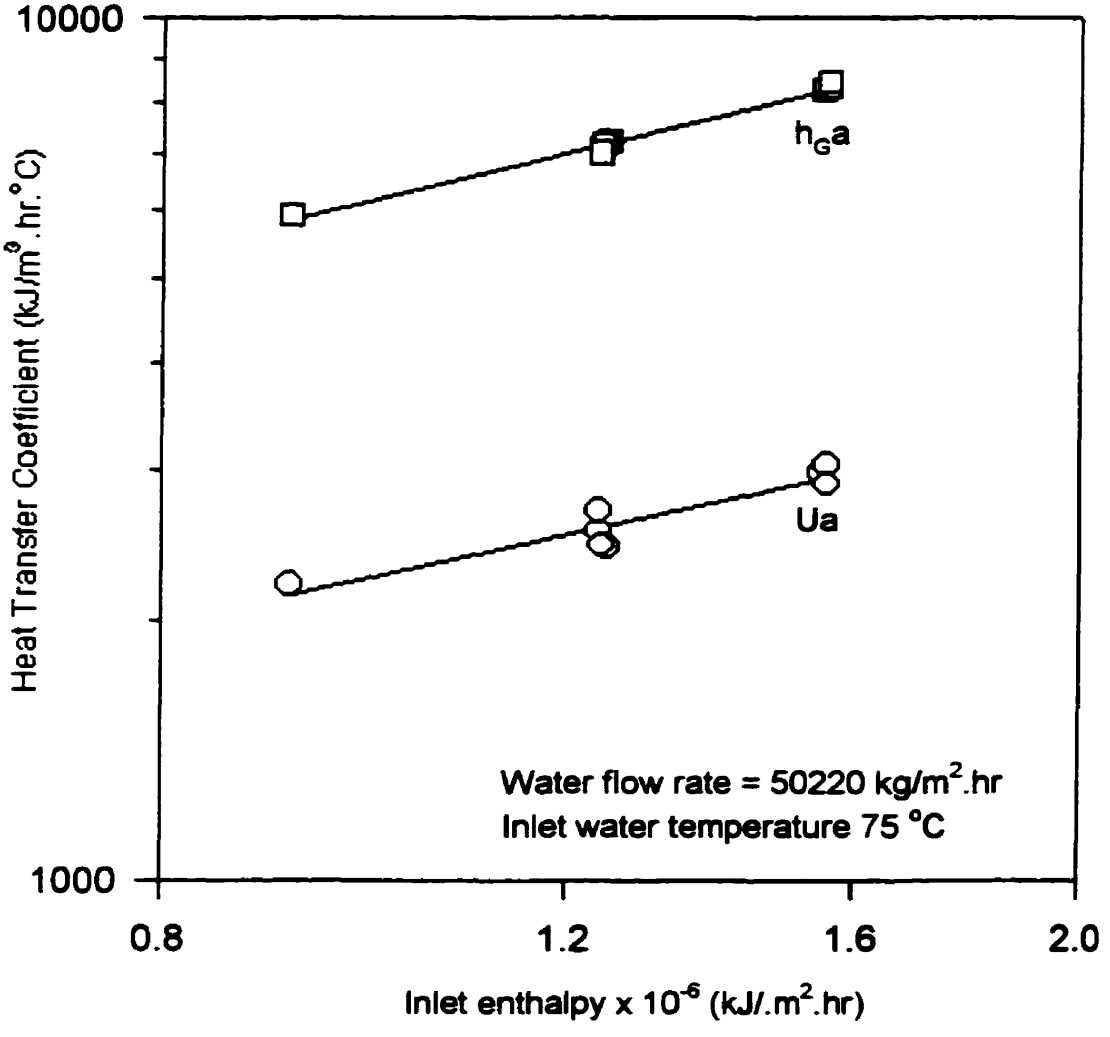

Fig(5.15): Heat transfer coefficient (1st direct section) vs. inlet enthalpy

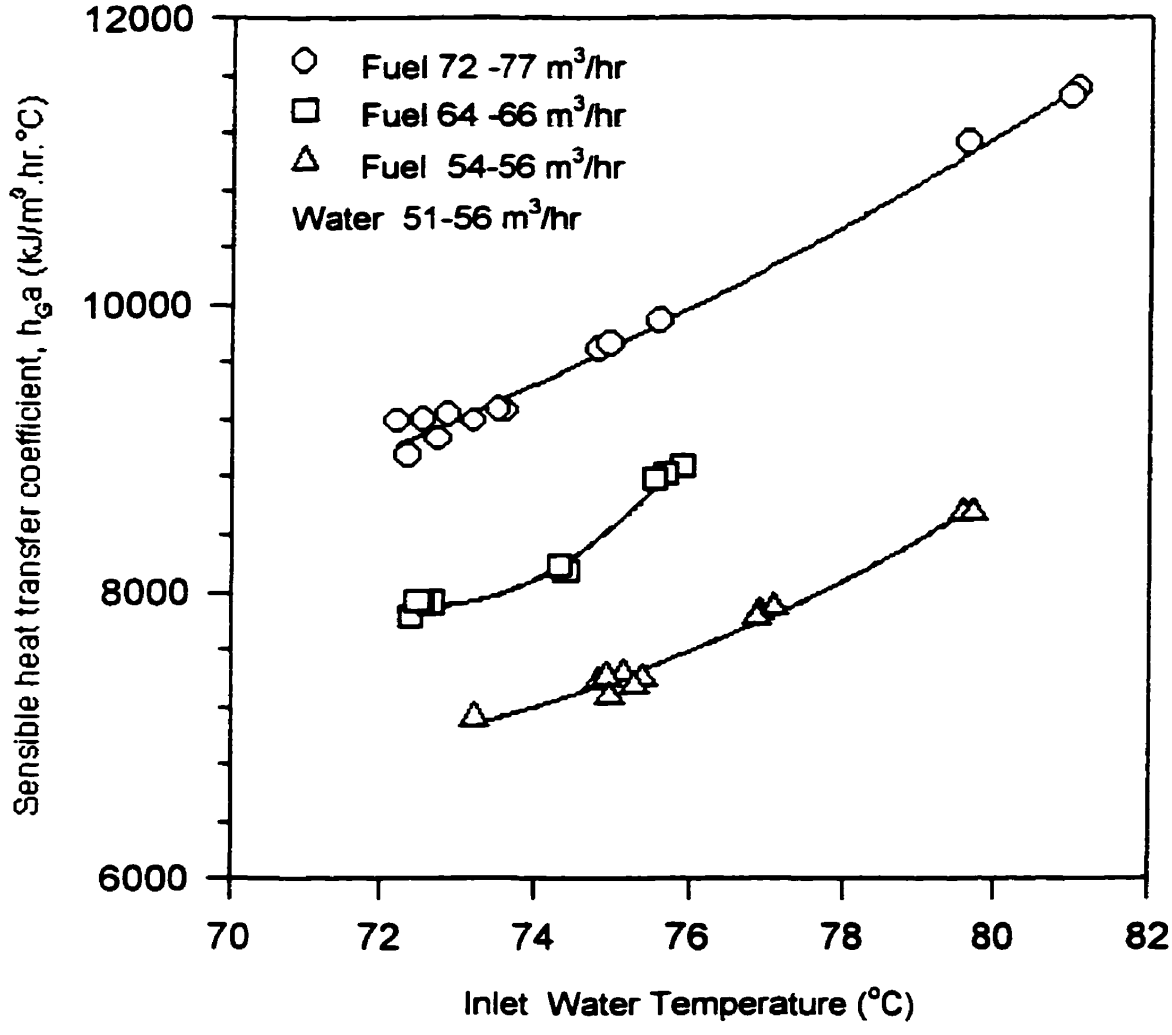

Fig(5.16): Heat transfer coefficient (1st contact section) at 40% excess air

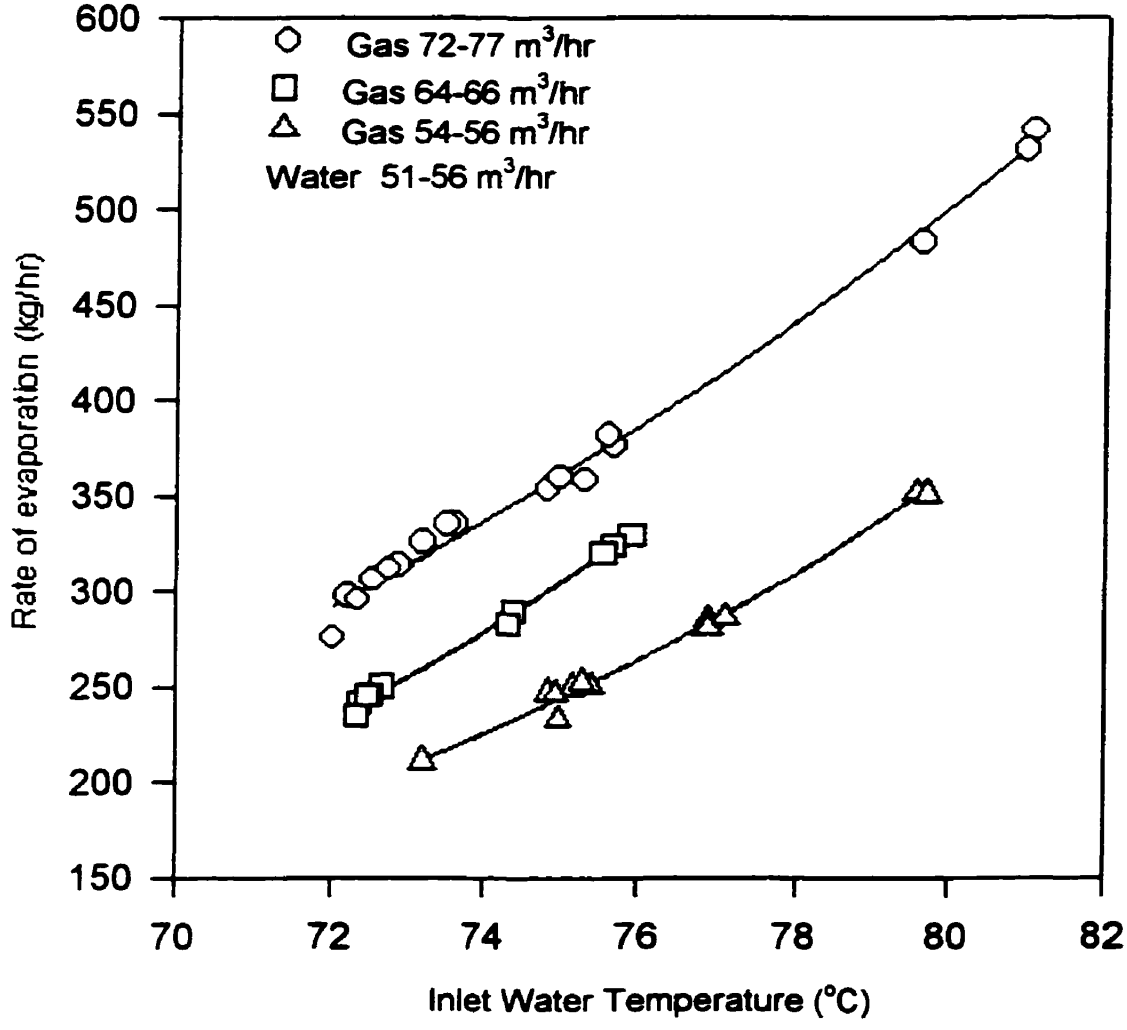

Fig(5.17): Rate of evaporation in the 1st unit at 40% excess air

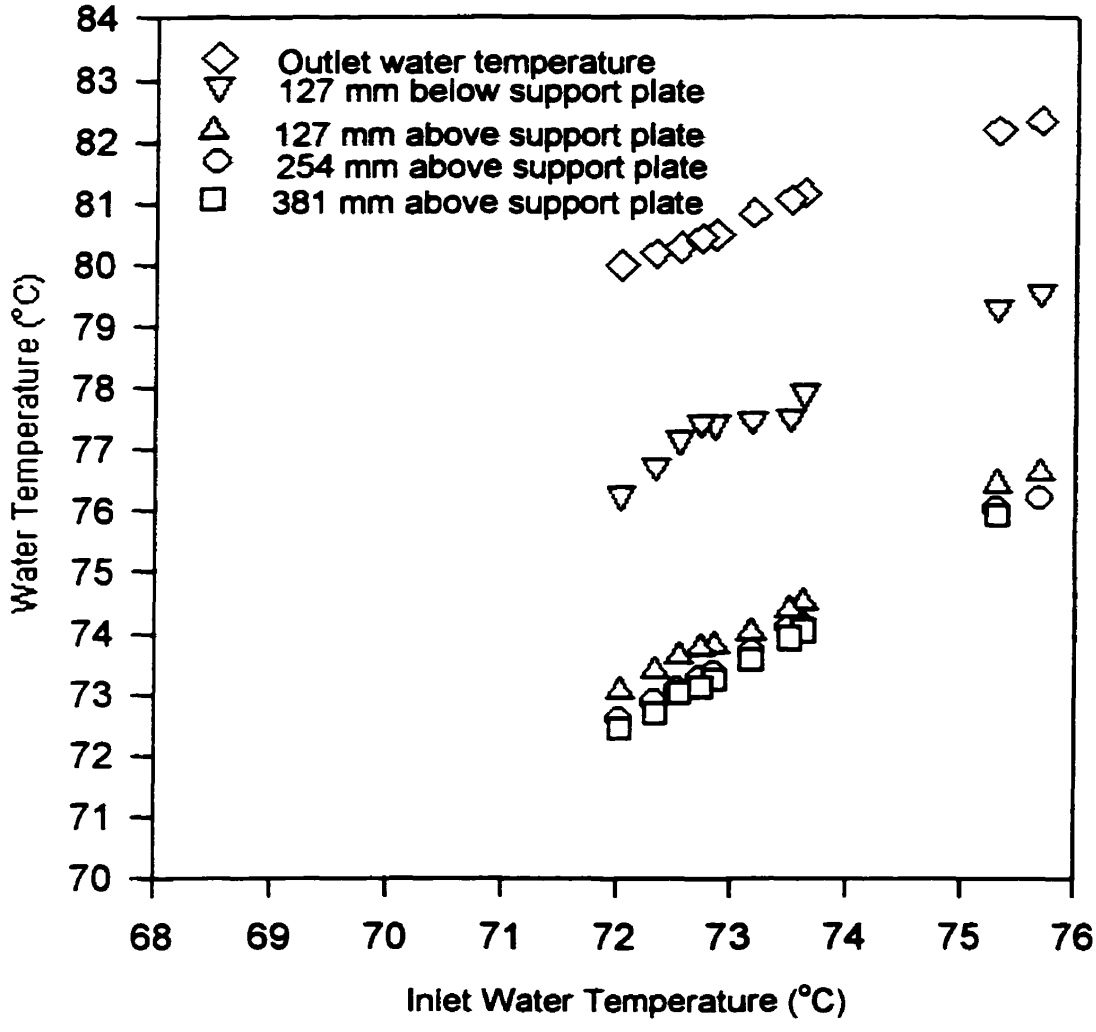

Fig(5.18): Water temperature profile along the first unit.
Gas = 76 m^3/hr, 40%excess air, Water 53 m^3/hr

5.2.3 Second Direct Contact Section

5.2.3.1 Mass Transfer

Mass transfer between hot wet flue gases and cold liquid water has been analyzed in terms of the overall volumetric mass transfer coefficient and the height of the overall gas transfer unit. The mass transfer coefficient was calculated using equation (3.45) while the height of transfer unit was calculated using equation(3.46).

The water vapor contant of the gas at the inlet of the unit ranges from 0.2 to 0.6 (kg.water/kg.dry gas) while at the outlet it is less than 0.1. The driving force has been calculated as the difference between the enthalpy of flue gases at the bulk gas temperature and the enthalpy at the bulk liquid temperature. The enthalpy driving force is corrected for high water vapor concentration and is estimated at the bottom, at the top, and at a point where 50% of the total heat is transferred. Estimation of the driving force along the unit has showed that 75% of the total heat transferred accompanied with a small change in the gas temperature and high mass transfer rates. Values of the enthalpy driving forces changes considerably along the unit. A mean driving force is obtained using a chart devised by Willmoson and Carey[1950].

The mass transfer coefficient has been calculated based on the total volume of the direct contact sections; the packing, and the spray zones above and below the packing. The average volumetric mass transfer coefficient ranges from 40 to 160 $kg/m^3.hr.kPa$, and the corresponding height of overall transfer unit is in the range of (0.3 - 0.6) m, varying with inlet gas enthalpy , inlet water temperature, and gas and liquid mass velocities.

Since the flue gas flow rate and its temperature or enthalpy entering the second unit are controlled by the performance of the first unit, the experimental study of the effect of one operating parameter while keeping the others constant is very difficult. For example, the flue gas flow rate and its enthalpy are coupled and controlled by the performance of the burner , firetube and the direct contact quenching section of the first unit. The water flow rate to the unit is the easiest parameter to manipulate without substantial change in the other operating conditions.

Figure (5.19) shows a logarithmic plot of the volumetric mass transfer coefficients K_Ga obtained with 304.8 mm bed of 25.4 mm Pall rings against the average liquid mass velocity, L_{avg}, at three values of gas velocity. It is found that a straight line could be drawn through the experimental points for each operating condition. The slopes of the regressed lines are higher in low liquid flow rate range and lower and nearly constant at higher liquid flow rates. This may be attributable to the larger change in the active interfacial area for mass transfer in the low water flow rate range. Expressing the relation between the average liquid mass velocity and the overall volumetric heat transfer coefficient as a power function, an average exponent of 0.62 is taken and hence $K_Ga \propto L_{avg}^{0.62}$. The overall mass transfer coefficient K_Ga, increases exponentially with liquid velocity.

The variation of overall mass transfer coefficient with dry gas mass velocity is shown in Fig(5.20). The slopes of the regressed lines vary with gas and liquid loading. In determining the effect of the flue gas velocity on the overall mass transfer coefficient, the values of $K_Ga/L_{avg}^{0.62}$ are plotted against the dry flue gas velocity on logarithmic coordinates. The data obtained using 25.4 mm Pall rings is regressed to the following equation:

$$K_Ga = 0.003(L_{avg})^{0.62}(G_s)^{0.57} \qquad (5.1)$$

The above equation is based on the following conditions:

Liquid flow rate: 11,000 - 21,000 $kg/m^2.hr$

dry gas flow rate: 2400 - 3400 $kg/m^2.hr$

Inlet flue gas enthalpy : 1000 -1250 kJ/kg.

Outlet water temperature: 40 - 60 °C

The fitting of the above equation to the set of experimental data is shown in Fig(5.21). Equation (5.1) reveals that the mass transfer coefficient is affected more by the liquid flow rate than by the gas flow rate. As the vapor concentration in the gas phase increases, the resistance to mass transfer decreases, resulting in a higher rate of mass transfer. At high water vapor concentration, the rate mass of transfer is less dependent on the gas mass velocity.

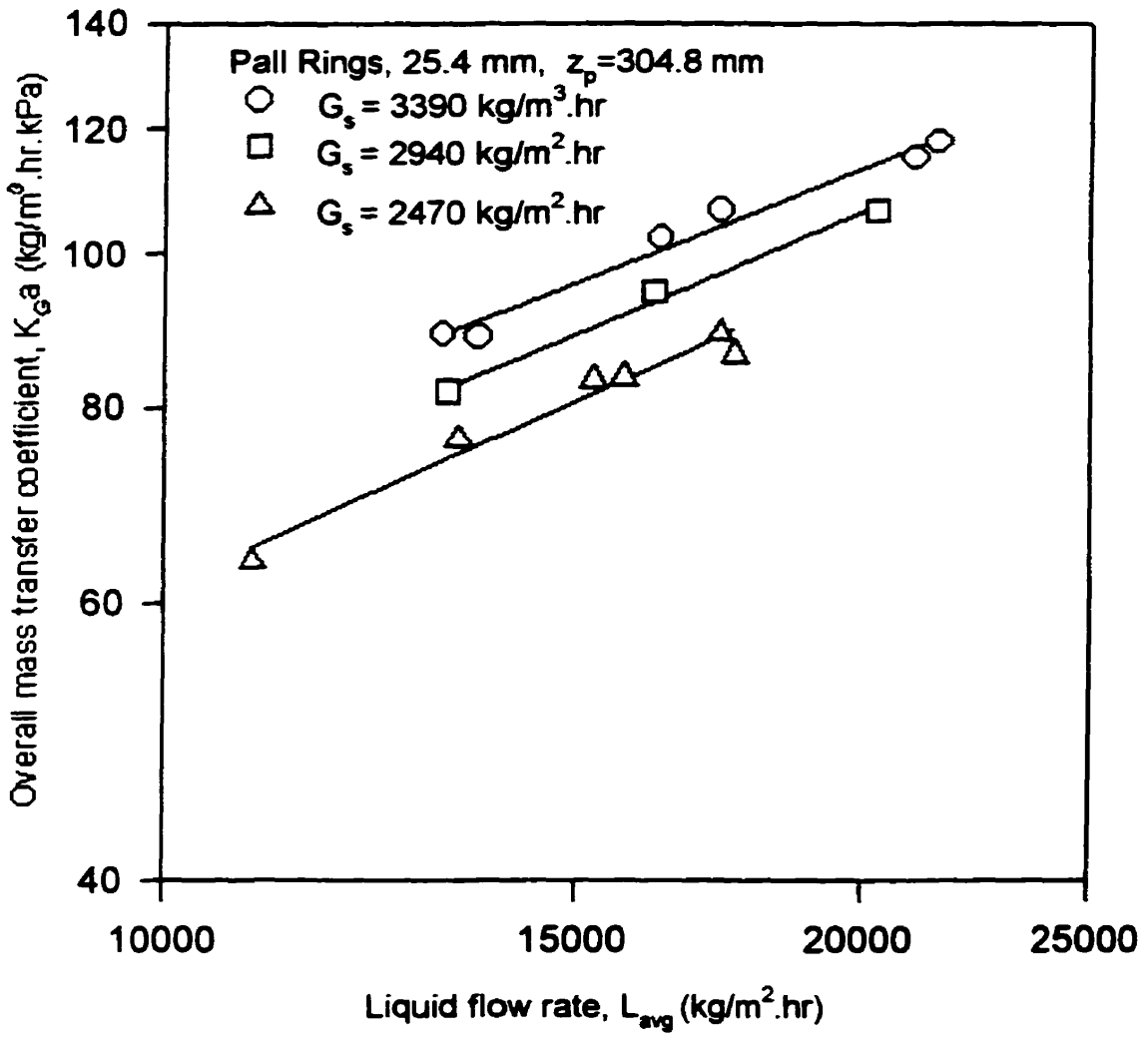

Fig(5.19): Effect of liquid flow rate on mass transfer coefficient (2nd unit)

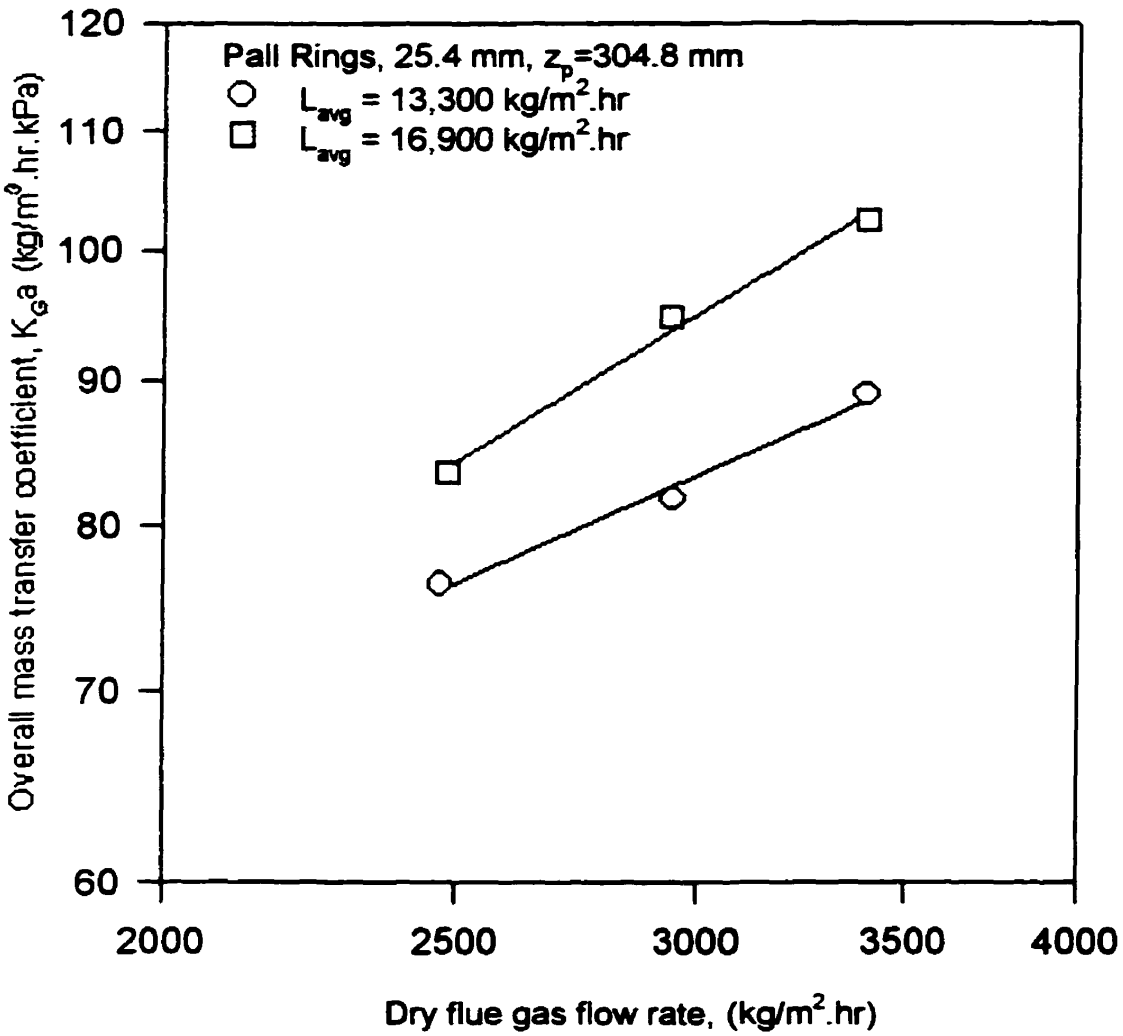

Fig(5. 20): Mass transfer coefficient vs. gas flow rate (2nd unit)

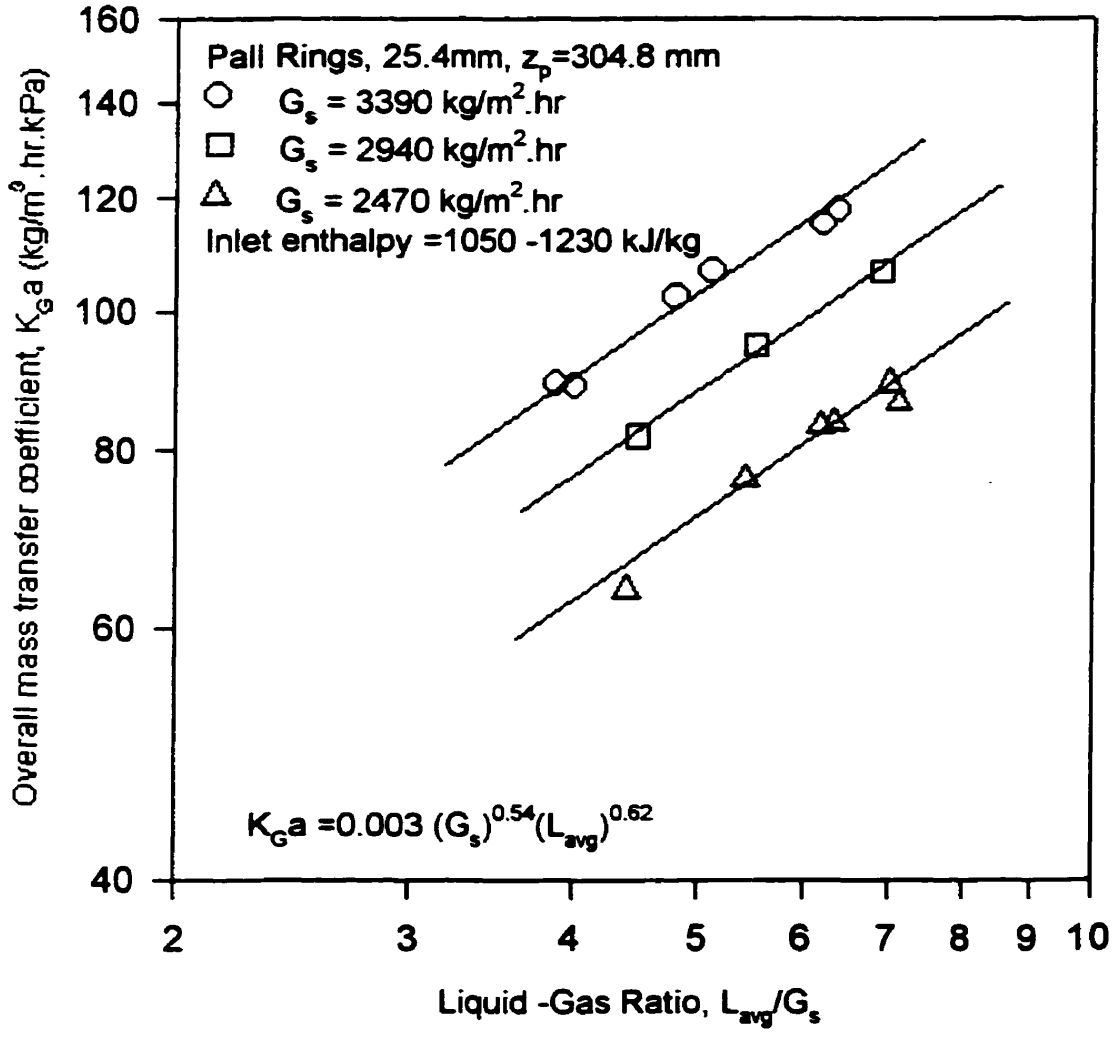

Fig(5.21): Measured mass transfer coefficient (2nd unit) vs. water-gas ratio.

The effectiveness of the direct contact section for mass transfer is best represented by the height of mass transfer unit. Fig(5.22) shows the variation of the height of transfer unit with liquid and gas flow rates for 25.4 mm Pall rings. The height of transfer unit is proportional to L_{avg}^{-n} . The values of n are function of the liquid flow rate. The height of gas transfer unit can be expressed as a power function of liquid and gas mass velocities by the following approximate expression:

$$HTU = 4.817 \frac{(G_{avg})^{0.528}}{(L_{avg})^{0.711}} \qquad (5.2)$$

The variations of the mass transfer coefficient and the height of the gas transfer unit with the inlet gas enthalpy and /or water temperature are not considered.

Measured overall mass transfer coefficients obtained using 304.8 mm bed of 50.8 mm Pall rings are shown in Fig(5.23). The overall mass transfer coefficient are plotted against the liquid flow rate at different gas flow rates on logarithmic coordinates. The data are regressed to straight lines for each operating condition. The slopes of the lines are less than that obtained with 25.4 mm Pall rings indicating that the transfer coefficients are less dependent on the liquid flow rates. However, the values of the transfer coefficients are lower than that obtained with 25.4 mm Pall rings. It may be concluded that increasing the size of the packing has the benefit of reducing the minimum wetting rate of the packing and hence enhance the flexibility of the unit. This may lead to the possibility of obtaining hot water at a higher level without loss in the efficiency. However, the height of the transfer unit is lower.

Originally the unit was filled to a height of 609.6 mm with 25.4 mm Pall rings. One spray nozzle was used. Measured overall mass transfer coefficients were in the range (35 - 80) kg/ m^3.hr.kPa. Fig(5.24) is a logarithmic plot of the rate of mass transfer calculated as (K_GA) obtained using 609.6 mm and 304.8 mm bed of 25.4 mm Pall rings against the liquid flow rate. Although the total height of contact was reduced from 1219.2 mm to 914.4 mm the mass transfer rate increased for the same operating conditions. This may be due to; a lack of wetting of the packing , a poor water distribution, and an excessive amount of packing being used. The water distributor was replaced by two spray nozzles.

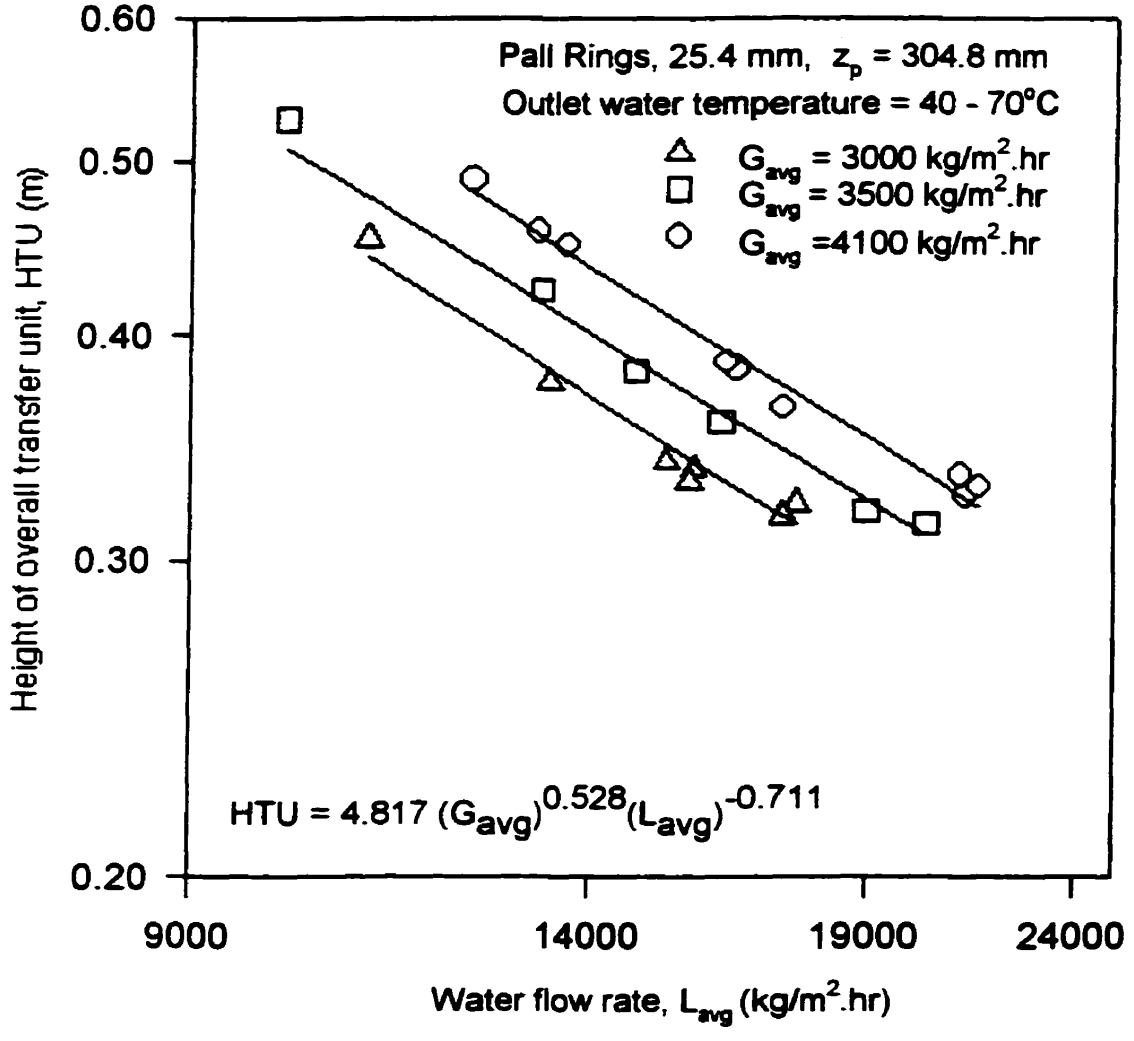

Fig(5.22): Effect of gas and liquid flow rates on the height of transfer unit.

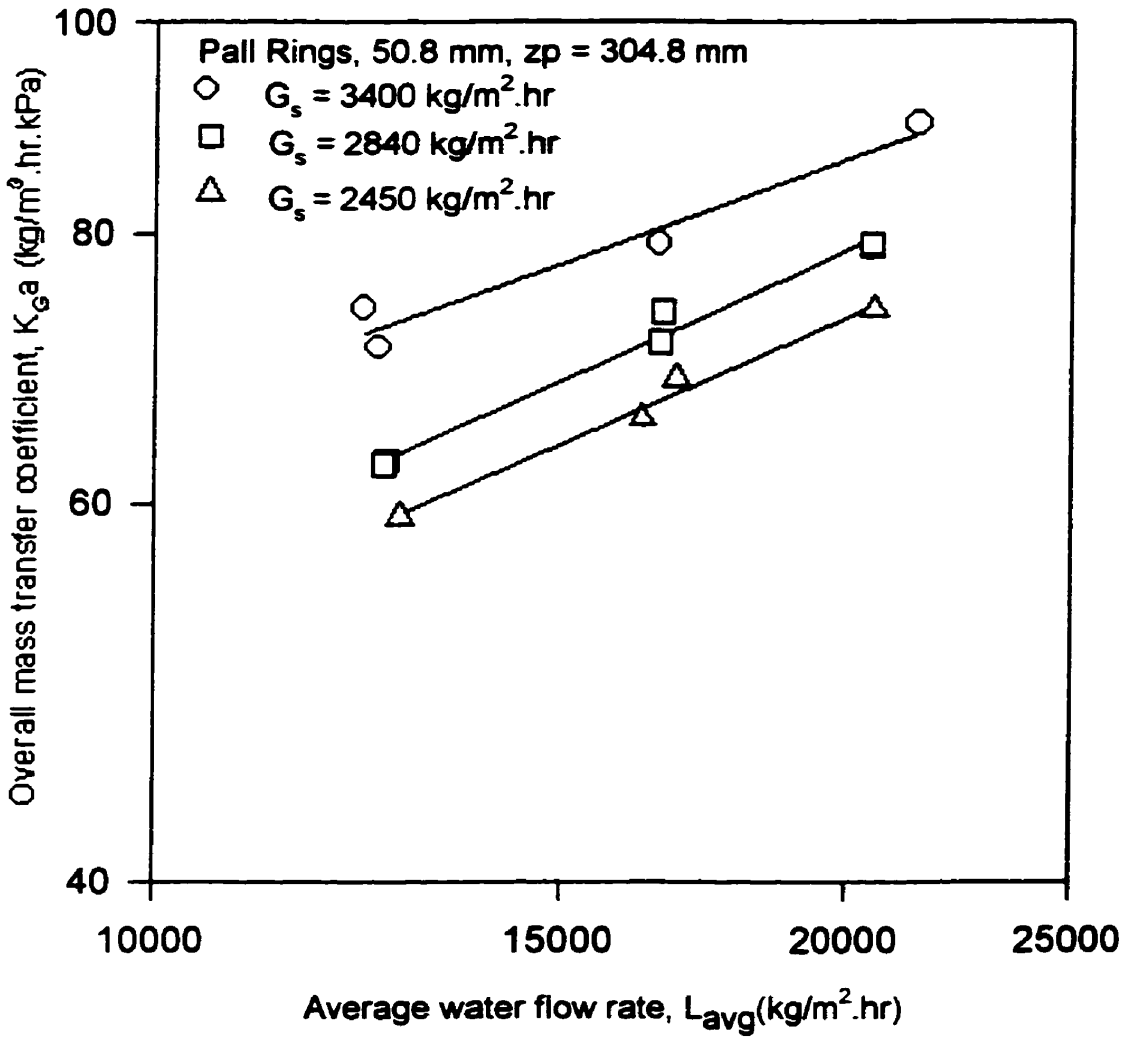

Fig(5.23): Variation of mass transfer coefficient in the second unit with liquid and gas flow rates, Pall Rings size = 50.8 mm.

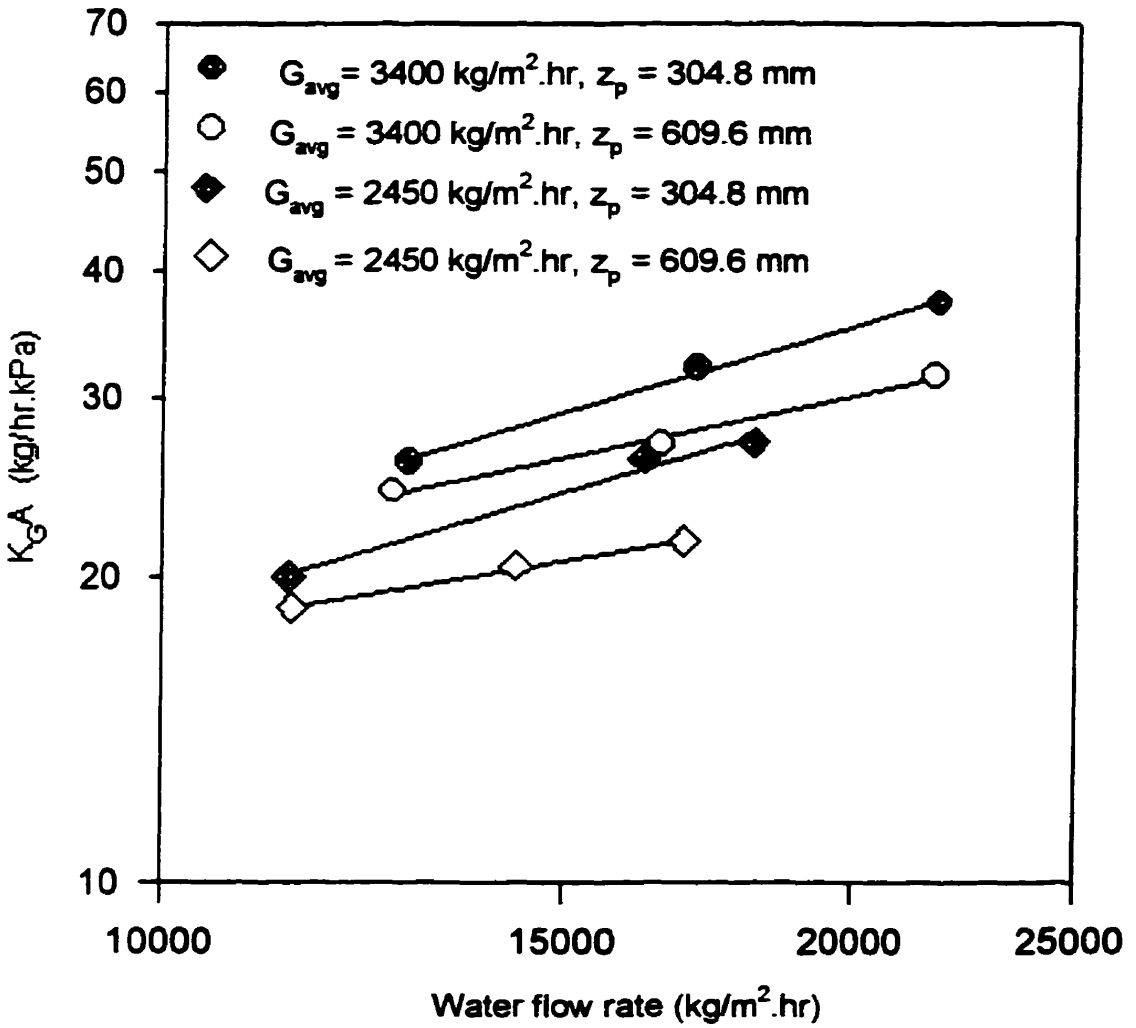

Fig(5.24): Effect of the height of packing on the rate of mass transfer.

5.2.3.2 Heat Transfer

Heat transfer between hot moist flue gases and cold water in the second unit has been analyzed using the volumetric overall heat transfer coefficient and the sensible heat transfer coefficient. The overall heat transfer coefficient has been calculated using equation (3.27a). The sensible heat gas transfer coefficient has been estimated as the sensible heat change of the gas per unit volume of the contacting section. The log-mean temperature difference between the gas and liquid at terminal conditions is used as the mean driving force. The sensible heat transfer represents less than 10 % of the total heat transferred.

Values of measured overall heat transfer coefficients are quite large and in the range of (30 - 100) $kW/m^3.\Delta_{LM}C$) varying with inlet gas enthalpy , inlet water temperature, and gas and liquid flow rates. Overall heat transfer coefficients obtained with 25.4 mm Pall rings are plotted against the average liquid flow rate at different gas flow rates on logarithmic coordinates. The data are fitted to straight lines for each operating condition as shown in Fig(5.25). The slopes of the lines are approximately 0.383, 0.405, and 0.412. The values of the slopes are affected by liquid and gas flow rates. The overall heat transfer coefficients are regressed as a power function of liquid flow rate, gas flow rate and gas enthalpy using the computer package, "Sigma Plot". The following approximate expression is obtained for 25.4 mm Pall rings:

$$Ua = 3.3 \times 10^{-4}(G_{avg})^{0.852}(L_{avg})^{0.400}(H'_g)^{0.691}(1.26/\rho_G)^{0.5} \qquad (5.3)$$

Where: Ua : Overall heat transfer coefficient ($kJ/m^3.hr.\ ^\circ C$)

H_g' : Inlet specific enthalpy of flue gases (kJ/k.mole)

The form of the equation is chosen to be similar to equation(3.58). Figure(5.26) shows a comparison between measured values of overall heat transfer coefficients and the calculated values using the above equation.

Sensible heat transfer coefficients are in the range of (2 - 6) $kW/m^3.^\circ C$. The variations of the height of heat transfer unit(equation 3.46b) with gas and liquid flow rates is shown in Fig(5.27). Comparisons between the measured sensible heat transfer coefficients obtained using 25.4 mm Pall rings and those predicted by the analogy(equation. 3.37) or by previous investigators are shown in Fig(5.28).

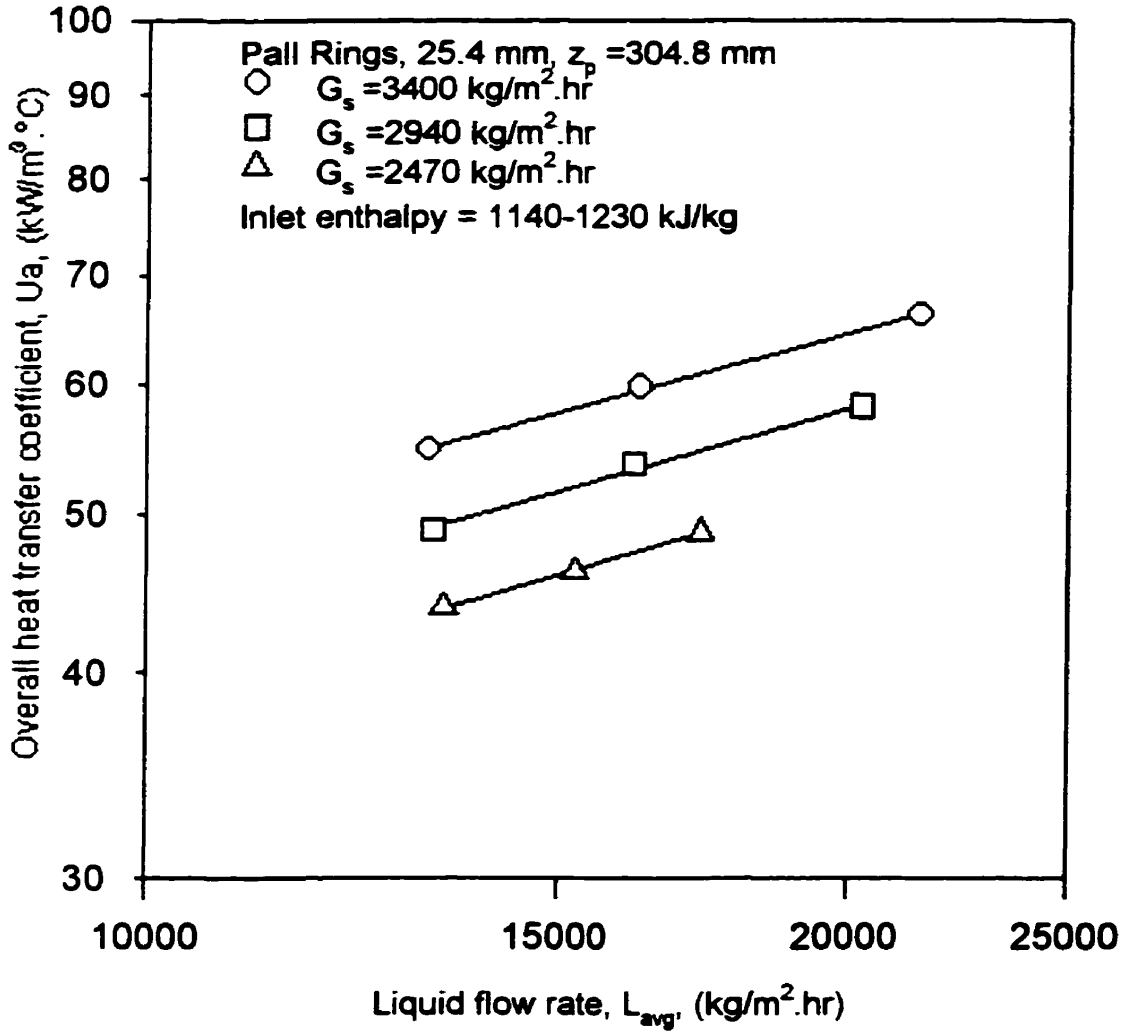

Fig(5.25): Overall heat transfer coefficient vs. liquid flow rates (2nd unit).

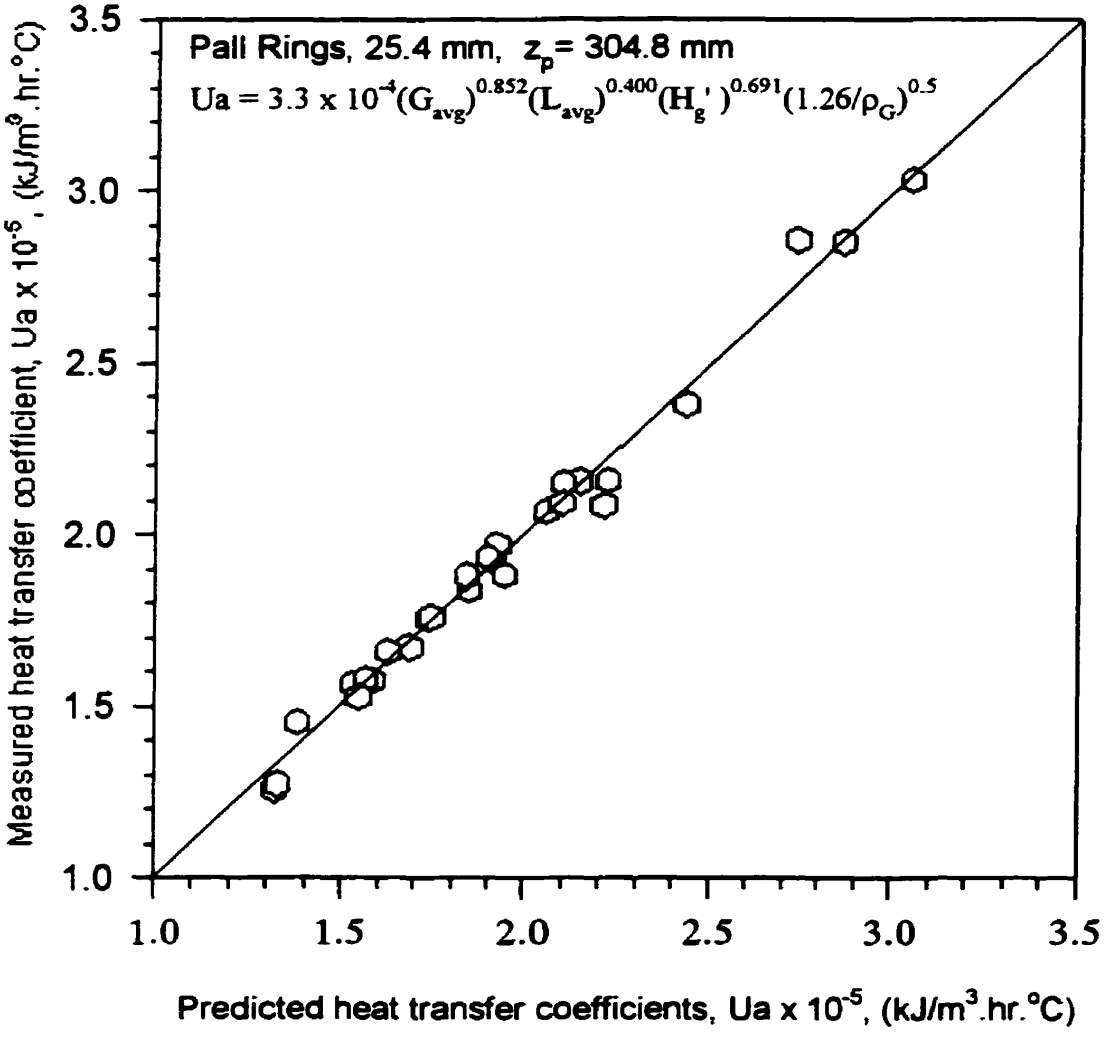

Fig(5.26): Parity plot, measured overall heat transfer coefficients vs predicted coefficients using (eq.5.3).

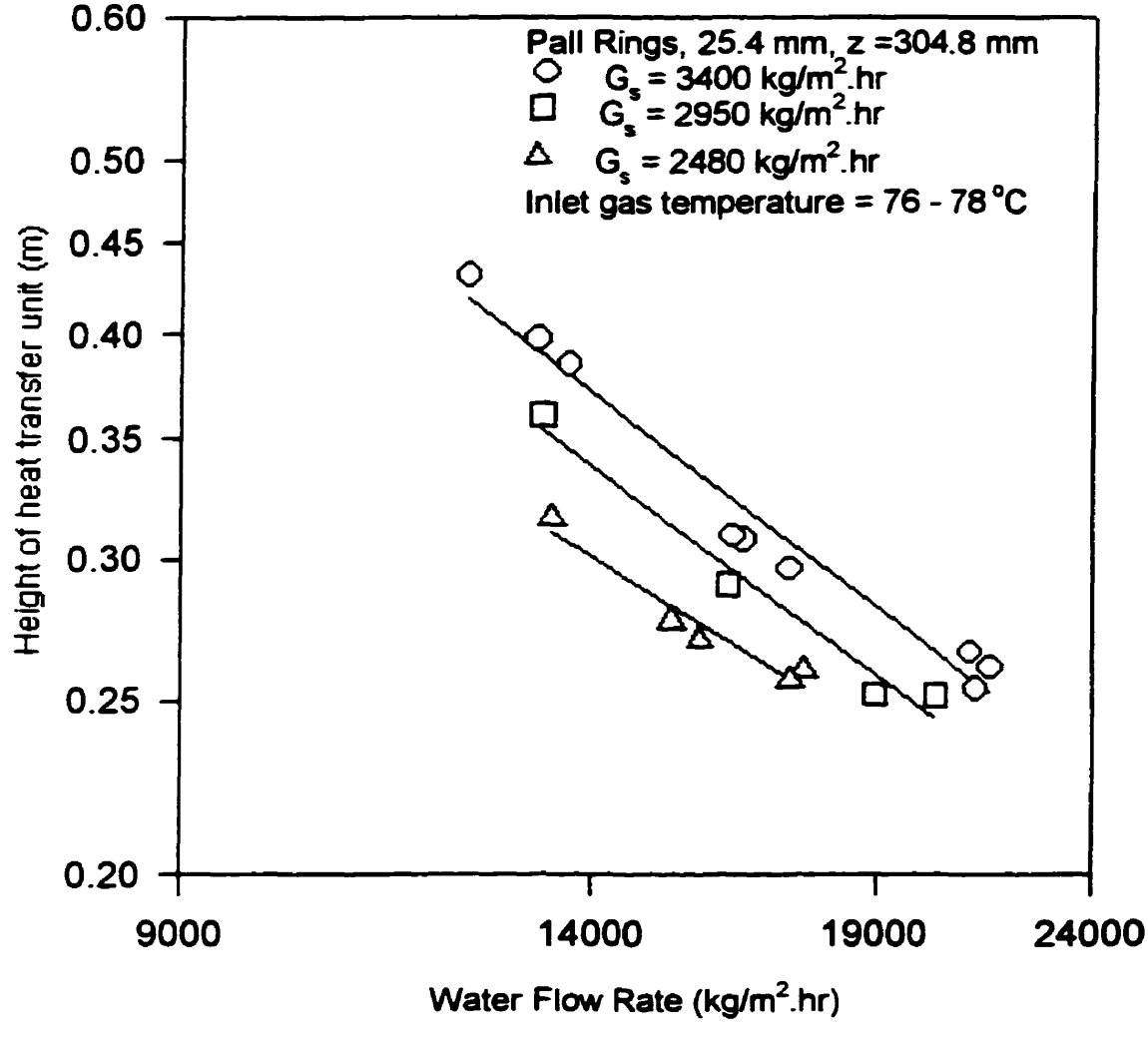

Fig(5.27): Variation of the height of heat transfer unit with gas and liquid flow rates in the 2nd unit.

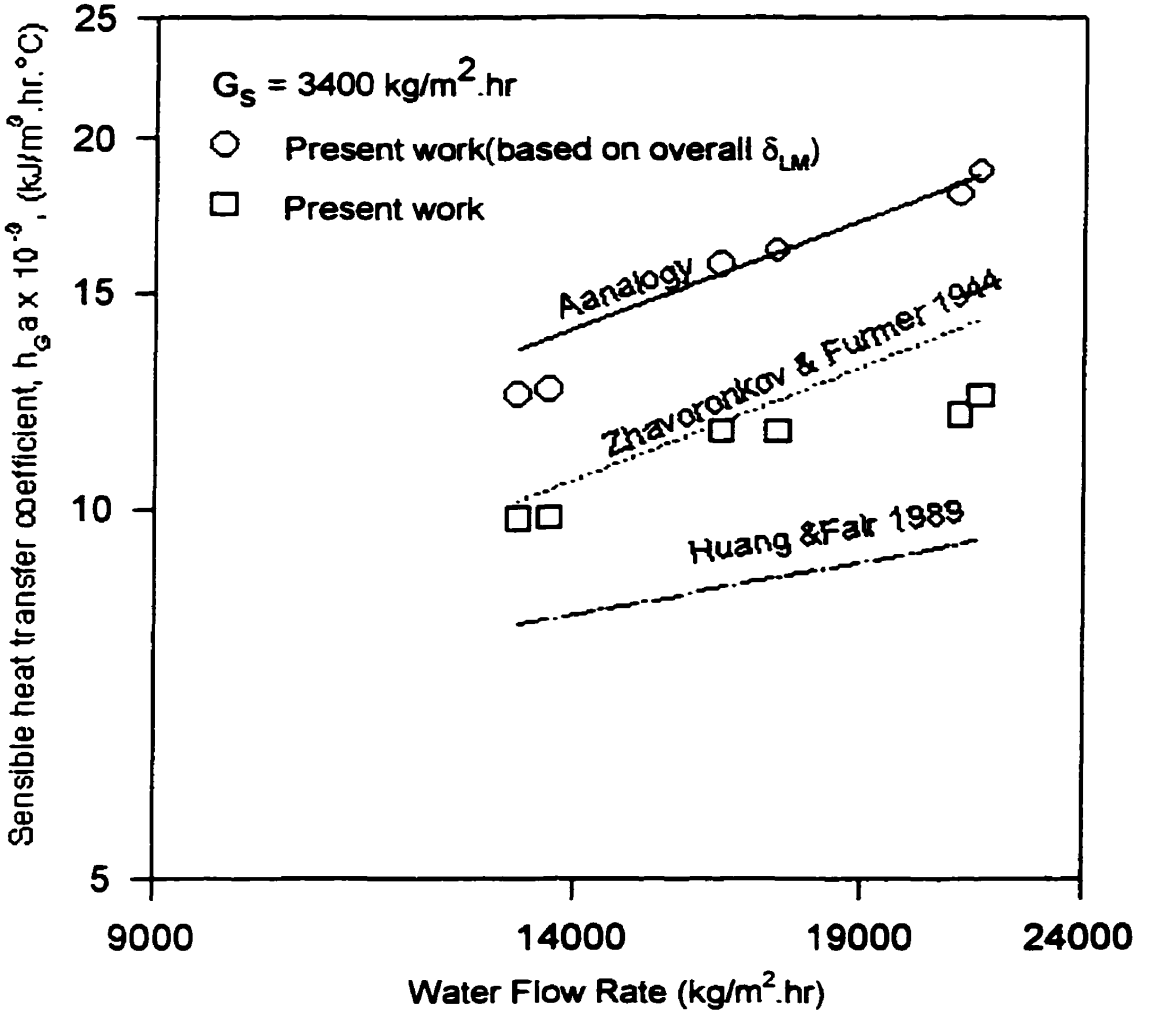

Fig(5.28): Comparsion of measured sensible heat coefficients with coefficients obtained by other investigations or methods.

□ Based on the mean value of (δ_{LM}) between bottom - 50% of heat is transferred level , 50% - 75 %, and 75% - top.

6.0 CONCLUSIONS AND RECOMMENDATIONS

1. Since the size of the first unit is determined by the size of the immersed firetube, a study of using ; a separate horizontal immersed firetube from the direct contact quenching section, a vertical fire tube, or a complete direct firing system is recommended All exposed parts of the firetube should be provided with double walls cooled by water.

2. The overall heat transfer coefficient between hot flue gases flowing through an immersed tube and water is in the range of (140 - 240) $kJ/m^2.hr.^oC$. The design of the tube based on the theoretical heat transfer principles and assumptions is practical and reasonable.

3. Quenching of hot dry gases by direct contact with water is very fast. The height of heat transfer unit is in the range of (0.15 - 0.25 m). It is function of the water temperature, water flow rate, and gas and air flow rates.

4. Since the liquid flow rate circulated through the first unit is approximately constant and very large and because of formation of solid deposits on the packing, it is recommended that the first direct contact section should be a spray tower or a packed tower filled with a bigger size of packing(50.8 mm). The design of water and gas distributors requires further investigation.

5. Complete combustion is obtained with (20 - 40) percentage excess air. There is a decreasing trend of the overall heat transfer coefficient and the thermal efficiency with increasing the level of excess air. The maximum firing rate is also reduced as the amount of excess air is increased.

6. Cooling of hot moist gases is also very fast. The height of transfer unit is in the range of (0.35 -0.55 m) varying with gas and liquid conditions. The heat and mass transfer analogy can be used to predict the transfer coefficients.

7. The total height of the second direct contact section should be not more than 1m. This includes 304.8 mm bed of 25.4 mm Pall rings, and two spray nozzles with a spray height of 304.8 mm. A cylindrical tower should be used to eliminate dry corners. The second unit could be located above the first unit.

7.0 NOMENCLATURE

Symbol	Meaning	Units
A	Cross section area	m^2
a	Interfacial area	m^2/m^3
C	Specific heat	kJ/kg.°C
Cp'	Volumetric specific heat	kJ/normal m^3. °C
C_s	specific heat	kJ/kg dry gas. °C.
D	Diameter	m
d	Differential operator	
F	Mass transfer coefficient	(General form)
f	heat transfer area/ mass transfer area	
G	Dry gas flow rate	kg/hr.
G_s	Superficial mass velocity of dry gas.	kg/m^2.hr
H	Specific enthalpy	kJ/kg
H'	Specific enthalpy	kJ/normal.m^3
HTU	Height of transfer unit	m
h_G	Heat transfer coefficient	kJ/m^2.hr.°C
h_Ga	Volumetric heat transfer coefficient	kJ/m^3.hr.°C
h'_Ga	Modified heat transfer coefficient	kJ/m^3.hr.°C
K_Ga	Volumetric mass transfer coefficient	kg/m^3.hr.(ΔP)
k_Ya	Volumetric mass transfer coefficient	kg/m^3.hr.(ΔY')
L	Superficial mass velocity of liquid	kg/m^2.hr
l	Tube length	m
Le	Lewis number (Equation 3.29)	
m	Empirical constant	
Nu	Nusselt number	
P_t	Total Pressure	kPa
P_A	Partial pressure of component A	kPa
P_{BM}	Logarithmic partial pressure of inert	kPa
N_A	Mass flux of component A	kg/m^2.hr
Pr	Prandtl number	
Q	Heat transfer rate	kJ/hr
q	heat transfer flux	kJ/m^2.hr
q_s	Sensible heat flux	kJ/m^2.hr
Re	Reynolds number	
t	Temperature	°C
Sr	Steam gas ratio	$m^3.H_2O$ vapor/ m^3dry gas
U	Overall heat transfer coefficient	kJ/m^2.hr.°C
Ua	Overall volumetric heat transfer coefficient	kJ/m^3.hr.°C
V_T	Total volume of contact	m^3
V_n	Flow rate of dry gases at normal conditions	Normal. m^3/hr

Symbol	Meaning	Units
x	Tube thickness	m
Y'	Humidity	kg.H_2O vapor/ kg.dry gas
Z	Height of direct contact	m
γ	Thermal conductivity	kJ/m.hr. °C
α	Ackermann correction factor	
$(\Delta t)_{LM}$	logarithmic mean temperature difference	°C
λ	Latent heat of vaporization	kJ/kg.
ρ_{ns}	density of water vapor at normal conditions	m^3/kg
ρ_{nG}	density of flue gases at normal conditions	m^3/kg
σ	Stefan Boltzmann constant(20412×10^{-8})	$J/m^2.hr.K^{-4}$
ε	Emissivty of gas	
η	Efficiency	
θ	Modified enthalpy potential	(Equation 3.33)
ζ	Absorptance of gas	
ω	A correction factor	(Equation 3.34)
Subscripts		
1 and 2	Positions 0, 1, and 2	
A	Substance A (water vapor)	
avg	Arithmetic average	
B	Substance B (dry flue gases)	
conv	Convection	
G	Gas	
H	Heat transfer	
i	Interface	
in	At the inlet	
L	Liquid	
m	Mass transfer	
n	Normal conditions (0°C, 101325Pa)	
o	At the reference temperature (0°C)	
out	At the outlet	
rad	Radiation	
t	Total	
w	At liquid water conditions.	
wall	At wall conditions.	
Superscripts		
-	Average	

8.0 REFERENCES

Ackermann, G., Warmeubergang und Molekulare Stofubtragung im gleichen Feld bei groben Tempertur und partialdruckdifferenzen, VDI-Forschungh. 382,1-16, 1937 (cited in Fair, 1972).

Bohn, M.S. and Swanson, L.W., A comparison of Models and Experimental Data of Pressure Drop and Heat Transfer in Irrigated Packed Beds, Int. J .Heat Mass Transfer, vol. 34, no. 10, pp. 2509-2519, 1991.

Bravo, J.L., Rocha, J.A., Fair, J.R., Mass Transfer in Gauze Packing, Hydrocarbon Processing, pp. 91-95, Jan. 1985.

Bras, G.H.P., Design of Cooler Condensers for Vapor-Gas Mixtures - I, Chem. Eng., pp. 223-226, April,1953.

Bras. G.H.P., A Graphical Method for Calculation of Cooler-Condenser, Chem. Eng. Sci., vol. 6, pp. 277-282, 1957.

Carey , W. F. and Williamson, B. A., Gas Cooling and Humidification: Design of Packed Towers from Small Scale Tests., Proc. Inst. Mech. Engs., vol. 163, pp..41- 53, 1950.

Chilton, T.H., and Colburn, A.P., Ind. Eng. Chem., vol. 26, pp. 1183, 1934 (Cited in Fair,1990).

Coker, A.K., Understand the Basics of Packed - Column Design, Chemical Engineering Progress, pp. 93-99, Nov. 1991.

Crib, G.S. and Nelson, E.T., The Simultaneous Transfer of Heat and Mass between Water and Moist Coal Gas, Chem. Eng. Sci., vol. 5, pp. 20-30, 1956.

Eckert, T.S., Selection of Proper Distillation Column Packing, Chem. Eng. Prog., vol. 66, no.3, pp. 39-44, 1970.

Fair, J.R., Designing Direct -Contact Coolers/Condensers, Chem.Eng. , vol. 79, no. 13, pp. 91-100, 1972.

Fair, J.R., Direct Contact Gas-Liquid Heat Exchange for Energy Recovery, Transaction of the ASME, vol. 112, pp. 216-222, Aug.1990.

Gambill, W. R., Chem. Eng. 74(18), 147,1967. Cited in [Sundstrom and DeMichiell 1971]

Heap, C.R., Direct Improvement in Water Heating, Gas Engineering & Management, pp.35 - 43, March 1992.

Hensel, S.L., Treybal, R.E., Adiabatic Humidifictaiion of Air with Water in a Packed Tower, Chem. En. Prog., vol. 48, no. 7, pp. 362 - 369, 1952.

Huang, C.C and Fair, J.R., Direct-Contact Gas-Liquid Heat Transfer in Packed Column, Heat Transfer Engineering, vol. 10, no. 2, pp. 19-28, 1989.

Griswold, J., Fuel, Combustion and Furnaces, McGraw-Hill Book Company, New York, 1946.

Kern, D.Q., Process Heat Transfer, McGraw-Hill Book Company Inc., New York, 1950.

Kreith, F. and Boehem, R.F. (Eds.), Direct -Contact Heat Transfer, Hemisphere, New York, 1988.

Laso, M.,and Bomio,P., Direct Contact Heat Transfer in Packed Column, Inst. Chem. Enger. Sympm. Series, Publ. by Inst. of Chemical Engineers, Davis Building, Rugby, England, vol.2, no. 128, pp. B95 -B102,1993.

Lewis, J.G., and White, R.R., Simplified Humidification Calculations Systems other than Air and Water, Ind.& Eng. Chem., vol. 45, no. 2, pp. 486-488, 1953.

Lydersen, A. L., Mass Transfer Practice, 1st ed., John Wiley & Sons., New York, 1983

Mersmann, A. and Deixler, A., Packed Columns, Ger.Chem. Eng., vol. 9, pp. 265-276, 1986.

McAdams, W.H., Pohlenz, J.B. and John, R.C., Transfer of Heat and Mass Between Air and Water in Packed Column, Chem.Eng.Prog., vol. 45, no. 4, pp. 241-252, 1949.

McAdams, W.H., Heat Transmission, 1st & 3rd ed., McGraw-Hill Book Company, New York, 1942 and 1954.

McCabe, W.L. and Smith, J.C., Unit Operation of Chemical Engineering, McGraw-Hill Book Co., New York, 1967.

Mickley, H.S., Design of Forced Draft Air Conditioning Equipment, Chem.Eng.Prog, vol. 45, no. 12, pp. 739-745, 1949.

Mizushina,T., Hashimoto, N. and Nakajima, M., Design of Cooler Condensers for Vapor-Gas Mixtures, Chem. Eng. Sci., vol. 9, pp. 195-204, 1959.

Nemunatitis, R.R. and Eckert, J.S., Heat Transfer in Packed Towers, Chem.Eng.Prog., vol. 71, no. 8, pp. 60-67, 1975.

Onda, K., Takeuchi, H. and Okumoto,Y., Mass Transfer Coefficients between Gas and Liquid Phases in Packed Columns, Journal of Chemical Engineering of Japan, vol.1, no.1, pp. 56-62, 1968.

Parekh, M.Sc.D, Report in Chemical Engineering, Massachuusetts Institute of Technology, 1941.[Cited in McAdams 1942].

Patrick, E.A.K. and Thornton, E., Immerison Tube Heating of Aqueoues Liquids, Trans. Inst.Gas. Eng., vol. 108, 1958. [Cited in Prithchard et.al 1977].

Prithchard, R., Guy, J.J. and Connor N.E., Handbook of Industrial Gas Utilization 1st ed., Van Nostrand Reinhold Ltd, New York, 1977.

Rao, D. N., and Mohtadi, M. F., PhD Thesis, A novel Direct Contact Heat Exchange System for Efficient Heating of Water., August 1982, Department of Chemical and Petroleum Engineering, University of Calgary , Calgary, Alberta, Canada.

Sherwood, T.K., Pigford, R.L, Wike, C.R., Mass Transfer, 3rd ed., McGraw-Hill Book Company, New York, 1975.

Stecher, P.G., Industrial and Institutional Waste Heat Recovery, Noyes Data Corporation, New jersy, 1979.

Sundstrom, D.W., and DeMichiell, R.L., Quenching Processes for High Temperature Chemical Reactions, Ind. Eng. Process Des. Develop.,vol. 10, no. 1, 1971.

Treybal, R.E., Mass Transfer Operation, 2nd ed., McGraw -Hill Book Company, New York, 1968.

Whitaker, S., Forced Convection Heat Transfer Relations for flow in pipes, Past Flat Plates, Single Cylinders, Single Spheres and for Flow in Packed Beds and Tube Bundles, A.I.Ch.E. Journal, vol. 18, no. 2., pp. 361-371, 1972.

Yohida, F., and Tanaka, T., Air Water Contact Operations in a Packed Column, Ind. Eng. Chem., vol. 43, no., 6, pp. 1467-1473, 1951.

Zhavoronkov, N.M. and Furmer, I.E., Heat Transfer in Packed Scrubbers and Towers., Khimicheskaya Prom., vol. 12., pp. 7 - 9, 1944 [Cited in Haung &Fair 1989].

9.0 APPENDICES

Appendix A Sample Calculation

Average input and Output readings of run no. 14 to be used in the sample calculation are shown in Appendix (B). The following equations are used in energy and material balances:

Water enthalpy = $L(4.19)(t_L)$

Flue gas enthalpy = $G_s[(1.04 + 1.88\ Y')(t_G) + 2501.6\ Y']$ for gas temperatures(0-100 °C)

Heat losses = $h_G\ A\ (t_{wall} - t_{air})$. The heat transfer coefficient inclueds both convection and radiation and is obtained from [Stecher 1979]

Vapor content of saturated flue gases is calculated using regressed relations given by Lydersen 1983]

Physical and chemical properties of fuel and flue gases are obtained from[Griswold 1946]

A computer Package called Sigma Plot is used in the calculation of the results of all runs.

7.1 Combustion Calculation

Fuel gas flow rate = 72.38 m^3/hr at (15.6°C, 101.325 kPa) = 3.05 k.mole/hr = 48.9 kg/hr.

Average heating value = 37591 kJ/m^3. [Griswold et.al 1946]

Heat generated by combustion = (37591)(72.38)= 2,720,837 kJ/hr.

O2% by mole in the dry flue gas = 4.67 % (measured)

Based on complete combustion, the percentage excess air = 25.6%

Amount of oxygen in the flue = 0.512 k.mol/k.mol of fuel.

Amount of air entering the burner = (2.512)(4.76)(3.05)(28.84) = 1052 kg/hr

Water content of air = 0.00238 kg.water/kg.dry air. (measured)

Air temperature = 19 °C, Enthalpy of air = 26, 767 kJ/hr

Total input enthalpy = 2, 720,837 + 26,767 = 2,747,604 kJ/hr.

Adiabatic flame temperature = 1730°C. (Obtained using a computer package called HSC)

Flue gas formed = [2 + 1 + (2.512)(3.76) + 0.512](3.05) = 39.62 kmol/hr = 1101 kg/hr.

Dry flue gas = 33.4 kmol/hr = 991 kg/hr.

Water vapor formed = (2)(3.05)(18) + (0.00238)(1052) = 112.3 kg/hr = 6.34 kmol/hr.

Initial water content of flue gases = (112.3)/(991) = 0.11332 kg.water/kg.dry gas.

Dew point of flue gases ≅ 60°C. , 101.325 kPa. (Steam Tables)

7.2 Second unit

Mass and energy balances

Inlet water flow rate = 5792 kg/hr

Inlet water temperature = 13.7°C

Inlet water enthalpy = 332,478 kJ/hr

Outlet flue gas temperature = 31.3°C (saturated).

Outlet flue gas humidity = 0.02873 kg.water/kg.dry gas (Steam Tables)

Outlet flue gas enthalpy = 105,159 kJ/hr.

Inlet flue gas temperature = 77.8 °C.

Outlet water temperature = 55 °C.

Average surface temperature = 54.7 °C, heat transfer coefficient = 40.9 kJ/m^2.hr.°C.

Surface area(walls) = 5.39 m^2.

Heat lost through the walls = 7870 kJ/hr

Heat lost through the inter-connecting pipe = 5526 kJ/hr and is calculated based on the following data: Max. surface temperature = 77.8 °C

Heat transfer coefficient = 53.1 kJ/m^2.hr.°C. Area = 1.77 m^2.

Total heat lost = 13,396 kJ/hr.

Solving the energy balance around the second unit with the water content of the inlet flue gas as the only unknown,

Water content of inlet flue gas = 0.43107 kg. water/kg. dry gas.

Inlet flue gas enthalpy = 1,211,326 kJ/hr.

Water condensed = (0.43107 - 0.02873)(991) = 399 kg/hr

Outlet water flow rate = 399 + 5792 = 6192 kg/hr.

Outlet water enthalpy = 1,426,946 kJ/hr

Rate of mass transfer

Height of packing section = 610 mm.

Total height of the contact section = 1219 mm

Cross section area = 0.348 m^2.

Volume of the contact section = 0.425 m^3.

Values of enthalpy driving forces are calculated at the bottom, top, and at a point where 50% of total heat is transferred and are shown in Table A1. In calculating the enthalpy driving force at the middle point it is assumed that the flue gas is saturated. The value of the driving force at 75% of heat is transferred is added for illustration. The mean driving force is obtained from a chart devised by [Williamson and Carey 19] as follows,

Ratio of driving force at the middle to that at the top = 5.73

Ratio of driving force at the middle to that the bottom = 0.864

From the chart, the mean driving force = 0.72 (481) = 346.

Overall mass transfer coefficient, K_Ga ,

K_Ga = 1.662 kg/m^3.s.atm = 59 kg/m^3.hr.kPa. (Equation.3.45)

Height of transfer unit, HTU,= $G_s/P_{BM}kGa$

G_S = 991/0.348 = 0.79 kg/m^2.s = 2848 kg/m^2.hr.

P_{BM} is calculated as the arithmetic mean between the logarithmic mean of partial pressures of dry gas in the gas film at each end of the unit.

P_{BM} = 0.84 atm = 85.113 kPa.

HTU = 0.573 m.

Table A1 Calculations of the enthalpy driving forces along the second unit.

Location	t_G °C	S_{rG} m^3.H_2O/ m^3.dry gas	H'_G kJ/m^3	t_L °C	S_{rw} m^3.H_2O/ m^3. dry gas	H'_w kJ/m^3	$H'_G/1+S_{rG}) - H'_w/(1+S_{rw})$ driving force
Bottom	77.8	0.710	1617	55.0	0.183	459	557
50%	67.1	0.372	878	35.0	0.059	169	481
75%	57.0	0.206	509	24.5	0.031	98	328
Top	31.3	0.047	140	13.7	0.016	51	84

Rate of heat transfer

Δt_{LM} = 19.7 °C

Overall heat transfer coefficient = (change of enthalpy of water)/(Δt_{LM})(volume).

= 130,722 kJ/m^3.hr.°C = 36.3 kW/m^3.°C.

Average sensible heat of flue gases = 1.47 kJ/kg.°C. [Griswold 1946]

Sensible heat change of flue gases = (991)(1.47)(77.8 - 31.3) = 67,740 kJ/hr.

Sensible heat transfer coefficient, $h_G a$, = (67,740)/[(19.7)(0.425)] = 8091 kJ/m^3.hr.°C

= 2.25 kW/m^3.°C.

Height of heat transfer unit = $G_s C_s/(h_G a)$ = (2848)(1.47)/(8091) = 0.517 m.

7.3 First unit

Heat and mass balances

Onlet flue gas enthalpy = 1,211,326 kJ/hr.

Inlet water temperature = 75.6 °C , Inlet water flow rate = 56,295 kg/hr

Inlet water enthalpy = 17,832,229 kJ/hr

Total heat input = 2,747,604 kJ/hr .

Water evaporated = (0.43107 - 0.11332)(991) = 315 kg/hr.

Outlet water flow rate = 56,295 - 315 = 55,980 kg/hr.

Outlet water temperature = 82.4 °C , Outlet water enthalpy = 19,327,431 kJ/hr.

Heat losses = 2,747,604 - (19,327,431 - 17,832,229 + 1,211,326) = 41,076 kJ/hr.

Surface temperature = 78.6 °C , heat transfer coefficient = 54.2 kJ/hr.m^2.°C,

surface area = 11.9 m^2. Calculated heat losses = 38,441 kJ/hr.

Total heat used =19,327,431 - 17,832,229 + 1,211,326 + 38,441 = 2,744,969 kJ/hr

% heat balance closure = [2,747,604 - 2,744,969)/ 2,747,604](100) = + 0.1%

Rate of heat transfer in the immersed firetube:

Area = 3.54 m^2.

Flue gas temperature at the exit of the firetube = 960 °C (measured)

Specific heat of water vapor = 2.388 kJ/kg.°C. (McAdams et.al 1954)

Specific heat of dry gases = 1.26 kJ/kg.°C. (McAdams et.al 1954)

Enthalpy of the flue gases at the exit of the fire tube

= 991{[1.26 + (2.388)(0.11332)](960) + (2501.6)(0.11332)} = 1,737,089 kJ/hr.

Heat losses = (5.4)(54.2)(82 - 19) = 18,439 kJ/hr

Solving the energy balance around the firetube:

Enthalpy of water leaving the packing = 18,335,355 kJ/hr

Water temperature = 78.2 °C

Δt_{LM} = 1226 °C

Heat transfer coefficient = (change of water enthalpy)/(Area)(Δt_{LM})

= 229 kJ/hr.m^2.°C = 63.5 W/m^2.°C.

Efficiency% = [(Change of water enthalpy)/(total heat input](100) = 36 %

Convective heat transfer

Re = 14,370, Pr = 0.77

Average gas temperature = (1730 + 960)/2 = 1345 °C = 1618.15^{0}K.

Convective heat transfer coefficient = 43.8 kJ/m^2.hr.°C (Equation.3.5)

Rate of heat transfer by convection = (43.8)(3.54)(1345 - 82.4) = 195,769 kJ/hr.

Radiation heat transfer:

Beam length = 0.9(tube diameter)

Gas emissivity = 0.125, Wall emissivity = 0.8 [Pritchard et.al 1977]

Rate of heat transfer by radiation = 557,335 kJ/hr (Equation.3.6)

Radiation heat transfer coefficient = 557,335/(3.54)(1345 - 82.4) = 125 kJ/hr.m^2.°C.

Total rate of heat transfer = 753,104 kJ/hr.

Enthalpy of flue gases leaving the firetube = 2,747,604 - 753,104 = 1,994,500 kJ/hr.

Calculated flue gas temperature = 1118 ° C > 960 ^{0}C.

Rate of heat transfer in first direct contact section:

Area = 1.1148 m^2., Height of packing = 457 mm, Total height of contact = 1067 mm.

Total Volume of contact = 1.19 m^3., Δt_{LM} = 145.9 °C.

Change in water enthalpy in the section = 18,335,355 - 17,832,229 = 504,126 kJ/hr.

Overall heat transfer coefficient = (504,126)/[(145.9) (1.19)]

= 2899 kJ/m^3.hr.°C = 805 W/m^3.°C.

Average specific heat of gases = 1.68 kJ/kg. Dry gas. ^{o}C. [McAdams 1954]

Sensible heat transfer coefficient

= [(991)(1.68)/(1.19)]ln{(960-78.2)/(77.8 - 75.6)} (Equation. 3.27b)

= 8385 kJ/m^3.hr.°C = 2330 W/m^3.°C.

The Dimensionless Temperature Parameter, DTP,

in the direct contact section

= (78.2 -75.6)/(75.6) = 0.0344.

and in the whole unit, DTP = (82.4 -75.6)/(75.6) = 0.09.

Appendix B Summary of some of experimental results

Appendix B1: Experimental results of the first unit obtained with 26% excess air and an average liquid flow rate 56 m^3/hr

Run	T_{Gi} °C	T_{gout} °C	Y'_{Gout} kg / kg.gas	T_{lin} °C	T_{lout} °C	Fuel m^3/hr	Q_{in} *106k J/hr	η% 1st unit	η% tube	η% Heater	h_{Gi} tube $W/m^2.°C$	Ua direct $W/m^3.°C$	$h_{Gi}a$ direct $W/m^3.°C$
1	869.0	79.9	0.495	78.9	83.1	47.5	1.8	48	42	94	51	271	1786
2	869.0	80.4	0.512	79.4	83.5	47.2	1.8	47	42	95	51	215	1774
3	869.0	80.2	0.504	79.2	83.3	47.0	1.8	48	42	95	50	238	1757
5	860.0	75.8	0.383	74.9	79.5	46.3	1.8	59	41	95	49	612	1648
6	891.0	80.2	0.522	79.1	83.8	54.5	2.1	46	40	96	56	274	2031
7	891.0	79.3	0.483	77.9	82.8	54.4	2.1	50	40	96	55	402	1903
8	917.0	77.3	0.432	75.6	81.5	60.0	2.3	55	39	96	59	678	2006
9	917.0	77.2	0.428	75.5	81.3	59.7	2.3	55	39	96	58	681	1990
10	917.0	76.9	0.421	75.1	81.0	59.6	2.3	56	39	95	58	706	1968
11	917.0	76.5	0.409	74.7	80.7	59.5	2.3	57	39	94	58	746	1945
12	949.0	78.6	0.455	76.3	82.8	70.5	2.7	52	36	96	63	689	2286
13	960.0	78.3	0.453	76.3	82.9	71.6	2.7	53	37	95	64	721	2361
14	960.0	77.8	0.431	75.6	82.4	72.4	2.7	54	36	94	64	803	2343
15	960.0	77.5	0.418	75.3	82.2	72.4	2.7	56	36	93	63	842	2311
16	960.0	77.0	0.417	75.0	81.8	71.0	2.7	56	36	96	62	868	2293
17	965.0	73.3	0.324	70.3	78.2	71.8	2.7	66	37	96	63	1213	2052
18	965.0	72.8	0.316	69.8	77.8	72.3	2.7	66	36	96	63	1249	2069
19	958.0	72.0	0.282	68.7	76.8	72.4	2.8	69	35	96	62	1343	2010
20	958.0	71.5	0.280	68.3	76.3	71.9	2.7	69	36	96	62	1354	1988
21	967.0	71.0	0.273	67.9	76.0	71.7	2.7	70	35	96	61	1387	1990
22	958.0	70.7	0.261	67.3	75.7	72.4	2.8	71	36	95	63	1425	1964
23	940.0	66.2	0.191	62.4	71.2	72.3	2.7	78	37	96	64	1610	1826
24	940.0	64.8	0.176	60.6	69.6	72.4	2.7	79	37	96	64	1641	1779

Appendix B2: Experimental results of the first unit obtained with 40% excess air.

Run	T_G °C est.	T_{gout} °C	Y'_{Gout} kg / kg.gas	T_{lin} °C	T_{lout} °C	Fuel m^3/hr	Q_{in} $*10^{-6}$ kJ/hr	Water m^3/hr	η% 1st unit	η% tube	η% Heater	h_G tube $W/m^2.°C$	Ua direct $W/m^3.°C$	h_Ga direct $W/m^3.°C$
1	856	76.6	0.393	75.2	80.6	55.8	2.1	51	52	36	96	54	601	2065
2	855	76.3	0.391	74.9	80.3	55.5	2.1	51	52	36	96	54	608	2057
3	857	74.8	0.347	73.2	78.9	56.1	2.1	52	57	35	96	53	773	1977
4	855	78.0	0.436	76.9	81.6	55.5	2.1	56	48	37	95	55	457	2182
5	855	78.2	0.438	77.1	81.7	55.5	2.1	56	47	36	96	55	435	2193
6	852	80.3	0.522	79.6	83.4	54.6	2.1	57	38	37	95	54	44	2375
7	854	76.8	0.398	75.4	80.7	55.1	2.1	51	51	36	95	54	572	2055
8	882	74.5	0.346	72.4	79.1	64.4	2.5	52	58	34	94	59	923	2176
9	881	76.3	0.398	74.4	80.6	63.8	2.4	52	52	35	95	59	706	2265
10	882	76.1	0.390	74.3	80.5	64.0	2.4	53	53	35	97	59	745	2274
11	882	74.7	0.355	72.6	79.2	64.3	2.5	53	57	35	96	59	902	2202
12	883	74.5	0.350	72.5	79.0	64.6	2.5	53	57	34	93	59	923	2203
13	887	77.5	0.427	75.9	81.5	66.1	2.5	56	49	34	97	60	610	2465
14	887	77.3	0.422	75.7	81.4	66.0	2.5	56	49	35	96	61	648	2452
15	887	77.2	0.417	75.5	81.3	66.2	2.5	56	50	34	94	61	667	2442
16	911	74.8	0.353	72.2	80.1	77.3	2.9	53	57	33	94	67	1106	2552
17	911	75.1	0.361	72.5	80.3	77.1	2.9	53	56	33	96	66	1057	2555
18	911	75.5	0.367	72.9	80.5	77.1	2.9	53	55	33	97	66	1017	2564
19	910	76.2	0.388	73.6	81.2	76.3	2.9	51	53	33	96	66	904	2573
20	910	75.8	0.380	73.2	80.8	76.3	2.9	51	54	33	94	66	944	2552
21	908	75.3	0.370	72.7	80.4	75.7	2.9	52	55	33	96	66	988	2519
22	910	76.9	0.403	74.8	81.6	76.4	2.9	56	51	33	93	66	855	2695
23	909	77.6	0.429	75.6	82.1	76.0	2.9	56	49	33	97	66	733	2747
24	905	80.7	0.528	79.6	84.2	73.7	2.8	64	38	34	96	66	213	3093

Table B3 : Experimental Results for the second unit . Pall Rings 25.4 mm, Z = 0.3048 m.

t_{Gin} °C	Y'_{Gin} kg/kg drygas	t_{Gout} °C	Y'_{Gout} kg/kg. drygas	$t_{L.in}$ °C	$t_{L.out}$ °C	G_s kg/m^2. s	H_G' kJ/kg. drygas	L_{avg} kg/m^2. s	η%	K_Ga kg/m^{3}s .atm	HTU m.	U_{OG} kW/m^3 .°C	h_G kW/m^3. °C	h_G analog kW/m^3. °C.
76.6	0.391	14.4	0.010	5.4	43.8	0.69	1113	4.4	95	2.35	0.34	43.5	3.7	3.6
76.3	0.388	29.1	0.025	5.4	56.9	0.69	1106	3.0	90	1.80	0.45	34.9	2.7	2.4
76.3	0.388	12.5	0.0088	5.3	39.6	0.69	1106	4.9	96	2.43	0.32	43.7	3.8	3.7
74.8	0.345	12.8	0.009	5.4	40.0	0.69	988	4.3	95	2.37	0.33	40.3	3.7	3.6
78.0	0.433	21.0	0.015	5.2	53.7	0.69	1228	3.7	94	2.15	0.38	43.9	3.3	3.2
78.2	0.435	13.3	0.0093	5.1	43.9	0.69	1234	4.8	96	2.51	0.32	48.8	3.9	3.9
78.0	0.429	16.0	0.011	5.1	48.0	0.68	1217	4.2	95	2.34	0.34	46.1	3.6	3.6
80.5	0.519	11.1	0.008	5.2	40.1	0.67	1460	6.3	97	2.76	0.29	58.0	4.3	4.4
76.1	0.387	12.7	0.0089	5.3	41.8	0.79	1104	5.3	96	2.84	0.32	52.2	4.4	4.4
74.7	0.353	18.6	0.013	5.4	47.5	0.79	1009	4.1	94	2.39	0.38	42.4	3.7	3.5
74.5	0.348	35.7	0.037	5.5	60.8	0.80	996	2.8	85	1.80	0.53	35.4	2.7	2.3
74.5	0.347	35.7	0.037	5.5	60.7	0.80	995	2.8	85	1.80	0.53	35.4	2.7	2.3
77.5	0.424	12.9	0.0091	5.1	43.6	0.82	1202	5.6	96	3.00	0.31	58.1	4.7	4.7
77.3	0.419	18.3	0.013	5.1	51.7	0.82	1189	4.5	95	2.67	0.36	53.7	4.1	4.1
77.2	0.414	27.2	0.022	5.2	59.6	0.82	1177	3.7	92	2.30	0.42	48.9	3.5	3.3
74.8	0.351	33.1	0.032	5.6	61.3	0.95	1004	3.4	87	2.33	0.49	46.5	3.5	3.1
75.1	0.358	19.6	0.014	5.4	51.0	0.95	1025	4.6	94	2.87	0.38	53.5	4.4	4.3
75.5	0.365	13.0	0.0091	5.4	42.4	0.95	1042	5.9	96	3.34	0.33	59.9	5.2	5.2
75.8	0.377	29.3	0.025	5.3	60.0	0.94	1076	3.8	90	2.49	0.45	51.0	3.8	3.5
76.2	0.385	18.8	0.013	5.3	51.5	0.94	1097	4.8	94	3.00	0.37	57.4	4.6	4.5
76.1	0.385	14.1	0.010	5.2	44.0	0.94	1097	5.9	96	3.24	0.34	59.9	5.0	5.0
76.9	0.401	32.9	0.032	5.3	64.3	0.94	1140	3.7	89	2.50	0.46	54.7	3.7	3.4
77.1	0.405	21.9	0.016	5.2	56.3	0.94	1153	4.5	94	2.88	0.39	59.7	4.4	4.4
77.6	0.426	14.5	0.010	5.1	46.8	0.94	1208	6.0	96	3.31	0.33	66.1	5.1	5.2

Table B4 : Experimental results for second unit. Pall Rings 50.8mm Z = 0.3048 m

t_{Gin} °C	Y'_{Gin} kg/kg drygas	t_{Gout} °C	Y'_{Gout} kg/kg. drygas	t_{Lin} °C	t_{Lout} °C	G_s kg/m^2. s	H_G' kJ/kg. drygas	L_{avg} kg/m^2. s	η%	k_Ga kg/m^2. s	HTU m.	U_{OG} kW/m^3 .°C	h_G kW/m^3. °C	h_G analog kW/m^3. °C.
79.7	0.424	24.1	0.018	2.0	41.1	0.68	1207	4.5	93	1.85	0.43	28.3	2.0	2.9
81.4	0.516	37.4	0.041	1.9	58.6	0.69	1453	3.6	89	1.69	0.50	33.7	1.8	2.5
81.5	0.533	28.6	0.024	1.8	48.7	0.68	1499	4.7	93	1.93	0.43	35.1	2.1	2.9
81.5	0.538	22.9	0.017	1.7	41.4	0.69	1512	5.7	95	2.08	0.39	36.2	2.3	3.2
79.1	0.398	34.9	0.035	2.1	53.6	0.79	1138	3.5	88	1.77	0.53	29.8	1.9	2.7
79.0	0.408	25.9	0.021	1.9	44.4	0.79	1163	4.6	92	2.02	0.46	32.1	2.3	3.1
78.9	0.418	20.9	0.015	1.8	37.7	0.79	1190	5.7	94	2.22	0.41	33.7	2.5	3.5
78.0	0.420	20.8	0.015	1.8	37.9	0.79	1194	5.7	94	2.23	0.41	34.3	2.5	3.5
77.6	0.400	34.7	0.035	1.9	53.4	0.79	1139	3.5	88	1.76	0.53	30.5	1.9	2.7
77.9	0.406	26.2	0.021	1.8	43.9	0.79	1155	4.6	92	2.00	0.46	31.7	2.2	3.1
77.9	0.356	38.1	0.043	1.9	60.2	0.97	1024	3.3	84	2.01	0.57	35.2	2.3	3.0
77.4	0.364	29.5	0.026	1.8	44.4	0.98	1043	4.9	90	2.22	0.51	33.0	2.4	3.5
76.8	0.374	26.0	0.021	1.8	39.8	0.97	1068	5.8	92	2.35	0.48	34.6	2.5	3.7
80.9	0.521	32.0	0.030	1.8	50.2	0.94	1467	6.0	92	2.47	0.46	45.4	2.6	3.7
80.8	0.506	39.3	0.046	1.8	59.8	0.94	1428	4.6	88	2.22	0.52	45.5	2.3	3.3
80.6	0.479	43.2	0.057	1.9	67.5	0.94	1355	3.7	85	2.18	0.54	48.2	2.4	3.1
78.6	0.453	26.0	0.021	1.8	45.7	0.95	1281	6.0	93	2.57	0.44	43.9	2.9	3.9
78.4	0.438	33.6	0.033	1.9	54.5	0.95	1242	4.6	90	2.28	0.50	41.8	2.5	3.4
78.5	0.425	43.8	0.059	1.9	64.7	0.96	1207	3.4	83	1.99	0.59	41.3	2.1	2.9
77.8	0.409	41.9	0.053	1.9	62.6	0.96	1165	3.5	84	1.99	0.59	39.7	2.2	2.9

Table B5 : Experimental Results for the second unit . Pall Rings 25.4 mm, Z = 0.6096 m.

TGin °C	Y'G kg/kg.dry gas	tGout °C	Y'Gout kg/kg dry gas	tLin °C	tLout °C	Gs $kg/m^2.s$	HGin kJ/kg	Lavg $kg/m^2.s$	kga $kg/m^3.s$	HTU (m)
80.9	0.547	35.9	0.037	11.7	59.0	0.50	1536	3.3	1.06	0.58
76.9	0.406	28.8	0.025	9.7	46.4	0.51	1153	3.3	1.02	0.58
75.8	0.383	25.3	0.020	9.6	42.5	0.51	1093	3.5	1.04	0.56
73.7	0.327	14.0	0.001	12.2	29.5	0.51	940	6.1	1.49	0.38
73.1	0.315	19.1	0.014	12.3	35.4	0.51	908	4.3	1.19	0.48
79.9	0.495	24.1	0.018	15.0	46.8	0.52	1396	4.8	1.38	0.45
79.8	0.484	33.0	0.032	15.0	58.7	0.52	1366	3.3	1.14	0.56
77.3	0.432	20.0	0.014	13.3	41.8	0.66	1225	6.1	1.78	0.43
76.9	0.421	26.7	0.022	13.2	48.5	0.65	1193	4.6	1.46	0.52
76.5	0.409	32.9	0.031	13.2	55.6	0.65	1160	3.6	1.30	0.60
77.1	0.405	25.1	0.020	12.2	47.3	0.77	1151	5.3	1.74	0.52
78.6	0.455	24.0	0.018	12.4	47.5	0.77	1286	6.0	1.87	0.48
77.5	0.418	36.4	0.039	13.7	61.7	0.79	1187	3.8	1.56	0.61
77.8	0.431	31.3	0.029	13.7	55.0	0.79	1222	4.8	1.66	0.57
78.3	0.453	25.2	0.020	13.6	49.7	0.78	1281	5.9	1.91	0.48
71.0	0.273	19.5	0.014	15.2	37.6	0.78	792	5.8	1.95	0.45
70.7	0.265	23.0	0.017	15.2	42.5	0.79	771	4.6	1.73	0.52
70.0	0.254	27.9	0.023	15.2	47.6	0.79	741	3.6	1.49	0.60
72.0	0.282	19.9	0.014	15.1	38.6	0.79	819	5.8	1.97	0.45
71.5	0.280	19.9	0.014	15.0	38.1	0.79	811	5.8	1.93	0.46
70.7	0.264	25.2	0.020	15.1	43.7	0.79	768	4.3	1.60	0.56
73.3	0.324	22.1	0.016	13.1	41.3	0.78	931	5.5	1.78	0.50
66.2	0.191	19.4	0.014	16.7	33.0	0.79	571	5.6	1.92	0.45
69.3	0.246	19.2	0.014	15.3	36.4	0.81	718	5.8	2.01	0.45
68.4	0.233	23.2	0.017	15.3	41.1	0.81	683	4.4	1.70	0.53